

**TOPOLOGY OPTIMIZATION OF SLIDER-CRANK  
MECHANISM UNDER DYNAMIC LOADING**

**DİNAMİK YÜKLEME ALTINDA KRANK-BİYEL  
MEKANİZMASININ TOPOLOJİ OPTİMİZASYONU**

**Muhammet Ali ESER**

**SUPERVISOR**

**Assoc. Prof. Dr. Can Ulaş DOĞRUER**

Graduate School of Science and Engineering of Hacettepe University

as a Partial Fulfillment to the Requirements

for the Award of the Degree of Master

In Mechanical Engineering

2021

i

## **ABSTRACT**

# **TOPOLOGY OPTIMIZATION OF SLIDER-CRANK MECHANISM UNDER DYNAMIC LOADING**

**Master of Science Degree, Department of Mechanical Engineering**

**MUHAMMET ALI ESER**

## **SUPERVISOR**

**Assoc. Prof. Dr. Can Ulaş DOĞRUER**

**September 2021, 98 Pages**

Parts in the mechanical system can be optimized individually regarding the static or modal analysis. However, during the motion of an assembly, parts move together and applied forces and configuration of assembly changes along with the motion. While the mechanism is in motion, situations different from those analysed and optimized in static conditions may be encountered. In addition, while the individual and statically optimized parts are in motion within the mechanism, the boundary conditions of each part in space change depending on time. Angle changes relative to the motion of the mechanism require modal analysis for each angle and static analysis again. In this case, mechanism type of structures and/or machine systems are simulated in dynamic environments and optimization processes include this type of dynamic analysis. The main purpose of this study is to test mechanism type of structures and machines in dynamic environments and to find the most suitable dimensional values according to stress and natural frequency constraints. Developing a parametric approach using Abaqus and SolidWorks in the Isight environment is the main goal of this study. The systems to be examined in this research are the simple and realistic crank-slider mechanism systems.

**Keywords:** Topology, parametric optimization, design of experiment, modal analysis, static analysis, dynamic analysis, slider-crank mechanism.

# ÖZET

## DİNAMİK YÜKLEME ALTINDA KRANK-BİYEL MEKANİZMASININ TOPOLOJİ OPTİMİZASYONU

**Yüksek Lisans Derecesi, Makina Mühendisliği Bölümü**

**Muhammet Ali ESER**

**TEZ DANIŞMANI**

**Doçent Dr. Can Ulaş DOĞRUEK**

**Eylül 2021, 98 Sayfa**

Mekanik sistemdeki parçalar, statik veya modal analize göre ayrı ayrı optimize edilebilir. Ancak, bir montajın hareketi sırasında parçalar birlikte hareket eder ve uygulanan kuvvetler ve hareketle birlikte montajın konfigürasyonu değişir. Mekanizma hareket halindeyken, statik koşullarda analiz edilen ve optimize edilenlerden farklı durumlarla karşılaşılabilir. Ayrıca mekanizma içerisinde tek tek ve statik olarak optimize edilmiş parçalar hareket halindeyken, uzaydaki her bir parçanın sınır koşulları zamana bağlı olarak değişmektedir. Mekanizmanın hareketine göre açı değişiklikleri, her açı için modal analiz ve tekrar statik analiz gerektirir. Bu durumda mekanizma tipi yapılar ve/veya makine sistemleri dinamik ortamlarda simüle edilir ve optimizasyon süreçleri bu tür dinamik analizleri içerir. Bu çalışmanın temel amacı, mekanizma tipi yapıları ve makineleri dinamik ortamlarda test etmek ve gerilme ve doğal frekans koşullarına göre en uygun boyutsal değerleri bulmaktır. Isight ortamında Abaqus ve Solidworks kullanarak parametrik bir yaklaşım geliştirmektir. Araştırmada incelenecek sistem basit ve gerçekçi krank-biyel mekanizma sistemleridir.

**Anahtar kelimeler:** Topoloji, parametrik optimizasyon ,deney tasarımı, modal analiz, statik analiz, dinamik analiz, krank-biyel mekanizma zinciri.

# CONTENT

ABSTRACT.....	ii
ÖZET .....	iii
CONTENT.....	iv
LIST OF FIGURES .....	vi
LIST OF TABLE.....	x
NOMENCLATURE .....	xii
1. INTRODUCTION.....	1
1.1 Literature Survey .....	1
1.1.1 Advanced Optimization Techniques.....	3
1.1.2 Traditional Methods.....	4
1.2 Slider Crank Mechanism.....	8
1.2.1 Kinematics of Inline Type Crank Slider .....	9
1.2.2 Equation of Motion on a Slider-Crank Mechanism.....	11
1.3 Scope of The Thesis.....	11
2. SOFTWARE.....	13
2.1 Isight and the SIMULIA Execution Engine.....	13
2.2 Abaqus .....	14
2.3 SolidWorks .....	15
2.4 Conclusion .....	15
3. SIMPLE CRANK SLIDER MECHANISM ANALYSIS.....	16
3.1 Introduction.....	16
3.2 SolidWorks Model.....	16
3.3 Abaqus Model.....	18
3.3.1 Modal Analysis Model.....	18
3.3.2 Dynamic Model .....	22
3.4 Isight Model.....	27
3.4.1 General Overview of Model .....	27
3.4.2 Design Inputs Selection .....	28
3.4.3 Output Selection.....	29
3.4.4 Design of Experiment .....	31
3.4.5 Results and Conclusion.....	31
4. SCALED SLIDER CRANK MECHANISM ANALYSIS .....	36
4.1 Introduction.....	36

4.2	SolidWorks Model .....	36
4.3	Abaqus Model .....	39
4.3.1	Modal Analysis Model .....	39
4.3.2	Dynamic Explicit Model .....	46
4.3.3	Static Model .....	51
4.4	Isight Model .....	56
4.4.1	General Overview of Model .....	56
4.4.2	Design Inputs and Outputs Selection .....	60
4.4.3	Design of Experiment .....	64
4.4.4	Results and Conclusion .....	74
4.4.5	Alternative Methods .....	75
5.	CONCLUSION .....	84
6.	REFERENCES .....	85

## LIST OF FIGURES

Figure 1-1. Global Maximum and Global Minimum.....	5
Figure 1-2. Inline Slider Crank Overview .....	9
Figure 1-3. Slider Crank Stick Model.....	9
Figure 1-4. Crank Slider Mechanism.....	10
Figure 2-1. Isight Overview .....	13
Figure 2-2. Isight Overview .....	14
Figure 3-1. Slider Part.....	16
Figure 3-2. Connecting Rod.....	16
Figure 3-3. Crank.....	17
Figure 3-4. Simple Crank Slider .....	17
Figure 3-5. Joints on System for Modal Analysis.....	18
Figure 3-6. Boundary Conditions on Assembly for Modal Analysis .....	18
Figure 3-7. Meshed Parts .....	20
Figure 3-8. 1 <sup>st</sup> Mode Shape .....	21
Figure 3-9. 2 <sup>nd</sup> Mode Shape .....	21
Figure 3-10. 3 <sup>rd</sup> Mode Shape .....	21
Figure 3-11. 4 <sup>th</sup> Mode Shape.....	21
Figure 3-12. 5 <sup>th</sup> Mode Shape.....	21
Figure 3-13. 6 <sup>th</sup> Mode Shape.....	21
Figure 3-14. 7 <sup>th</sup> Mode Shape.....	21
Figure 3-15. 8 <sup>th</sup> Mode Shape.....	21
Figure 3-16. 9 <sup>th</sup> Mode Shape.....	21
Figure 3-17. 10 <sup>th</sup> Mode Shape.....	21
Figure 3-18. Assembly after 3.4 rad turn .....	22
Figure 3-19. Step Definition of Dynamic Explicit Analysis.....	22
Figure 3-20. Joints on Assembly for Dynamic Explicit Analysis .....	23
Figure 3-21. Force and Boundary Conditions on Assembly for Dynamic Explicit Analysis..	23
Figure 3-22. Maximum Stress at the End of the Analysis .....	24
Figure 3-23. Maximum Displacement at the End of the Analysis.....	24
Figure 3-24. Displacement at 0.08 s .....	25
Figure 3-25. Displacement at 0.16 s .....	25
Figure 3-26. Displacement at 0.24 s .....	25
Figure 3-27. Displacement at 0.32 s .....	25
Figure 3-28. Displacement at 0.40 s .....	25
Figure 3-29. Displacement at 0.48 s .....	25
Figure 3-30. Displacement at 0.56 s .....	25
Figure 3-31. Displacement at 0.64 s .....	25
Figure 3-32. Displacement at 0.72 s .....	25
Figure 3-33. Displacement at 0.80 s .....	25
Figure 3-34. Stress at 0.08 s.....	26
Figure 3-35. Stress at 0.16 s.....	26
Figure 3-36. Stress at 0.24 s.....	26
Figure 3-37. Stress at 0.32 s.....	26
Figure 3-38. Stress at 0.40 s.....	26
Figure 3-39. Stress at 0.48 s.....	26
Figure 3-40. Stress at 0.56 s.....	26

Figure 3-41. Stress at 0.64 s.....	26
Figure 3-42. Stress at 0.72 s.....	26
Figure 3-43. Stress at 0.80 s.....	26
Figure 3-44. General Overview of Isight Model .....	27
Figure 3-45. SolidWorks Input Selection .....	28
Figure 3-46. Data Exchanger Input Selection for the Displacement Boundary Condition .....	28
Figure 3-47. Von Misses Stress Interested Area on Simple Crank Mechanism.....	29
Figure 3-48. Output for Explicit Model.....	29
Figure 3-49. Output for Modal Analysis Model .....	30
Figure 3-50. DOE Input Variations from DOE Component.....	30
Figure 3-51. Outputs of DOE Weight Function.....	32
Figure 3-52. Mapping the Inputs and Outputs .....	32
Figure 3-53. Result of DOE.....	33
Figure 3-54. Mode Shape and Design Number in DOE Analysis .....	33
Figure 3-55. Displacement and Design Number in DOE Analysis .....	34
Figure 3-56. Correlation of Input and Output.....	34
Figure 3-57. Every Input's effect on Outputs .....	35
Figure 4-1. General View of Crank Slider .....	36
Figure 4-2. Slider/Piston .....	36
Figure 4-3. Slider Fitting -Slider Road .....	37
Figure 4-4. Connecting Rod.....	37
Figure 4-5. Crank Arm.....	38
Figure 4-6. Crank Arm Fitting .....	38
Figure 4-7. Simple Slider Crank Isometric View .....	39
Figure 4-8. Step Definition .....	40
Figure 4-9. Joints on the Assembly.....	41
Figure 4-10. Boundary Conditions on the Assembly .....	41
Figure 4-11. Body Type Demonstration on the Assembly .....	41
Figure 4-12. Meshed Parts .....	42
Figure 4-13. 1 <sup>st</sup> Mode Shape.....	43
Figure 4-14. 2 <sup>nd</sup> Mode Shape .....	43
Figure 4-15. 3 <sup>rd</sup> Mode Shape .....	43
Figure 4-16. 4 <sup>th</sup> Mode Shape.....	43
Figure 4-17. 5 <sup>th</sup> Mode Shape.....	43
Figure 4-18. 6 <sup>th</sup> Mode Shape.....	43
Figure 4-19. 7 <sup>th</sup> Mode Shape.....	43
Figure 4-20. 8 <sup>th</sup> Mode Shape.....	43
Figure 4-21. 9 <sup>th</sup> Mode Shape.....	43
Figure 4-22. 10 <sup>th</sup> Mode Shape.....	43
Figure 4-23. 0° Configuration- 1 <sup>st</sup> Mode .....	44
Figure 4-24. 0° Configuration- 2 <sup>nd</sup> Mode .....	44
Figure 4-25. 90° Configuration- 1 <sup>st</sup> Mode .....	44
Figure 4-26. 90° Configuration- 2 <sup>nd</sup> Mode .....	44
Figure 4-27. 180° Configuration- 1 <sup>st</sup> Mode .....	44
Figure 4-28. 180° Configuration- 2 <sup>nd</sup> Mode .....	44
Figure 4-29. Step Definition .....	45
Figure 4-30. Amplitude for Input Moment.....	46
Figure 4-31. Joints on the Assembly.....	47

Figure 4-32. Moment and Boundary Conditions on Assembly .....	47
Figure 4-33. Body Type Demonstration on Assembly .....	47
Figure 4-34. Meshed Parts .....	48
Figure 4-35. Dynamic Explicit Job .....	48
Figure 4-36. Displacement at 0.04 s .....	49
Figure 4-37. Displacement at 0.08 s .....	49
Figure 4-38. Displacement at 0.12 s .....	49
Figure 4-39. Displacement at 0.16 s .....	49
Figure 4-40. Displacement at 0.20 s .....	49
Figure 4-41. Displacement at 0.24 s .....	49
Figure 4-42. Displacement at 0.28 s .....	49
Figure 4-43. Displacement at 0.32 s .....	49
Figure 4-44. Displacement at 0.36 s .....	49
Figure 4-45. Displacement at 0.40 s .....	49
Figure 4-46. Acceleration at 0.04 s .....	50
Figure 4-47. Acceleration at 0.08 s .....	50
Figure 4-48. Acceleration at 0.12 s .....	50
Figure 4-49. Acceleration at 0.16 s .....	50
Figure 4-50. Acceleration at 0.20 s .....	50
Figure 4-51. Acceleration at 0.24 s .....	50
Figure 4-52. Acceleration at 0.28 s .....	50
Figure 4-53. Acceleration at 0.32 s .....	50
Figure 4-54. Acceleration at 0.36 s .....	50
Figure 4-55. Acceleration at 0.40 s .....	50
Figure 4-56. Step Definition of Static Analysis .....	51
Figure 4-57. Joints on Assembly .....	52
Figure 4-58. Boundary Conditions on Assembly .....	52
Figure 4-59. Body Type Demonstration on Assembly .....	52
Figure 4-60. Analytical Field Creation of Static Analysis .....	53
Figure 4-61. Loading Process of Static Analysis .....	53
Figure 4-62. Applied Force on the System .....	54
Figure 4-63. Meshed Parts .....	54
Figure 4-64. Von Mises Stress at the end of The Analysis .....	55
Figure 4-65. Von Mises Stress at the end of The Analysis .....	55
Figure 4-66. Acceleration on the Case Study Time-End of the Analysis .....	55
Figure 4-67. Von Mises Stress investigated Zone .....	56
Figure 4-68. General Overview of Isight Model .....	56
Figure 4-69. General View of Isight Design .....	58
Figure 4-70. General View of Isight Design .....	59
Figure 4-71. SolidWorks Input Selection .....	60
Figure 4-72. Dynamic Analysis Workflow .....	61
Figure 4-73. Data Exchanger-1 Input Selection .....	61
Figure 4-74. Matlab Function Calculator and Printer .....	62
Figure 4-75. Data Exchanger Output Selection- Max Kinetic Energy of Dynamic System ...	62
Figure 4-76. Data Exchanger-3 Input Selection- Static-Modal Model, Angle .....	63
Figure 4-77. Static and Modal Analysis Workflow .....	63
Figure 4-78. Data Exchanger-2 Output Selection- Static Model Average Stress .....	64
Figure 4-79. Data Exchanger-4 Output Selection- Modal Analysis-Mode 2 .....	64



Figure 4-80. DOE Inputs.....	66
Figure 4-81. DOE Outputs.....	66
Figure 4-82. Investigated Zone Von-Misses Stress vs Design Number .....	69
Figure 4-83. Kinetic Energy vs Design Number .....	69
Figure 4-84. Mode Shape vs Design Number.....	70
Figure 4-85. Pareto Table between Input and Outputs .....	70
Figure 4-86. Correlation Graph of Rod Length and Other Parameters.....	71
Figure 4-87. Correlation Graph of Angle (Frame) and Other Parameters.....	71
Figure 4-88. Correlation Graph of Width of Rod and Other Parameters.....	72
Figure 4-89. Local Effects for Stress .....	72
Figure 4-90. Local Effects for Kinetic Energy .....	73
Figure 4-91. Local Effects for Mode Shape.....	73
Figure 4-92. NLPQLP Inputs.....	75
Figure 4-93. NLPQLP Outputs .....	75
Figure 4-94. Stress vs Number of Design.....	80
Figure 4-95. Kinetic Energy vs Number of Design .....	80
Figure 4-96. 2 <sup>nd</sup> Mode Shape vs Number of Design.....	81
Figure 4-97. Local Effects for Investigated Zone Von-Misses Stress .....	81
Figure 4-98: Local Effects for Kinetic Energy .....	82
Figure 4-99. Local Effects for Mode Shape.....	82

## LIST OF TABLE

Table 3-1. Slider Geometrical Properties.....	16
Table 3-2. Connecting Rod Geometrical Properties .....	17
Table 3-3. Crank Geometrical Properties .....	17
Table 3-4. Mechanical Properties of Steel .....	18
Table 3-5. Element Type and Node Number .....	19
Table 3-6. Mesh Quality Analysis .....	20
Table 3-7. Modal Analysis Results for Simple Crank Slider.....	20
Table 3-8. Element Type and Node Number .....	24
Table 3-9. Geometrical and Displacement Input Table .....	31
Table 4-1. Slider Geometrical Properties.....	36
Table 4-2. Slider Fitting Geometrical Properties .....	37
Table 4-3. Connecting Rod Geometrical Properties .....	37
Table 4-4. Crank Arm Geometrical Properties .....	38
Table 4-5. Crank Arm Fitting Geometrical Properties .....	38
Table 4-6. Element Type and Node Number .....	42
Table 4-7. Mesh Quality Analysis .....	42
Table 4-8. Natural Frequency Results for Simple Crank Slider .....	45
Table 4-9. Element Type and Node Number .....	48
Table 4-10. Element Type and Node Number .....	54
Table 4-11. Frame- Angle Conversion .....	65
Table 4-12. Design Matrix for DOE-Full Factorial .....	67
Table 4-13. Result Table of DOE .....	68
Table 4-14. Investigated Angle-Frame .....	76
Table 4-15. NLQP Design Inputs and Outputs Results .....	77
Table 5-1. General Overview Comparison .....	84

## ACKNOWLEDGEMENTS

I am excited and proud to complete my master's thesis, which I prepared with serious effort and devotion. I will use this part of my thesis as an opportunity to thank the people who have supported me during my thesis.

I would like to express my endless thanks to my thesis advisor, Associate Professor Can Ulaş Dođruer, who guided me in my work, did not spare his support and efforts, encouraged me and broadened my perspective on engineering and life. I am grateful that he worked with me until midnights when I was close to despair while preparing this thesis. Working with him is a great opportunity for me.

I would like to thank my professors who took part in my thesis evaluation committee and helped shape the research with their valuable opinions.

I would like to thank the lecturers of Hacettepe University Mechanical Engineering Department, which I will always be proud of completing my graduate education, for sharing their experiences and being a light on my path.

I would like to thank my manager Hasan Püskül, my colleagues, Barış Canitez, Mehmet Yahşi, and Fatih Çetin for their help during the implementation process of my work.

I would like to express my gratitude to my precious and invaluable mother, father and brother who have supported me throughout my life and whose rights I will never be able to repay. Thanks to the efforts of my parents and their value to education and to me as a child, I have achieved the position I am in now. Although he likes to walk around with a sullen face, I thank my brother who made the world laugh when he laughed.

I would like to express my gratitude to my dear wife, my life partner, the dearest Cansu Düzleyen Eser, who followed me closely during this process and provided all the support she could during my thesis period and my lecture period. I would like to thank her for always being understanding and helping me when I have to study, even on holidays, and for doing her best for my comfort in sickness and health and for the ease of my work. I would not have been able to finish this thesis without her help.

## NOMENCLATURE

$a$	<i>Vector representing <math>i</math>th link length</i>
$a_i$	<i>Magnitude of <math>a_i</math> the link length</i>
$A$	<i>Area of region defining link shape</i>
$J$	<i>Moment of Inertia</i>
$H$	<i>Height</i>
$L$	<i>Length of connecting rod</i>
$M$	<i>External Moment</i>
$R$	<i>Crank arm</i>
$V_{c0}$	<i>AB rod velocity</i>
$V_b$	<i>OA rod velocity</i>
$W$	<i>Width</i>
$W$	<i>Work</i>
$\beta$	<i>Angle between Slider and Connecting Rod</i>
$\rho$	<i>Material density</i>
$\omega$	<i>Rotational Speed</i>
$\varphi$	<i>Angle between crank and crankshaft</i>
$\varphi_{c0}$	<i>AB rod angular velocity</i>

# 1. INTRODUCTION

An optimization task focuses on obtaining an elemental set that minimizes or maximizes an objective function, a certain response, which is affiliated with each elemental set. In this thesis, we are interested in minimizing the selected zone stress, total kinetic energy and mode shape of the system.

Optimization methods are divided into many sub-categorizes. Generally, it is classified as local optimization methods and global optimization methods

There are huge research made for local optimization approaches. The most common known local-optimization approach methods are generalized as a model base and pattern search methods. These methods are derivative-free algorithms. Local investigation of the cost function on a given pattern which is a set of a given input parameter is the pattern search methods' operation algorithm. The Nelder–Mead [1] simplex method and The Hooke–Jeeves[1] method are the most well known models of local pattern search.

Computing the cost function using function evaluations are the main way to work on Model-based search methods. Furthermore, obtaining derivatives of the model is performed. Most of the Model-Based algorithms are trust-region methods that interpolate the cost function in a certain region. This region is a suitable area that is a good estimation of the cost function [2,3].

Since most of the engineering problems require multi-modal issues, local optimization techniques are inadequate to achieve the optimization, in order to overcome this issue, global optimization methods were developed. Many global optimization algorithms utilise random search and heuristics methods. Some of the thriving well-known methods of global optimization techniques are evolutionary algorithms, simulated annealing algorithms, differential evolution algorithms, particle swarm optimization algorithms, estimation of distribution algorithms, and ant colony optimization algorithms [2,3]

## 1.1 Literature Survey

Optimization techniques are used almost everywhere, from in our daily activates to every aspect of engineering and industry. The main idea is the maximize the efficiency of system and at the same time reduce the effort, mass or price of product. A mechanical design must include optimization steps in which engineers pay attention specific aspirations, which are strength of the part, deflection under the loading process, total mass, damage, corrosion, etc.

For a long time, analytical and numerical methods to calculate the extreme values of a function has been applied to engineering problems. Although, these methods mostly work well for the most engineering practices, they do not show the same performance for complex systems. To able to decide the problems complexity, objective function and design matrix needs to be controlled. Based on the requirement set, the optimization process guides to an extensive objective function. This objective function may have a huge number of design variables. To overcome the objective function may be ineffective for complex systems. Since the process of analysis might be more expensive than the possible benefits of the solution. Thus, in general, optimization techniques are applied on simple systems or individual parts, applying these techniques are not desired on complex systems. For instance, automobile gearbox optimization is more basic than optimization of the entire automobile system in terms of complexity and mathematically [4,5].

Increasing the entanglement of the problem causes selection of the incorrect optimization method and receiving not the best feasible solution. No optimization method can give the guarantee to find the best answer. Due to the nonlinear effects in real design problems, total number of design parameters can be enormous and their effects on the goal function can be complicated.

Physical problems can be expressed in mathematical functions. These functions involve dependent or independent variables. When the function includes some requirements such as efficiency, performance, it becomes the objective function. Minimizing or maximizing the objective function become the central issue of optimization. To be able to maximize or minimize the objective function, derivation tool is used. The derivation process ends up with zero which is equivalent to optimal solution. As a result, optimum solution is achieved by this operation. However, not every zero of derivation of function results does not guarantee the best optimum result. Furthermore, the optimization function may have several local extreme points, whereas the real interest is the global extreme. In this kind of problems old-fashioned methods (such as: gradient methods) does not work properly, to be more accurate, most of the time old methods focus on computing local points. For complex systems, advanced optimization methods propose different solutions, because their working principle allow them to find a solution near the global optimum point in an acceptable time and computational costs [5].

Increasing the design variable causes complexity and nonlinearity. Due to the nonlinearity, some optimization techniques become inadequate and new methods needed to be implemented.

In general, two types of optimization method exist:

**Traditional optimization methods:** These ones are deterministic algorithms. They work some specific rule, which is calculating step by step.

Traditional Method calculate a solution after they pass to another solution. These methods have been used for a long time, and they have proven themselves with different engineering cases. These techniques can be given as an example; quadratic programming, nonlinear programming, dynamic programming, geometric programming, etc.[6]

**Advanced optimization methods:** Advanced methods are based on probabilistic rules. These methods are popular in Industry since they are new and fully unexplored and they have better specialties in certain areas when compared to traditional methods. To give examples to advanced optimization techniques; Particle Swarm Optimization, Genetic Algorithm, Differential Evolution (DE), Artificial Bee Colony, etc [5,6].

Although, traditional methods are widely used in the mechanical design, they have some limitations:

- Traditional methods not always give good performance for a huge range of design function.
- Traditional methods are mostly used for local optimum and they are not suitable for multi-constraints cases.
- A large number of constraints may be obstacle to perform efficiently for traditional methods.
- Results of traditional methods depend on the initial selection and there is no certainty the result is globally optimal one.
- Gradient based traditional methods in some cases may be congested at local optimum.

Because of the disadvantages of traditional optimization techniques, advanced optimization methods are used in certain cases. Genetic Algorithm is one of the most commonly preferred

advanced optimization method. Although being popular among the optimization techniques, there are some drawbacks. The genetic Algorithm provides an optimal result for the problems that contain large input and constraints matrices. However, there are some difficulties to accomplish. Because of, assignment of control parameters which are cross over rate, mutation rate, the population is difficult. Therefore, modifying existing algorithms and mixing them as hybrid methods give more powerful, robust and accurate solutions [4,5].

### **1.1.1 Advanced Optimization Techniques**

The industry tends to mimic nature, and in nature, some problems are solved with evolution. Biology, chemistry and physics processes are modelled by researchers to investigate and understand the mechanism of the natural processes. As a consequence, advanced optimization methods are artificially developed.

There are huge number of advanced optimization methods, such as genetic algorithms, simulated annealing, genetic programming, evolution strategies, ant colony optimization, particle swarm optimization and etc. Some of the will be explained below:

#### **1.1.1.1 Genetic Algorithm:**

Genetic Algorithm is inspired from Charles Darwin's evolution theory. This algorithm based on 'the strongest one lives', which means survival of the fittest.

The search algorithm runs in solution space, which is created, by genetic operators and natural selection tools. Mutation, crossover and the mutation rate are these tools.

One of the main differences between traditional methods and Genetic Algorithms is the working style. Traditional methods work directly with inputs and decision factors, however, the Genetic Algorithm creates inner keywords linked with input and decision factors, which ultimately increase speed. This method, hide the decision factors and inputs into solution with string format. Furthermore, one of the strong sides of Genetic Algorithms is actually their search algorithm, which works on a populated design solution rather than only one point on the design solution space. The population of individual elements of the design solution space is built randomly. Genetic operators are used in order to create the global optimum in the current population. These genetic operators are [7,8,9]:

- Selection
- Crossover
- Mutation.

#### **1.1.1.2 Particle Swarm Optimization**

Kennedy and Eberhart discovered Particle Swarm Optimization and its computational method based on evolution similar to Genetic Algorithm. A population of random solution space is generated as the initial of analysis after then starts to search for the optimal solution. This process updates the design solution space simultaneously. It is called particles to potential solutions, they are following the optimum particles into problem design space.

Historically, this method was invented to simulate bird drove's unpredictable movements and human social systems. Each particle keeps track of its coordinates in the problem space, which is associated with the best solution (fitness) it has achieved so far. The local best solution is being called 'pBest'. There is also a global best solution which is called 'gBest' and this point is also to seek out by particles in the design space. The particle swarm optimization allows changing velocity or acceleration of every single particle movement towards 'pBest' and 'gBest' [10,11].

### 1.1.2 Traditional Methods

Traditional methods mostly begin with chosen initial solution or value and begin to search for the optimum solution with many iterations. Optimization algorithms decide the step length and search movement direction.

In historically since the oldest optimization method is the traditional method, there is a vast number of techniques that can be evaluated as traditional methods. However, it can be divided two groups which are gradient-based and direct solution methods.

Direct search method does not require the gradient of the objective function. This method starts to investigate with the area of given current point, searching for the point which its objective function result is under the current point. This method includes, pattern search, univariate search and random search.

Quasi-Newton method, steepest descent method, conjugate gradient method are given as an example to gradient-based methods. Gradient-based methods control the search direction with gradient of objective function. One of the reasons of selection these methods is being fast. The deficiency of this method is, since the gradient is a local speciality of objective function, getting into local minima and being stuck in there is more common. The most widely using method is steepest descent method.

Single variable, multi variable optimization techniques are classified as traditional method since they involve gradient methods. Bisection, Newton's Method for Root Finding, Secant Method, Polynomial Interpolation, Linear Programming, Nonlinear Programming and other traditional methods are breakdowns of single and multi-variable methods.

#### 1.1.2.1 Single-Variable Optimization

In real life, most of the practical optimization problems have more than one variable. Optimization of multi-variable problems require powerful computation and time. In order to accomplish the optimization in limited computation and time, the variables are investigated individually. Furthermore, the study of single variable minimization can be seen reasonable.

Nonetheless, the optimization of both single and multivariable functions can be investigated in two parts [10]:

- Search direction finding
- Values minimizing in the found direction.

Single variable optimization's motivation is minimizing the values in the given direction.

Consider a scalar function which can be written like  $f: R \rightarrow R$ , that depends on single variable, which is  $x \in R$ . The  $f(x)$  shall be minimized. Moreover, our intention is also:

- Use low computational force as possible as
- Avoid using high memory need
- Encounter with errors less as possible as

In most engineering case, computing of  $f$  and its derivation are expanse in terms of computational cost, so the requirements can be reduced into 2 parts: Evaluating the  $f(x)$  function and taking derivative, which is  $df/dx$ , which it is taken so much time.



A single-variable optimization problem is trying obtain  $x^*$  value that in a specific interval  $([a, b])$ , enables to minimize the design problem function  $f(x)$ . There are two theorems procure the sufficient and necessary environment for the minimum value of a function. [6]

- Necessary Condition:

Let us define a  $f(x)$  function that in an interval which is  $a \leq x \leq b$  and  $f(x)$  has a minimum point at  $x = x^*$  relatively in which  $a \leq x^* \leq b$  and if the derivative  $df / dx = f'(x)$  exists a certain finite number at  $x = x^*$ , then  $f^j(x^*) = 0$  [10].

It is given that:

$$f'(x^*) = \frac{f(x^*+h)-f(x^*)}{h} \quad (2.1)$$

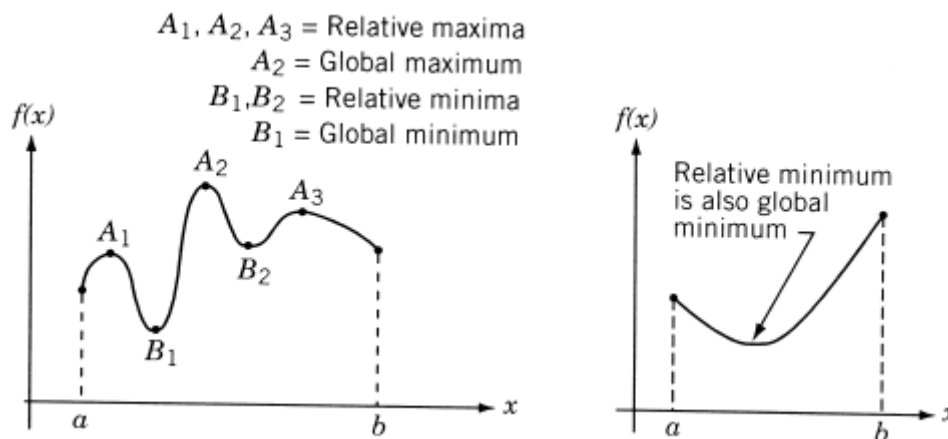


Figure 1-1. Global Maximum and Global Minimum

There is a definite number, that it should be zero.  $x^*$  is a relative minimum and that leads to:

$$f(x^*) \leq f(x^* + h) \quad (2.2)$$

for all values of  $h$  variable is enough close to zero. Hence:

if  $h > 0$ ;

$$\frac{f(x^*+h)-f(x^*)}{h} \geq 0 \quad (2.3)$$

If  $h < 0$ ;

$$\frac{f(x^*+h)-f(x^*)}{h} \leq 0 \quad (2.4)$$

$$f'(x^*) \geq 0 \quad (2.5)$$

$$f'(x^*) \leq 0 \quad (2.6)$$

The only way to ensure the both Eqn. 2.5 and 2.6 is :

$$f'(x^*) = 0 \quad (2.7)$$

- Sufficient Condition:

Let  $f'(x^*) = f''(x^*) \dots = f^{(n-1)}(x^*) = 0, f^{(n)}(x^*) \neq 0$ . Then  $f(x^*)$ ;

- (i) a minimum value of  $f(x)$  if  $f^{(n)}(x^*) > 0$  and  $n$  is even
- (ii) a maximum value of  $f(x)$  if  $f^{(n)}(x^*) < 0$  and  $n$  is even
- (iii) neither a maximum nor a minimum if  $n$  is odd [10].

For  $0 < \theta < 1$ ;

$$f(x^* + h) = f(x^*) + hf'(x^*) + \frac{h^2}{2!}f''(x^*) \dots + \frac{h^{n-1}}{(n-1)!}f^{(n-1)}(x^*) + \frac{h^n}{(n)!}f^{(n)}(x^* + \theta h) \quad (2.8)$$

Since  $f'(x^*) = f'' = \dots = f^{(n-1)}(x^*) = 0$ , so Eqn. 2.8 becomes;

$$f(x^* + h) - f(x^*) = \frac{h^n}{(n)!}f^{(n)}(x^* + \theta h) \quad (2.9)$$

### 1.1.2.2 Multivariable Optimization

Multivariable algorithms show the search of optimum point in multiple output matrix. These algorithms are defined as Gradient Based Techniques whether or not it is used on the method [10, 11].

- Global max/min: If a value in the (a, b) is bigger than any point on the space matrix which is  $R \times R$ , then the function  $f(a, b)$  is called the global maximum. Same rule applies for global minimum.
- Local max/min: The value in (a, b) is contrasted within the values nearby. Then it becomes Local Max/Min.
- Extreme values are called Maxima/Minima.

If the function  $f$  is not discrete on the region  $R$  and the boundary conditions, then the global max/min values exist for this function. Also, if the local max/min exist in the interior area, they are considered as critical points. The max/min on a structure given by constraints where there are no interior points. If the max/min happens on the boundary of the region or the structures without interior points, other methods should be used (Lagrange multiplier, reducing the number of variables etc) [11].

The constraints in the design function have functional connection within the inputs that represents physical phenomenon and source limitations. The user can implement these constraints in formula.

As an example, maximum stress or maximum deflection is a constraint of a structural system. And these constraints have mathematical relationship with structure's shape and dimension [11].

There are two kind of constraints in optimization problems:

#### 1.1.2.2.1 Multivariable Optimization with Equality Constraints

In mathematics, equality is a relationship between two quantities or, more generally two mathematical expressions, a descriptor that the quantities have the same value.[8]

Optimization of continuous functions depend on the equality constraints in multivariable techniques:

**Minimize**

$$f = f(X) \text{ subject to } g_j(x) = 0, j = 1, 2, \dots, m$$

$$X = \{x_1 \ x_2 \ x_3 \ \dots \ x_n\}$$

Above equation, the number of 'x' which is 'm' is less than or equal to n; the opposite which is  $m > n$  makes the problem overdefined which cause no solution. There are several methods available for the solution of this problem. The methods of direct substitution, constrained variation, and Lagrange multipliers are discussed in the following sections [12].

For a problem with n variables and m equality constraints, it is theoretically possible to solve simultaneously the m equality constraints and express any set of m variables in terms of the remaining  $n - m$  variables. With substituting these expressions into the original objective function, the results that involve only n and m variables as notation and physical meaning. Obtaining the new objective function, makes the function independent from constraints and its optimum value can be found by applying unconstrained techniques. This method can be described as simple; however, it is not practical. Because, most of the case constraints are mostly nonlinear. Eliminating them is useless and make the problem more inextricably most of the time. However, the method of direct substitution might prove to be very simple and direct for solving simple problems [12].

#### **1.1.2.2.2 Multivariable Optimization with Inequality Constraints**

Inequality constraints suggest that the relationship between variables can be either bigger, smaller or even equal to original value [13].

The following problem is the main concern:

$$g_j(X) \leq 0, \quad j = 1, 2, \dots, m \quad (2.10)$$

The inequality constraints equation in Eqn. 2.10 can be written again to become equality constraints by adding variable that is non-zero, slack variables,  $y_j^2$ , as

$$g_j^2(X) + y_j^2 = 0 \quad j = 1, 2, \dots, m \quad (2.11)$$

Still added slack variables are unknown and the problem turns below:

Minimize  $f(X)$

$$G_j(X, Y) = g_j(X) + y_j^2 = 0 \quad j = 1, 2, \dots, m \quad (2.12)$$

$Y = \{y_1, y_2, \dots, y_m\}^T$  is the vector of slack variables [13]. This problem can be solved conveniently by the method of Lagrange multipliers. For this, the Lagrange function L is constructed as;

$$L(X, Y) = f(X) + \sum_{j=1}^m \lambda_j G_j(X, Y) \quad (2.13)$$

where  $\lambda = \{\lambda_1, \lambda_2, \dots, \lambda_m\}^T$  is the vector of Lagrange multipliers [13].

## 1.2 Slider Crank Mechanism

Crank slider mechanism was selected in this work as case study, because its usage area is enormously wide. Almost every complex system in industry has some sort of slider crank mechanism as a subsystem.

Slider crank mechanism was investigated with optimization techniques to find the best optimal design. The design process is based on parametric design rules. When a part's geometric dimension is changed, its dependencies change according to the given new dimension. The design objectives are finding the minimum stress of inspected area, minimum kinematic energy of mechanism and minimum value of the requested mode shape [14].

The slider-crank mechanism is constituted with a four-link mechanism with has in total of four joints. Three of them is revolute and on the prismatic joint. Linear motion is converted to rotational motion via the crank slider mechanism or vice versa. The essential parts of mechanism are connecting rod and slider mass that drives the beam. The sliding mass only move linear direction and has no degree of freedom on rotational axis. Only connecting rod and driving beam have rotational degree. Although, each body of the system obtain six degree of freedom, the system has one degree of freedom due to the kinematic constraints.

The most common example is internal combustion engines. The linear motion is created with combustion which occurs in a cylindrical structure and that creates pressure which drives the piston. After that, the piston's linear motion is converted into rotational motion with help of connecting rod. As long as this motion converting process continues, the forces that are produced during progress cause shakes in certain periodic times. The vibration will disrupt the operation of the engine at a certain time later [14].

To able to rotate fully,  $L > R + E$  must be provided,

' $R$ ' is the 'crank length', ' $L$ ' is the 'connecting rod length' and ' $E$ ' is the 'offset of the slider'.

Some Applications of Crank Slider Mechanism:

- Oscillating cylinder: Toys, models, hydraulic motors.
- Reciprocating Engine: Automobiles' engine, motorcycles, tractors.
- Rotary Engines: Some Aircrafts, automobiles, motorcycles.

There are 2 types of crank-slider:

- Inline Type: In line slider crank mechanism slider lies on the same plane with the joint between crank and ground. Being in the same plane causes the symmetrical movement for slider while crank rotates.
- Offset: When there is distance between slider and crank-ground joint's planes it makes the system offset crank-slider mechanism. Offset types, break the symmetrical movement of slider and slider moves faster than other side. Also this situation is called 'quick return'. [11]

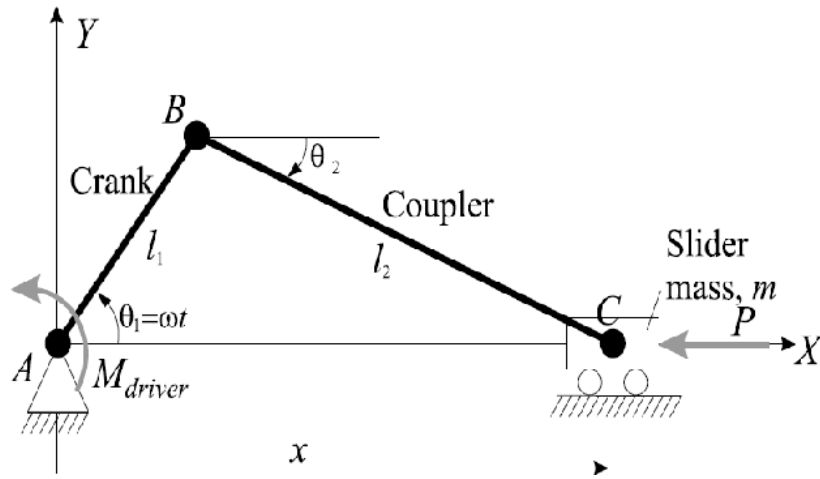


Figure 1-2. In-line Slider Crank Overview

In this work, inline type (Figure 1-2) was studied.

### 1.2.1 Kinematics of In-line Type Crank Slider

The connecting rod displacement is approximately proportional. It depends on the ‘cosine’ function of the angle of rotation of the crank. The reference point is taken as when it is on the top dead center (TDC). Hence, the back-and-forth movement is created by rotating crank and connecting rod. The motion can be considered as harmonic [14]:

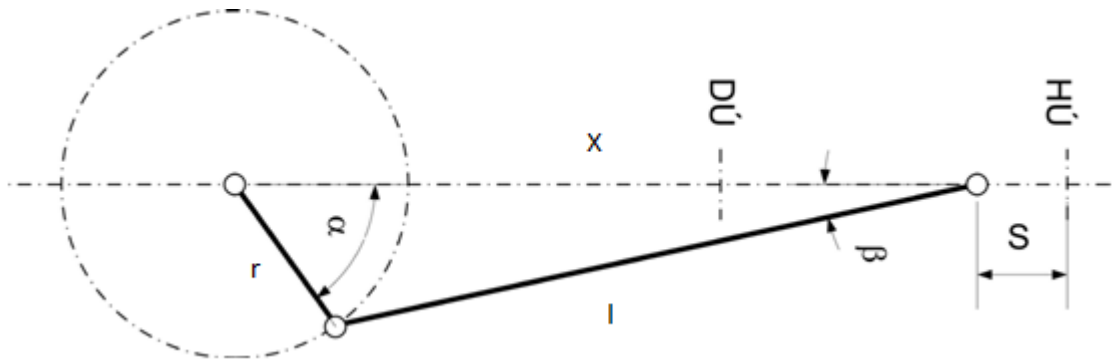


Figure 1-3. Slider Crank Stick Model

$$X = r \cos \alpha + l \cos \beta \quad (2.14)$$

The Figure 1-3 shows length of links in slider-crank mechanism.

- $x$ : the distance of the end of the connecting rod from the crank axle ,
- $l$ : the connecting rod length ,
- $r$ : the radius of crank ,
- $\alpha$ : the angle of crank, this angle measured from the top dead center .

The triangular area in Figure 1-3, between connecting rod, crank and ground, helps derivation of the necessary equations:

$$r \sin \alpha = l \sin \beta \quad (2.15)$$

With help of Eqn. 2.15 is transformed to Eqn. 2.14, below the new equation given:

$$X = r(\cos\alpha + 1/\lambda(\sqrt{1 - \lambda^2 \sin^2\alpha})) \quad (2.16)$$

Mathematical function of reciprocating motion of connecting rod can be described as sinusoidal function. Hence, to be more accurately, the piston motion equation becomes more elaborately can be described below:

$$X = r\cos\alpha + \sqrt{l^2 - r^2 \sin^2\alpha} \quad (2.17)$$

The differences between Eqn. 2.14 and 2.17 is negligible if  $l \gg r$ . The connecting rod is much longer than the crank in this situation. However, for high speed system the variance between Eqn. 2.14 and 2.17 are significant and cause serious vibration and damage [15].

To find the piston velocity equation, the derivative of the piston displacement equation should be calculated (Eqn. 2.17) :

$$v(\alpha) = \frac{dX}{d\alpha} \quad (2.18)$$

By making the necessary calculations the below equation is obtained:

$$V = \left(-r\sin\alpha - \frac{r^2 \sin\alpha \cos\alpha}{\sqrt{l^2 - r^2 \sin^2\alpha}}\right) \frac{d\alpha}{dt} \quad (2.19)$$

In Eqn. 2.19 the term  $\frac{d\alpha}{dt}$  is the rotational speed of crank and it symbolizes as ' $\omega$ '. When the same principle is used for finding acceleration equation and the below equation is obtained:

$$a = -r\omega^2(\cos\alpha + \lambda\cos 2\alpha) \quad (2.20)$$

The relationship between crank and connecting rod is given below equation. This equation is given in terms of torque on the shaft and it changes via the crank's cycle.

$$\tau = Fr\sin(\alpha + \beta) \quad (2.21)$$

$\tau$  is the torque on the shaft and  $F$  is the force applied on the connecting rod [15].

When  $\alpha = 90^\circ$  or less from the Top Dead Center (TDC) from a given position, torque reaches its maximum. As it can be seen from above equations  $\alpha$  angle is the driver parameter and piston speed needs to be known to calculate this angle [15]. While the crank is at top or bottom dead center ( $0^\circ, 180^\circ$ ), no torque occurs. Hence, crank is stationary on these point, it cannot be started by moving connecting rod [15].

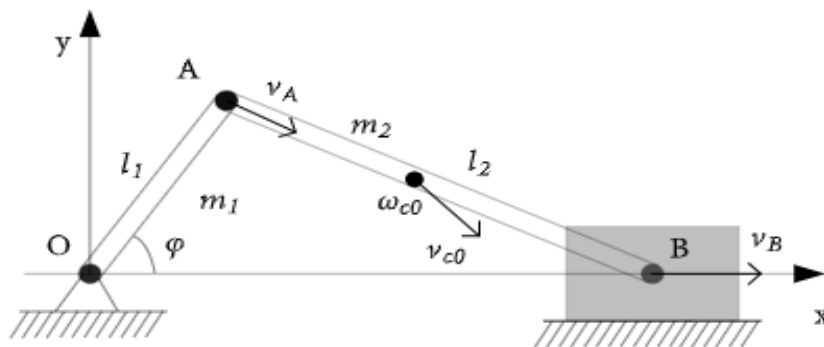


Figure 1-4. Crank Slider Mechanism

### 1.2.2 Equation of Motion on a Slider-Crank Mechanism

Cyclic-bending moment  $M$  is applied on the crank. It can be considered OA and AB links are rigid. Lagrange equations will help us to write the mechanism motion [16, 20]

The general scheme of the slider crank is given Figure 1-4. The mechanism has one-degree freedom.

$\alpha$  symbolizes variable set in the system,

$M$  symbolizes the external moment.

The crank angle  $\alpha$  is the angle between rod OA and the horizontal direction [16].

length of OA is  $l_1$ , mass of OA is  $m_1$ ,

length of AB is  $l_2$ , mass of AB is  $m_2$ .

Inertia of OA:

$$J_1 = \left(\frac{m_1}{l_1}\right) \int_0^{l_1} x^2 dx = (1/3)m_1 l_1^2 \quad (2.22)$$

Inertia of AB:

$$J_2 = \left(\frac{m_2}{l_2}\right) \int_0^{l_2} x^2 dx = (1/3)m_2 l_2^2 \quad (2.23)$$

AB rod velocity= $V_{c0}$

AB rod angular velocity= $\varphi_{c0}$

OA rod velocity= $V_b$

The kinetic energy formula is given below:

$$T = \sum_{n=1}^3 T_n = \frac{1}{2}J_1\varphi^2 + \left(\frac{1}{2}m_2\varphi^2V_{c0}^2 + \frac{1}{2}J^2\varphi_{c0}^2\right) + \frac{1}{2}m_2V_b^2 \quad (2.24)$$

The generalized force:

$$\begin{aligned} Q_\delta &= \sum \frac{W_\delta}{\delta_\psi} \\ &= M + m_1gl_1\cos\psi + m_2gl_1\sin\psi\cos\psi \end{aligned} \quad (2.25)$$

### 1.3 Scope of The Thesis

In order to obtain more realistic, suitable and effective systems and products for industry parametric optimization of mechanical systems were made in the thesis.

In general, the optimization of the objects for their natural frequencies and maximum stress zones has been made via Abaqus-Tosca and Isight. Abaqus-Tosca works in non-parametric methods. While optimizing in Abaqus-Tosca, the general topology algorithms embedded in the program were worked. Due to the being non-parametric, Abaqus-Tosca may obtain non-producible designs results. However, Isight was run with geometric design data received from the SolidWorks program, it has been observed that optimization eliminates impossible results in terms of production and gives only physically possible results.

Overall, it is aimed to design the most suitable topology / shape considering more than one purpose in this work. The topology optimization will be made using Abaqus CAE and SolidWorks software in the Isight optimization environment. Although the methodology that is developed in this work is applicable to a broad range of engineering systems, this study exclusively deals with dynamic systems. The objectives that are sought in this work are stress minimization under dynamic loading and minimization of the output of modal analysis i.e.

natural frequency of the system. Both objectives may be subject to constraints on the part geometry.

Topology optimization of more than one mechanical structure will be made within the scope of this thesis study. When performing optimization, more than one goal and target will be considered. Minimum weight/volume, min-max stress values, placing natural frequencies in certain ranges, etc. The systems that will be examined within the scope of the study will be dealt with under two loadings basically: static loading and dynamic loading.

The above-mentioned optimization issues may be solved relatively easily for static loading. On the other hand, working on optimization studies under dynamic loading is a challenging case study. A basic approach used in the analysis of flexible multiple body dynamics will be adopted while topology optimization of a mechanical structure operating under dynamic load. This approach is known as elasto-dynamic modelling.

In modelling, the total motion of the system is expressed as the sum of the rigid movement of the parts forming the system and the micro-movements resulting from the elasticity, and the problem is solved sequentially: First the rigid motion, then the micro-motion can be solved. This method will be used in the topology optimization of systems operating under dynamic load.

It is planned to use Isight and ABAQUS programs for topology optimization. In the thesis study, as a reference model, firstly, the crankshaft mechanism will be studied and then, after sufficient experience on the method and software, complex mechanical systems will be designed.



## 2. SOFTWARE

### 2.1 Isight and the SIMULIA Execution Engine

In order to work on the natural frequency and dynamic response of model, co-simulation is required. Isight software is used as co-simulation. Isight Optimization Tool is used to merge multi-disciplinary problems and related applications (components) together in one simple simulation. The software helps the automation process, examine the results of optimizations, and identify the best optimal parameters that requires necessary constraints [17].

Co-simulation also helps,

- Incredibly, reduce design cycle time through incorporated workflow
- More reliable products among the evaluated vast design alternatives.
- Reduce the investments on the computational force, thanks to efficient distribution analysis.



Figure 2-1. Isight Overview

Hence, in this thesis Simulia Isight Execution Engine is used as co-simulation tool [17].

In Isight, there are optimization and design of engineering methods. Some of them are listed below:

- Single Objective Optimization Methodologies:

Gradient methods should be used for differentiable functions. The gradient methods are very suitable for parallel execution because of being separately computing the gradients. Some of the methods are:

- Nonlinear Programming by Quadratic Lagrangian (NLPQL)
- Modified Method of Feasible Directions (MMFD)
- Large-Scale Generalized Reduced Gradient (LSGRG)
- Hooke-Jeeves Direct Search
- Nealder & Mead Downhill Simplex
- POINTER - Pointer Automatic Optimizer
- The Deterministic Multi-Objective
- Adaptive Simulated Annealing (ASA)
- Multi-Island Genetic Algorithm (MIGA)

- Multi-Objective Optimization Methodologies:

Since multi-objective optimization is widely used in the industry besides from the academic environment, they become more popular in the last decade.

The evolutionary-based multi-objective optimization algorithms take more attention than other methods. These algorithms (EAs) methods are created based on the idea that Charles Darwin's

theory of evaluation. The Evolutionary algorithm has adaptive nature since it mimics nature and thanks to this ability suitable different operators and functions can be produced. One of the evolutionary techniques that have been used as an optimization method is The Genetic Algorithm (GA). In general, the Genetic Algorithm runs by a populated solution set not just one solution. Thanks to this speciality of GA, it makes it one of the perfect candidates for solving multi-objective optimization problems. The population approach also makes GA more robust to not encounter premature convergence which is the local best option [17].

Some of the methods are given below:

- Archive-based Micro Genetic Algorithm (AMGA)
- Neighbourhood Cultivation Genetic Algorithm (NCGA)
- Non-dominated Sorting Algorithm (NSGA-II)

Simple workflow of Isight is given Figure 2-2:

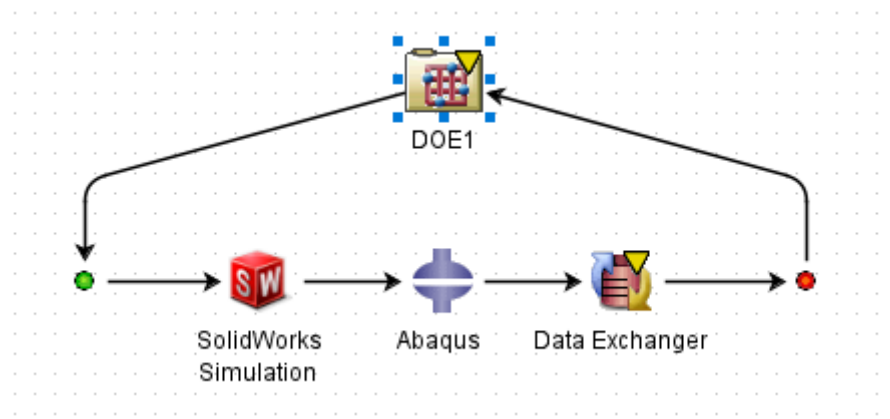


Figure 2-2. Isight Overview

It can be seen in Figure 2-2, geometrical optimization of a system requires CAD data, analysis file and a data exchanger. The geometrical data is an input for the analysis file and data exchanger exported required output. Inputs and outputs are evaluated in Design of Experiment (DOE) tool.

## 2.2 Abaqus

Abaqus FEA is a software suite for finite element analysis and computer-aided engineering. Abaqus has some packages that are specialized for different tasks [18]:

**Abaqus/CAE, (Complete Abaqus Environment)**, It is used to model and analyse a mechanical component, subsystem or system. It has embedded visualization and post-processor tools.

In addition, Abaqus/CAE including only the post-processing module can be launched independently in the Abaqus/Viewer [18].

**Abaqus/Standard**, Finite Element analyser that runs implicit modelling [18].

**Abaqus/Explicit**, Finite Element analyser that runs explicit modelling to solve highly nonlinear systems that involve complex contacts, transient loads, etc. [18].

**Abaqus/CFD**, Computational Fluid Dynamics program that able to calculate and model advanced fluid dynamic problems with extended and empowered post processing [18].

In this work, ‘Abaqus/CAE’ and ‘Abaqus/Explicit’ was used for analysis.

### **2.3 SolidWorks**

SolidWorks is a CAD program that enables to design simple or complex system. In market there are other CAD design tools but, in this work SolidWorks was preferred. There are some reasons:

- User friendly (Easy to learn)
- SolidWorks has many integrated tools and applications; such as, Abaqus, HEEDS, Matlab, ANSYS, SOLID CAM, etc. Import and export operations are made easily.
- SolidWorks enables complex motion analysis.
- Rendering properties are realistic.
- Complex surfaces can be designed and their patterns can be viewed.
- Cost estimation can be done is realistic and durability of the given product can be obtained.
- Easy to communicate with both Isight and Abaqus [19]

### **2.4 Conclusion**

The software was mentioned in this chapter are Abaqus, SolidWorks and Isight were evaluated that, they can co-operate with each other. Since their capabilities and performances' are compatible with each other, during the co-simulation process there should not be any problems regarding software.

### 3. SIMPLE CRANK SLIDER MECHANISM ANALYSIS

#### 3.1 Introduction

In this thesis, a slider-crank that is similar to piston crankshaft was investigated. To understand the mechanism dynamics and optimization techniques, a simple model was built at the beginning of the analysis process.

Furthermore, the construction of a simple model helps to understand Isight, Abaqus and SolidWorks tools and their communication in co-simulation. One of the reasons behind constructing the simple model is that analysis of the realistic crank-slider model analysis in Abaqus requires so much time and if there is an error in the Isight model, the whole process will start over and giving no exact solution. This causes enormous computational time loss. Hence, because of these reasons, it was decided that a simple crank slider mechanism model was built in the first place.

#### 3.2 SolidWorks Model

In SolidWorks part model option, three-part were modelled.

First one is representative piston/slider:

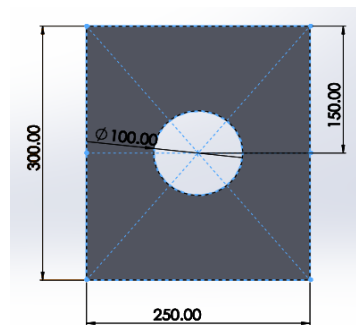


Figure 3-1. Slider Part

Table 3-1. Slider Geometrical Properties

Geometrical Feature	Dimension (mm)
Width	250
Length	300
Depth	100
Hole Diameter	100

Second one is connecting rod/coupler link:

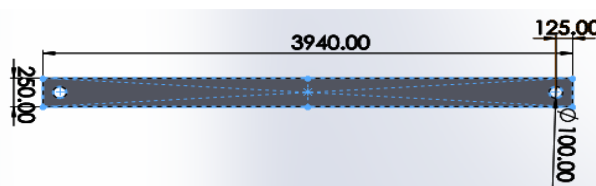


Figure 3-2. Connecting Rod

Table 3-2. Connecting Rod Geometrical Properties

Geometrical Feature	Dimension (mm)
Width	250
Length	3940
Depth	100
Hole Diameter	100

Third one is crank/slider:

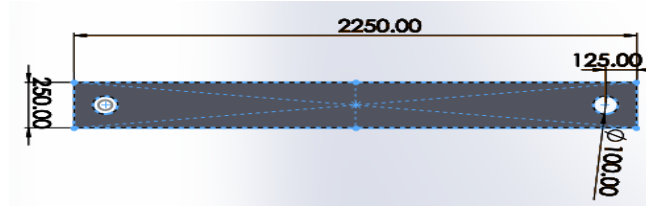


Figure 3-3. Crank

Table 3-3. Crank Geometrical Properties

Geometrical Feature	Dimension (mm)
Width	250
Length	2250
Depth	100
Hole Diameter	100

Isometric view of assembly is displayed in Figure 3-4:

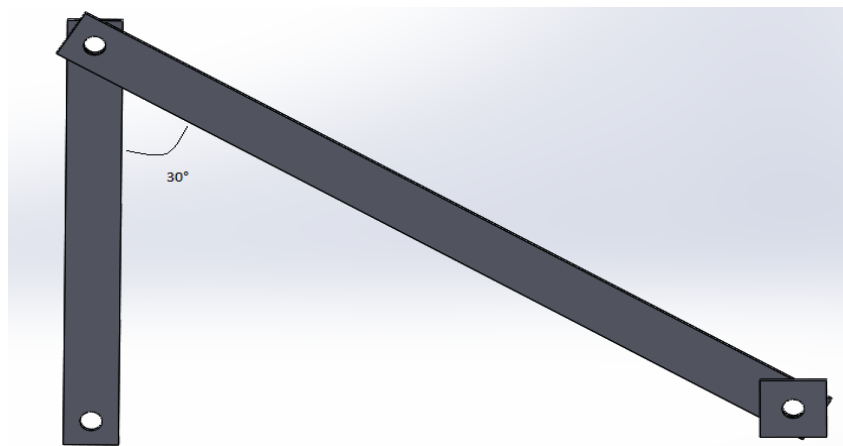


Figure 3-4. Simple Crank Slider

At start-off, the angle between crank and connecting rod is 30°.

### 3.3 Abaqus Model

Since this thesis's interests both modal analysis and dynamic response of the system, two different separated models were constructed for each analysis.

#### 3.3.1 Modal Analysis Model

##### 3.3.1.1 Introduction

In the Abaqus model first, the SolidWorks model is imported as a '.sat' file type. Importing the assembly rather than '.SLDASM' helps one create a python file that assists the automation process. The automation process is obligatory since the design optimization requires an autonomous analysis model.

After the model is imported as the '.sat' file, an Abaqus type assembly file should be created. However, the material is assigned as a first step in the process. In this study, steel AISI 4340 was chosen.

Required Material Properties of 4340 in given Table 3-4:

Table 3-4. Mechanical Properties of Steel

Mechanical Properties of Steel	
E/Young Modulus	$2 \times 10^9$ Pa
$\nu$ /Poison Ratio	0.3
$\rho$ /Density	7800 kg/m <sup>3</sup>

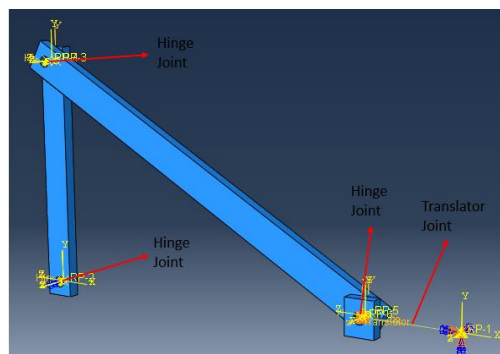


Figure 3-5. Joints on System for Modal Analysis

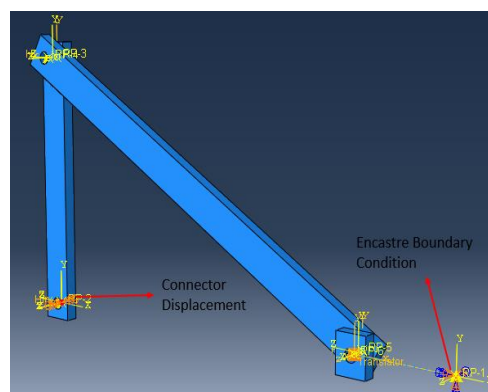


Figure 3-6. Boundary Conditions on Assembly for Modal Analysis

### 3.3.1.2 Analysis Step

In Abaqus, the modal analysis will be made for a specific angle and displacement configuration. However, in order to investigate the different configuration angle's effect on the modal analysis in the optimization part, the system should be moved and modal analysis should be made at certain angle configurations synchronized to this movement.

To create the required environment for the analysis, firstly, a static step was created and in this step, movement was provided with the connector displacement boundary condition. The external force or moment should not be used on the system for the modal analysis which is implemented after the static step and the displacement boundary condition method requires no force. Secondly, the modal analysis step was constructed and ten mode-shapes were requested as outputs.

### 3.3.1.3 Interaction and Load Step

In this section, required joints and boundary conditions are assigned. As it can be seen from the below figure, there are two types of connectors and two types of boundary conditions are defined. For rotational movement 'hinge' and for translational movement 'translator' joints are defined. The translator joint assigned between the ground and piston. To assigned the joint correctly, the encastre boundary condition was used on the point. Furthermore, connector displacement was used on the hinge joint that is located on the crank part.

In addition, for the connector displacement boundary condition, 3.4 rad was given. This boundary condition adjusted the system to its new configuration. The mechanism crank angle turns 3.4 rad and settles to its new position. Modal analysis was made in the original position and this new position. The reason, performing modal analysis twice, is to be able to compare natural frequency values in the optimization step.

### 3.3.1.4 Meshing

In the aspect of total computational time, meshing is a crucial issue. Because, if not enough seed is assigned to the parts, the analysis may give incoherent and meaningless results, if more than the required seed is assigned to the parts, this only increase the computational time. For only one analysis, analysis time increment may not be a problem. The real issue is optimization total time; small increments of total time increments have an enormous effect on the total process time.

In this case, for each part mesh assigned as it shown in Figure 3-7:

Table 3-5. Element Type and Node Number

Part	Element Type	Element	Node
Connecting Rod	C3D8R	81	224
Piston	C3D8R	237	408
Crank	C3D8R	91	248

Table 3-6. Mesh Quality Analysis

Part Name	Number of Elements	Quality
Connecting Rod	81	Analysis errors: 0 (0%), Analysis warnings: 0 (0%)
Piston	237	Analysis errors: 0 (0%), Analysis warnings: 0 (0%)
Crank	91	Analysis errors: 0 (0%), Analysis warnings: 2 (2.1978%)

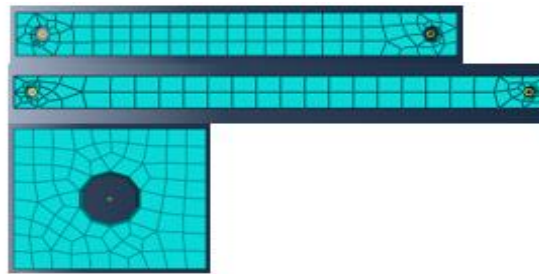


Figure 3-7. Meshed Parts

The main reason not to assign fine mesh in the system is trying to minimize the total computational time. In addition, the mesh quality is at an acceptable level.

### 3.3.1.5 Results and Conclusion

In this section, analysis job was built and run the job. After given the run for the 3.4 rad displacement boundary condition results are:

Table 3-7. Modal Analysis Results for Simple Crank Slider

MODE NO	EIGENVALUE	FREQUENCY/(RAD/TIME)	FREQUENCY/(CYCLES/TIME) Hz
1	139.77	11.823	1.8816
2	933.94	30.56	4.8638
3	4640.8	68.123	10.842
4	6517.1	80.729	12.848
5	8795.7	93.785	14.926
6	25056	158.29	25.193
7	31070	176.27	28.054
8	62432	249.86	39.767
9	79714	282.34	44.935
10	87766	296.25	47.15



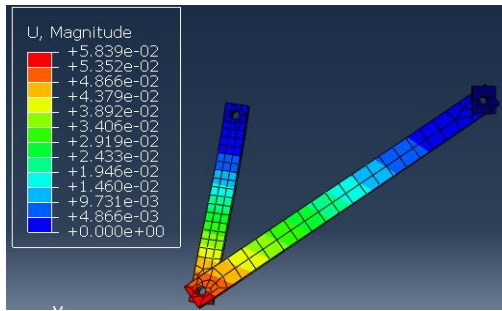


Figure 3-8. 1<sup>st</sup> Mode Shape

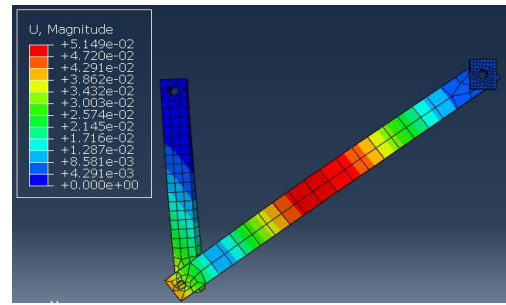


Figure 3-9. 2<sup>nd</sup> Mode Shape

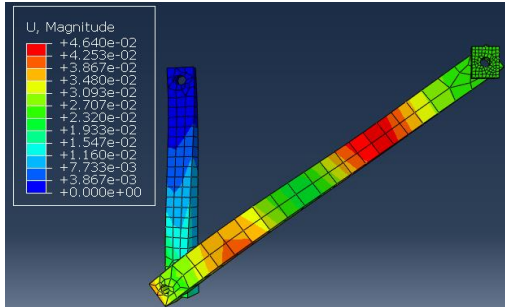


Figure 3-10. 3<sup>rd</sup> Mode Shape

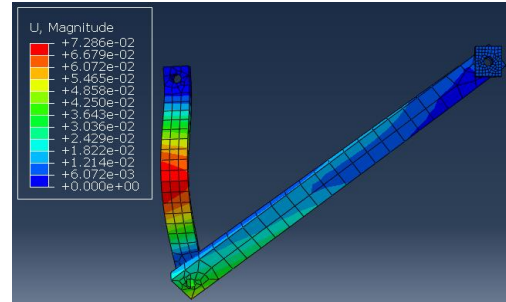


Figure 3-11. 4<sup>th</sup> Mode Shape

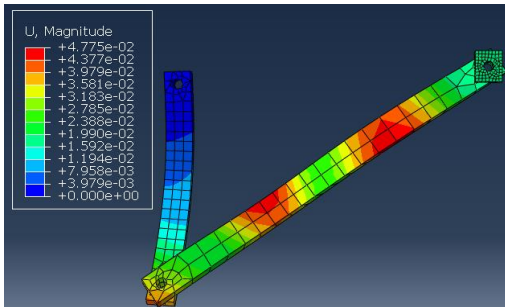


Figure 3-12. 5<sup>th</sup> Mode Shape

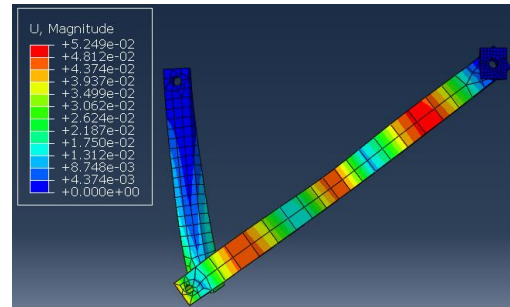


Figure 3-13. 6<sup>th</sup> Mode Shape

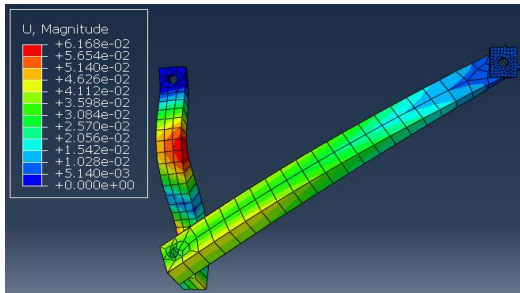


Figure 3-14. 7<sup>th</sup> Mode Shape

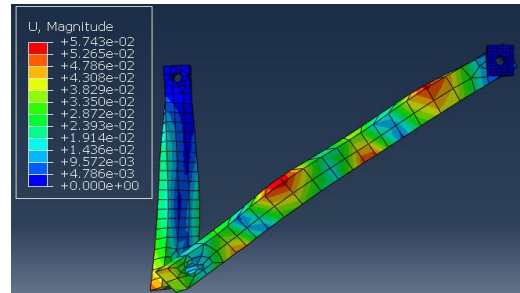


Figure 3-15. 8<sup>th</sup> Mode Shape

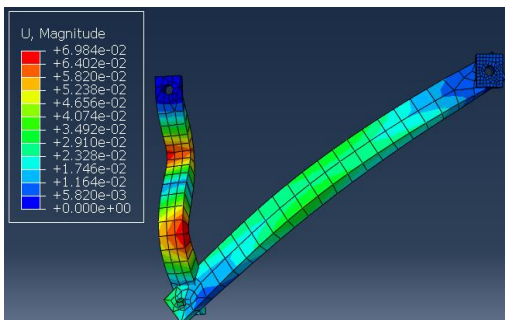


Figure 3-16. 9<sup>th</sup> Mode Shape

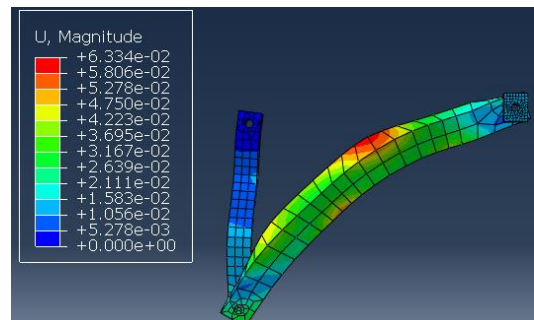


Figure 3-17. 10<sup>th</sup> Mode Shape

After the mechanism was turned 3.4 rad. assembly would be like:

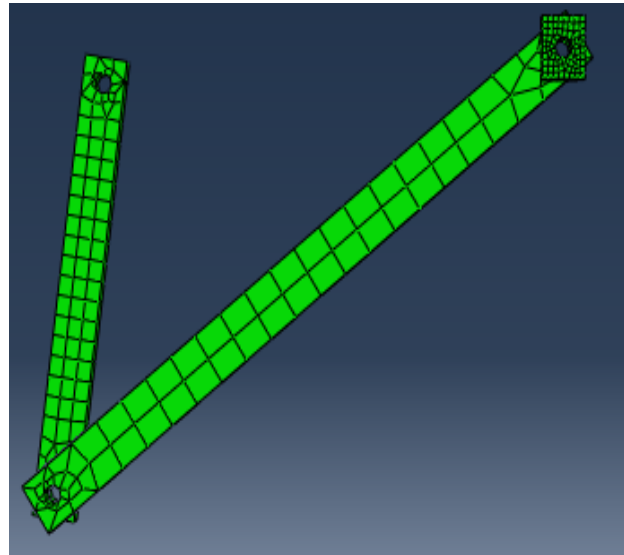


Figure 3-18. Assembly after 3.4 rad turn

Furthermore, 10 mode shape and their displacement figures are given below.

For modal analysis, all mode shapes changed due to the angle configuration changes. The change is observable in first three modal shapes. Furthermore, first three mode shape are similar to each other. The distortion increase rest of the mode shapes in certain parts. 4th, 7th and 9th mods shapes effects crank more than connecting rod, while other mode shapes have influence on the connecting rod.

### 3.3.2 Dynamic Model

#### 3.3.2.1 Introduction

In this section, the main goal is constructing a simple dynamic system that can move according to force or momentum and obtaining Von-Misses stress results for a selected zone. Furthermore, geometric parameters should be modifiable for the design optimization side. Because the main aim is finding the optimum geometry parameters for the selected zone stress value.

#### 3.3.2.2 Analysis Step

In this section, 'Dynamic-Explicit' option was selected as step type.

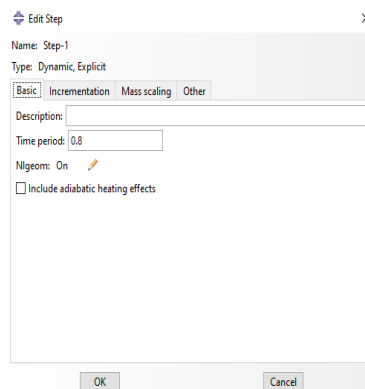


Figure 3-19. Step Definition of Dynamic Explicit Analysis

Table 3-9 shows the setting for dynamic explicit analysis. The time period of dynamic explicit analysis was set to 0.8 second. Nonlinear geometry was set to on.

### 3.3.2.3 Interaction and Load Step

Since the mechanism must move according to force, the same joints were applied as it was used in 'Modal Analysis': Hinge and Translator Joints. However, only one boundary condition which was the encastre type was sufficient for this case. Encastre boundary condition was assigned between the crank and the ground. In addition, the displacement boundary condition is unnecessary for this case since the continuous movement of the assembly is required. In order to accomplish movement, the hinge joint on the crank provided the necessary freedom.

This analysis requires external force. Since the idea of building this model is the representing the real crank-shaft mechanism, the force is applied on the edge points of the piston itself.

The Force was applied on the 4 points and equally distributed between these points. At each point, 1000N was applied and a total of 4000N was applied to the assembly. Additionally, force was applied to the global 'x' coordinate.

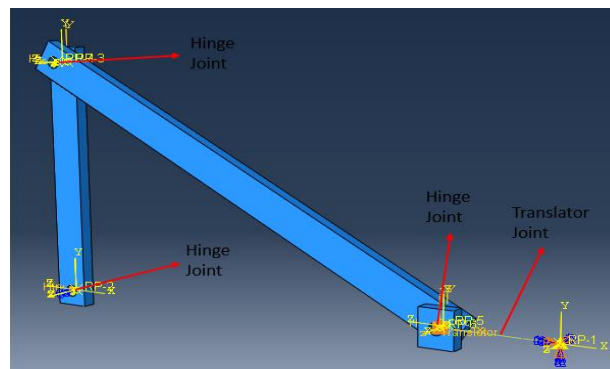


Figure 3-20. Joints on Assembly for Dynamic Explicit Analysis

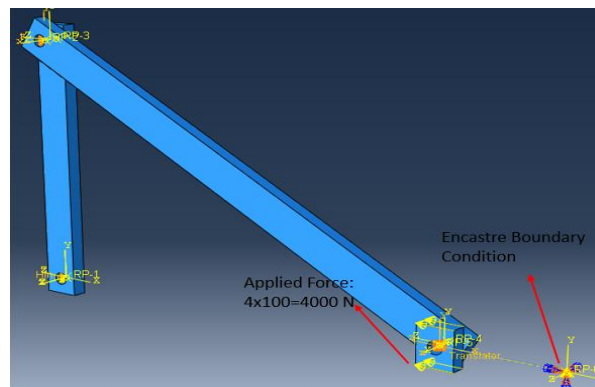


Figure 3-21. Force and Boundary Conditions on Assembly for Dynamic Explicit Analysis

### 3.3.2.4 Meshing

The same number of meshes were discarded as in the 'Modal Analysis Model'. If the mesh was made finer than earlier analysis, the analysis would take more computational time; on the other hand, if the meshes were assigned coarse, the results are incoherent or meaningless.

Table 3-8. Element Type and Node Number

Part	Element Type	Element	Node
Connecting Rod	C3D8R	81	224
Piston	C3D8R	237	408
Crank	C3D8R	91	248

In Table 3-8, parts and their element types, element and node numbers are given.

### 3.3.2.5 Results and Conclusion

In this section, an analysis job whose time step 0.8s was created and run.

Displacement and Stress values at the end of the analysis are given below figures.

From the below figures, as it can be seen maximum stress occurs at the crank ground connection zone and stress concentration occurs in this area. The connection rod is the most deflected part as predicted. The increment of the length of a body makes deflection more perceivable. Also, the crank ground connection has been exposed the torque that the system produced, so it is experienced more stress in other locations.

From stress figures Von Misses stress at the beginning of the analysis, approximately  $10^3$  Pa values however at the end of the analysis it reaches  $10^5$  stage. It is reasonable since at the end of the analysis system moves its maximum position and momentum effects apparent. The same rationale is applied to the displacement figures.

Maximum displacement and stress occurred at 0.8 s which is end of the analysis, Figure 3-22 and Figure 3-23 are given below:

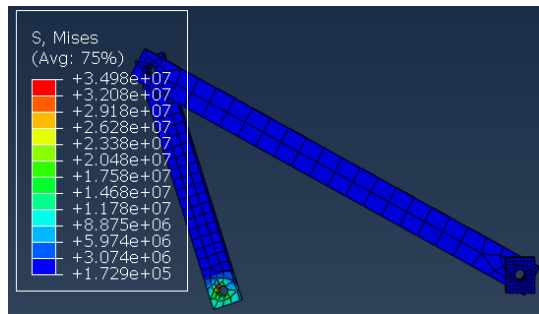


Figure 3-22. Maximum Stress at the End of the Analysis

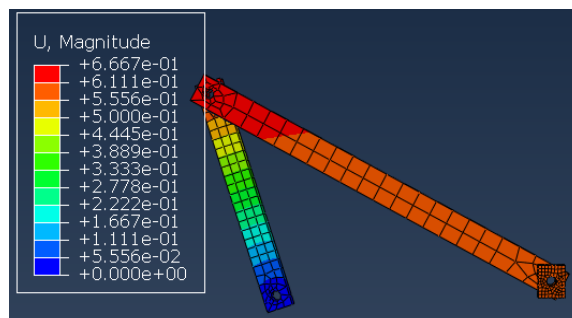


Figure 3-23. Maximum Displacement at the End of the Analysis

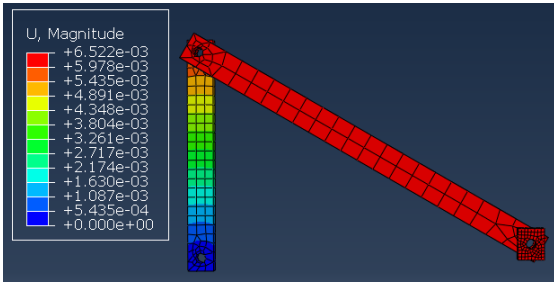


Figure 3-24. Displacement at 0.08 s

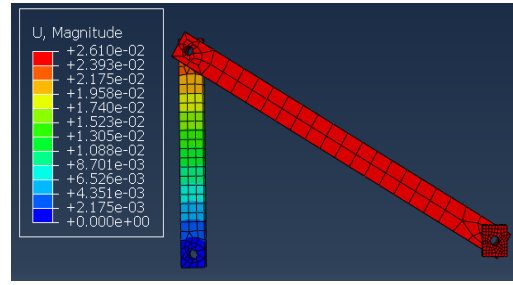


Figure 3-25. Displacement at 0.16 s

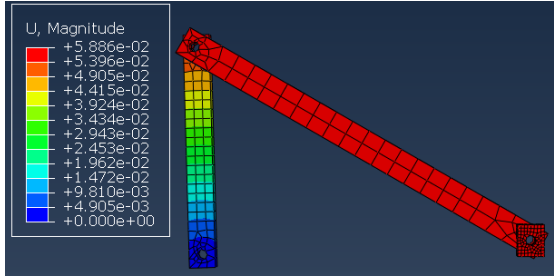


Figure 3-26. Displacement at 0.24 s

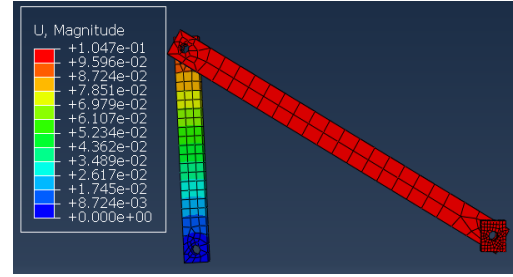


Figure 3-27. Displacement at 0.32 s

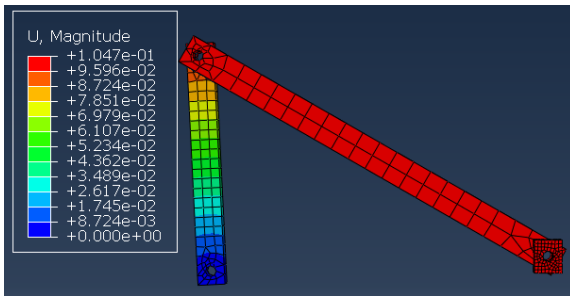


Figure 3-28. Displacement at 0.40 s

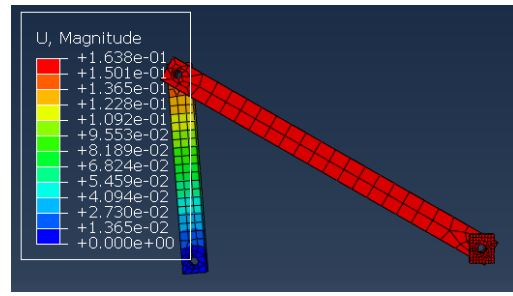


Figure 3-29. Displacement at 0.48 s

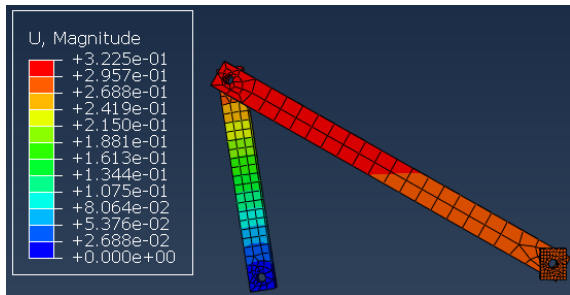


Figure 3-30. Displacement at 0.56 s

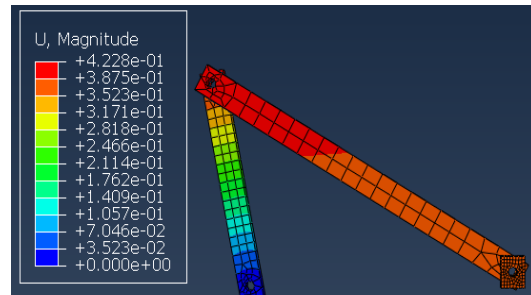


Figure 3-31. Displacement at 0.64 s

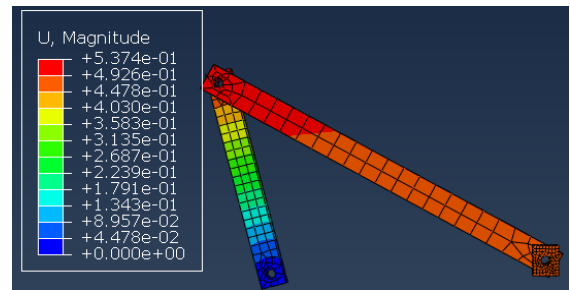


Figure 3-32. Displacement at 0.72 s

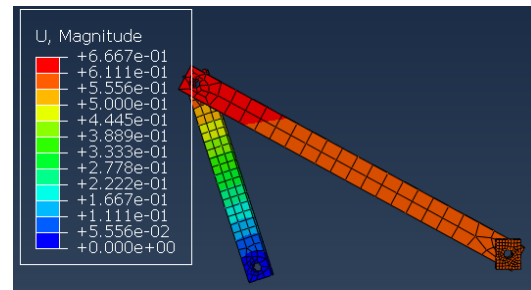


Figure 3-33. Displacement at 0.80 s

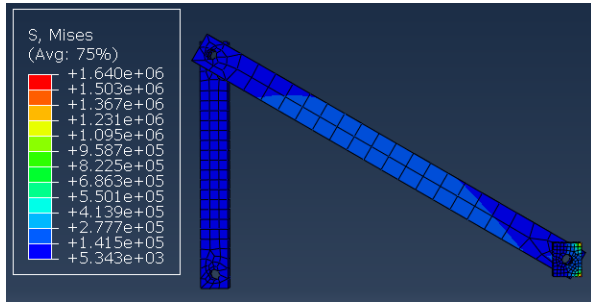


Figure 3-34. Stress at 0.08 s

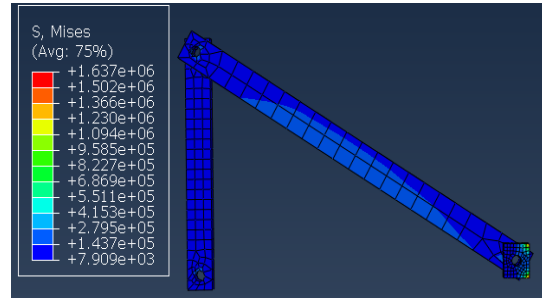


Figure 3-35. Stress at 0.16 s

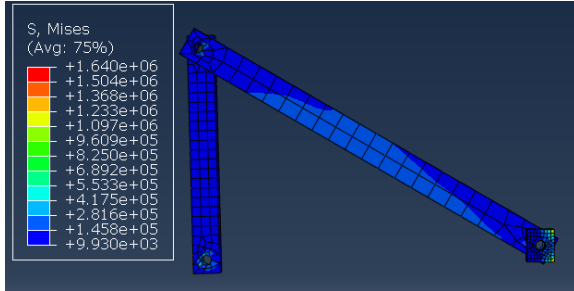


Figure 3-36. Stress at 0.24 s

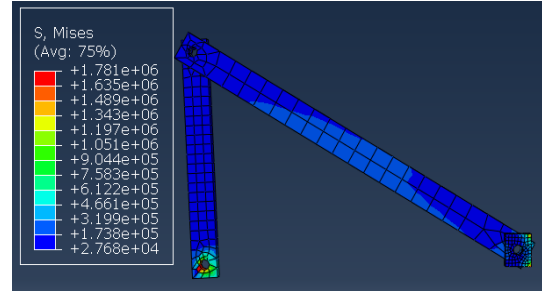


Figure 3-37. Stress at 0.32 s

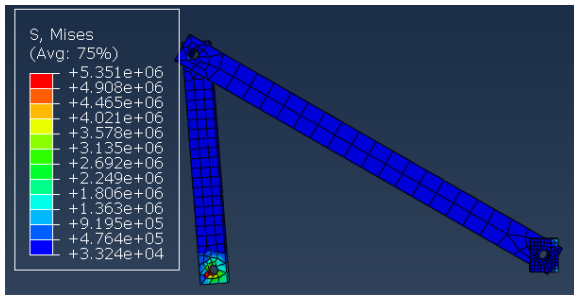


Figure 3-38. Stress at 0.40 s

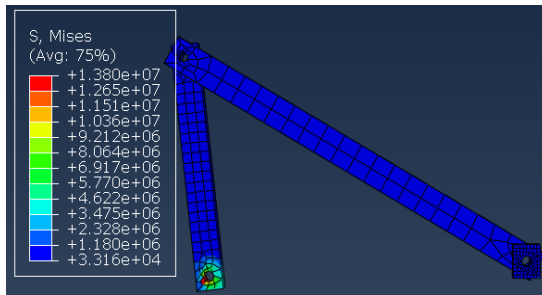


Figure 3-39. Stress at 0.48 s

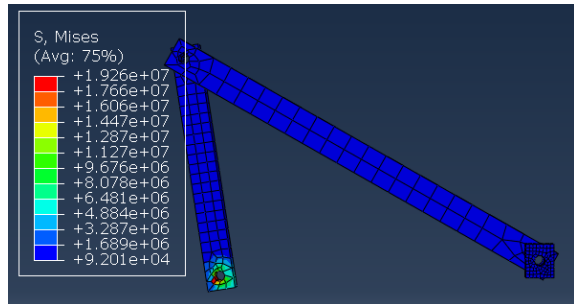


Figure 3-40. Stress at 0.56 s

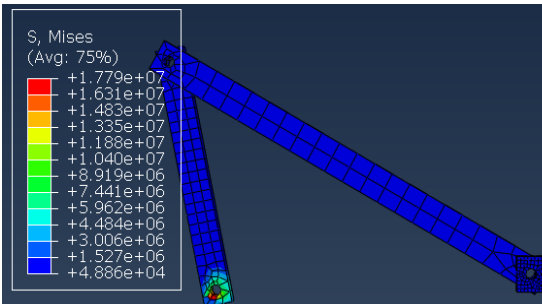


Figure 3-41. Stress at 0.64 s

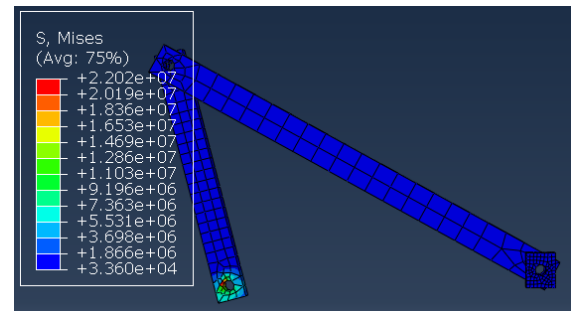


Figure 3-42. Stress at 0.72 s

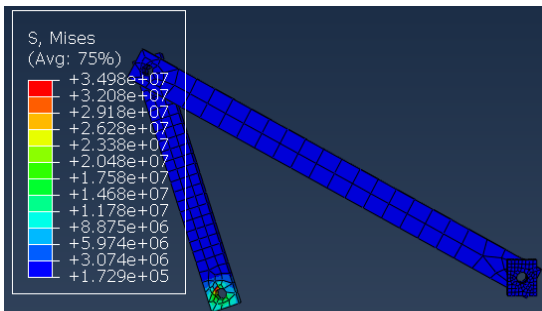


Figure 3-43. Stress at 0.80 s

### 3.4 Isight Model

In the Isight model, the goal is to create a multi-model that access both ‘Modal Analysis’ and ‘Dynamic Explicit’ models, running them and extracting the solutions. The extracted solutions served as inputs for constructing the design solutions.

#### 3.4.1 General Overview of Model

General overview of Isight model is given in Figure 3-44:

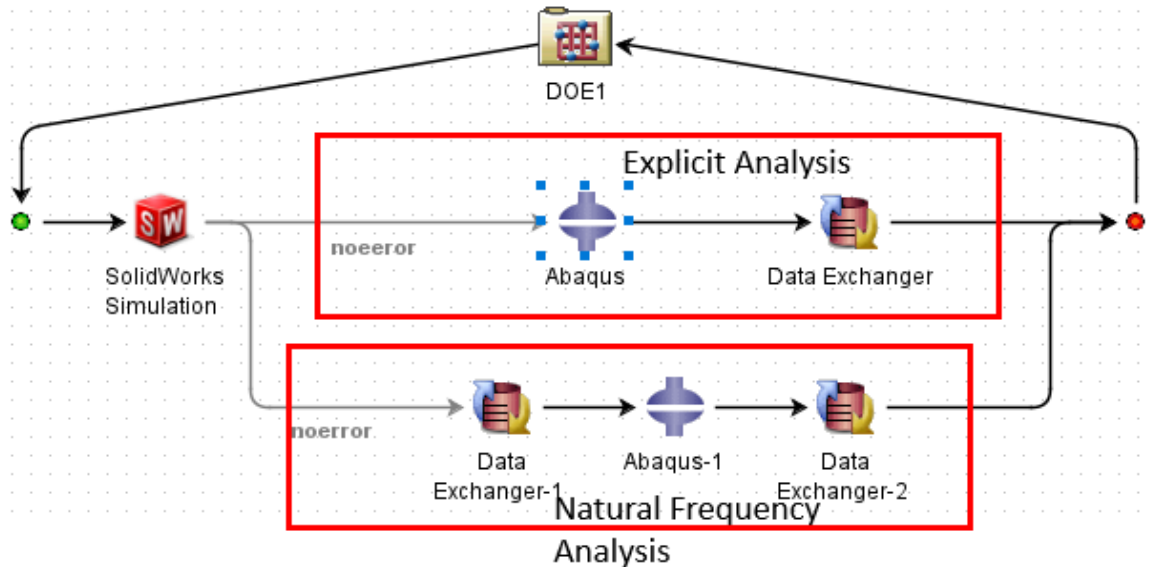


Figure 3-44. General Overview of Isight Model

As it can be seen there are 2 analysis workflow: Dynamic Explicit and Modal Analysis.

Since these models use the same SolidWorks model, both of the workflows is fed by the same SolidWorks Model.

For Explicit Workflow, first Abaqus imports the SolidWorks via Python Code macro. Python process the ‘.SAT’ file and starts to construct the model and run the job. This action reproduces the initial Abaqus Explicit Model. It builds the same explicit analysis. After the analysis job is finished in the Abaqus component, the ‘Data Exchanger’ component extracts the solution from the ‘Abaqus .odb’ file. The solution then is sent to the ‘Design of Experiment’ component.

For Modal Analysis Workflow, the Data Exchanger component procures the ‘connector displacement’ value from a ‘.csv’ file. It is processed via python and implemented as a connector displacement value. To enable successfully obtain and change the connector displacement ‘.csv’ file is required, since, in python code that generates the Abaqus model does not allow the change connector displacement. To be more specific, it is reachable in the Abaqus component. However, in every analysis step, python code runs and change the parameter it's the initial value. To overcome this issue, an extra Data Exchanger and ‘.csv’ file were used. After running the Modal Analysis Model, the second data Exchanger works and extract the results from the ‘Abaqus .dat’ file The solution then is sent to the ‘Design of Experiment’ component.

### 3.4.2 Design Inputs Selection

SolidWorks provides the main input option, which is the geometry of the model. In the Isight SolidWorks component, the whole design parameter can be accessible and can be selected as input from Isight Model (Figure 3-45).

In this case, only the width of the connecting rod was selected as a design parameter for both Modal Analysis and Dynamic Explicit model (Figure 3-45).

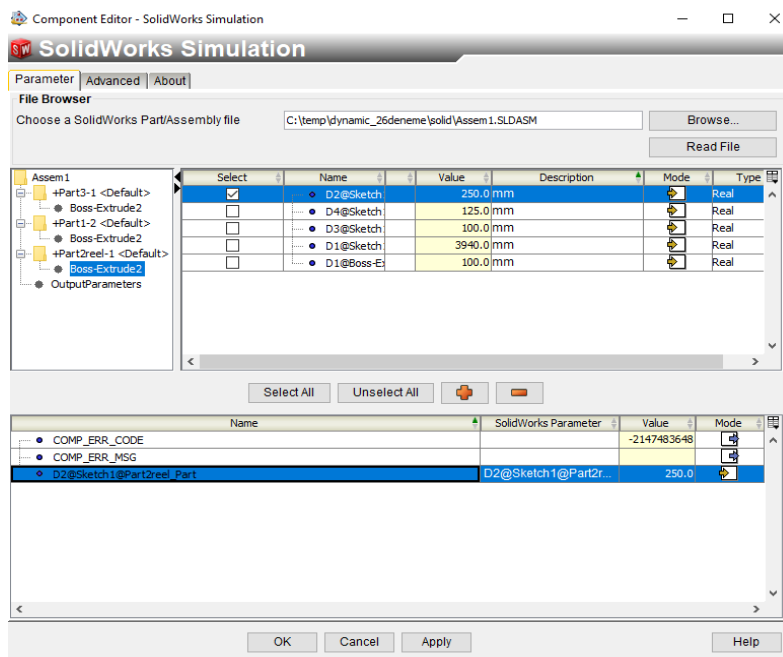


Figure 3-45. SolidWorks Input Selection

Moreover, for the Modal Analysis section, displacement of the boundary condition was required as input and it was imported from the '.csv' file. This input is procured via the Data Exchanger component.

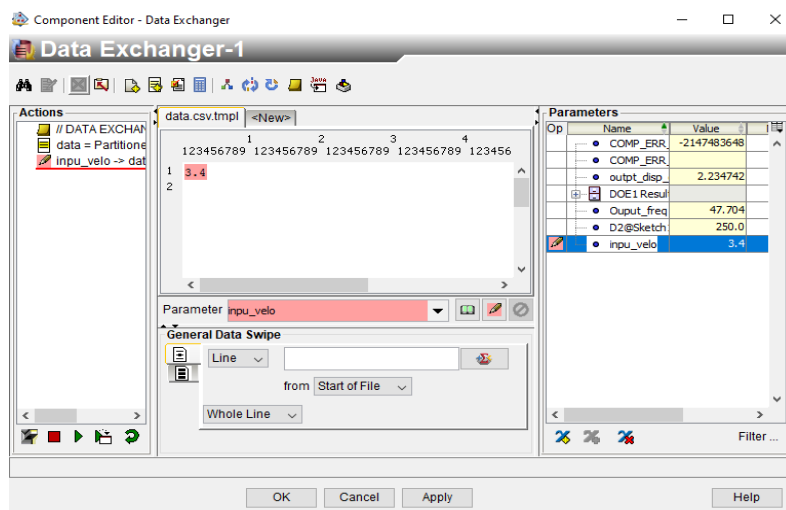


Figure 3-46. Data Exchanger Input Selection for the Displacement Boundary Condition

In Figure 3-46 displacement of boundary condition for Abaqus Modal Analysis is imported from a '.csv' file via Data Exchanger Isight component. This is crucial for working properly Python Code Automation.



### 3.4.3 Output Selection

To be able to obtain meaningful output from explicit dynamic analysis, firstly a preselected area during the initial Abaqus modelling, and with help of python extracted the '.odb' file results into a text file format. In this case, the hole that is between connecting rod and piston (connecting rod side) was selected as the result data investigated zone.

The extraction of the solution via python is made because any geometrical change affects the mesh number with the result table. This issue causes obstruction for the extraction of the output. Because, Abaqus selects the geometry with their node numbers and record them in python specific numbers, but since the node numbers change in every design iteration, these specific numbers in python cannot match the new numbers with the old ones. In order to overcome this issue, a python code was written which is enable to read the node numbers that are on the selected area and reach stress and displacement values without the effects of node number changes.

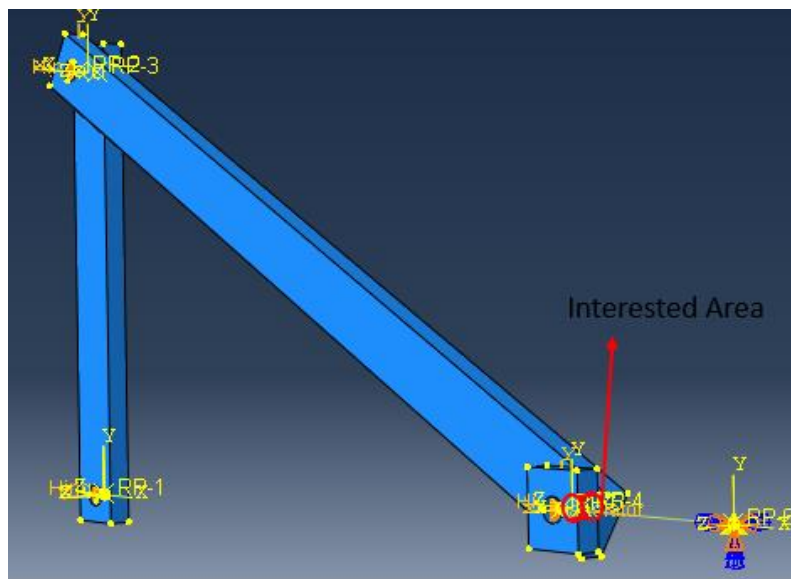


Figure 3-47. Von Misses Stress Interested Area on Simple Crank Mechanism

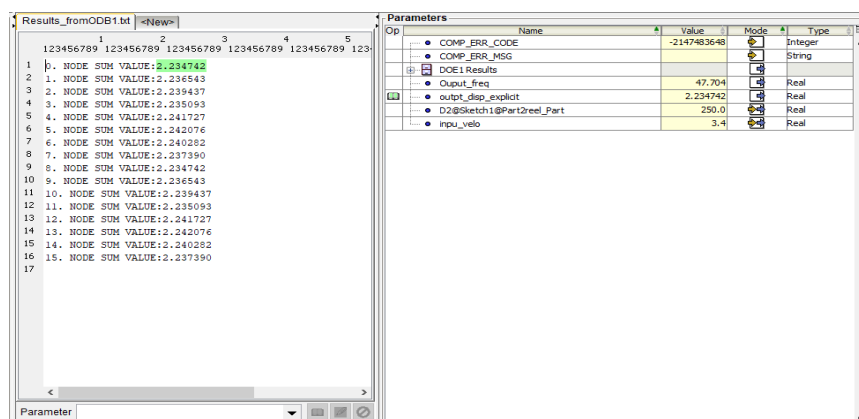


Figure 3-48. Output for Explicit Model

In the selected area there are 15 nodes for the initial design, however, this will be changed as long as the geometry changes. Yet, Python code reads all of the nodes in the selected area without the node number restriction as it was shown in Figure 3-48.

In Figure 3-48, all the node counts are shown independently from Abaqus annotation and this demonstration can be changed at every iteration of the DOE analysis. This is important to be independent of the initial Abaqus Explicit Analysis.

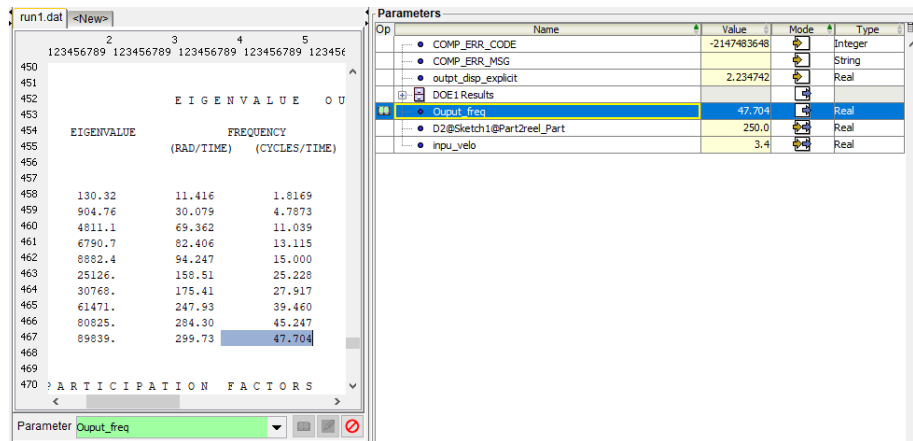


Figure 3-49. Output for Modal Analysis Model

In Figure 3-49, Modal Analysis output selection. 10<sup>th</sup> eigenvalue of the system was selected as the investigated eigenvalue. The main reason is beside the last five eigenvalues, the first eigenvalues are less confronted in real life slider-crank. Furthermore, since the 10<sup>th</sup> eigenvalue is the biggest among the others, the effect of the change of the Design Optimization Component (DOE) make it observable.

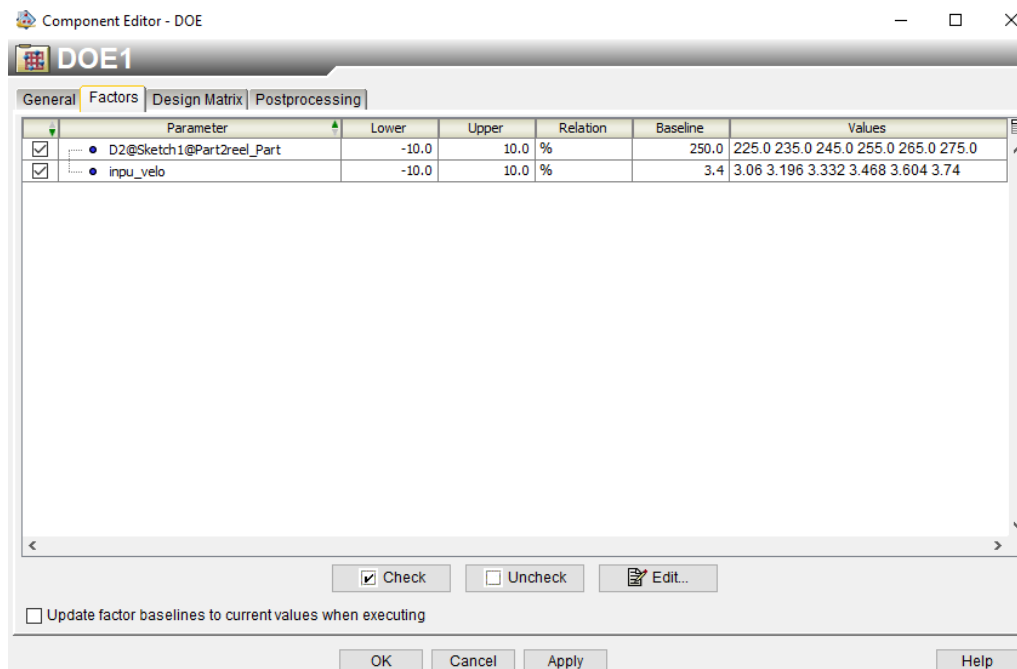


Figure 3-50. DOE Input Variations from DOE Component

### 3.4.4 Design of Experiment

In this case 'Design of the Experiment' was selected as an optimization technique:

In 'Design of Experiment', the number of levels for each factor is equal to a number of points with random combinations.

- **Advantages:**

Allows as many as possible points and more combinations can be studied for each factor. It gives the freedom to select the number of designs to run as long as it is greater than the number of factors.

- **Disadvantages:**

They are not reproducible unless the same random seed is used consecutively. As the number of points decreases, the chance of missing some regions of the design space increases.

The selected design inputs will be evaluated  $\pm 10\%$  based on their initial values.

In Figure 3-50 and Table 3-9 geometrical input and displacement values for every iteration in DOE is given.

Table 3-9. Geometrical and Displacement Input Table

Run#	Length of Connecting Rod	Displacement Input (Rad)
1	225	3.06
2	235	3.196
3	245	3.468
4	255	3.332
5	265	3.74
6	275	3.604

Moreover, outputs that come from Abaqus results were weighted equally and it is 0.5 (Figure 3-51). The objective of the DOE is to minimize the initial values of the 10<sup>th</sup> Modal Shape and Displacement of Investigated Zone.

In Figure 3-52, it can be observable the relation between the input component and output component.

### 3.4.5 Results and Conclusion

According to Analysis results, the best option of geometry and connector displacement is 2<sup>nd</sup> design. It gives for natural frequency 35 Hz and for explicit analysis 2.51799 mm in displacement.

Output frequency and iteration number changes are given in Figure 3-53.

As it can be seen from the Figure 3-54 and Figure 3-55, although, the natural frequency value holds one of the best optimum values, the displacement value fitted one of the bigger results. There are in total 6 designs and DOE choose the 2<sup>nd</sup> design as the best optimum design. From

the perspective of displacement value, it is not the best design, it is selected because its weighted function is equal to Mode Shape values'. The digits of both output responses values are not equal and there is a difference. Hence, the modal analysis results should be more dominant in the design optimization process. In Figure 3-54 and Figure 3-55, it can be seen.

Furthermore, changing the displacement of the boundary condition and readjusting the configuration of the system is more effective than the geometrical change. Since the configuration adjusts the momentum effect, this is reasonable for both analysis types. Following, building necessary relations between components, the Isight relation configuration is given in Figure 3-52. Moreover, changing the configuration of the system affect the stiffness matrix which directly influences the eigenvalue.

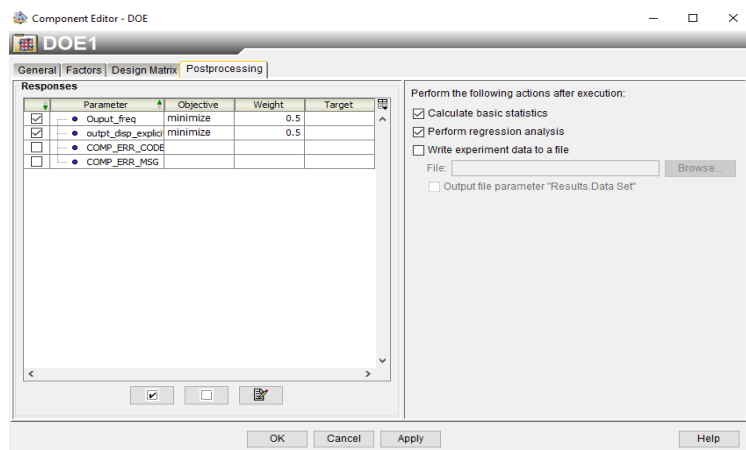


Figure 3-51. Outputs of DOE Weight Function

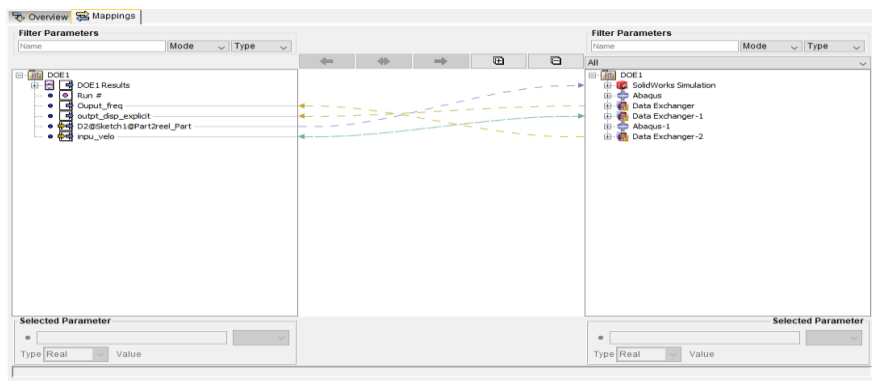


Figure 3-52. Mapping the Inputs and Outputs

Run Path		Parameters for all iterations (Done)			
		D2@Sketch1@Part2reel_Part	input_velo	Output_freq	outpt_disp_explicit
1	1	225.0	3.468	35.084	2.548825
1	2	255.0	3.604	35.1	2.517977
1	3	245.0	3.06	57.707	2.395762
1	4	255.0	3.74	53.167	2.375919
1	5	265.0	3.332	49.487	2.297653
1	6	275.0	3.196	47.704	2.234742

Figure 3-53. Result of DOE

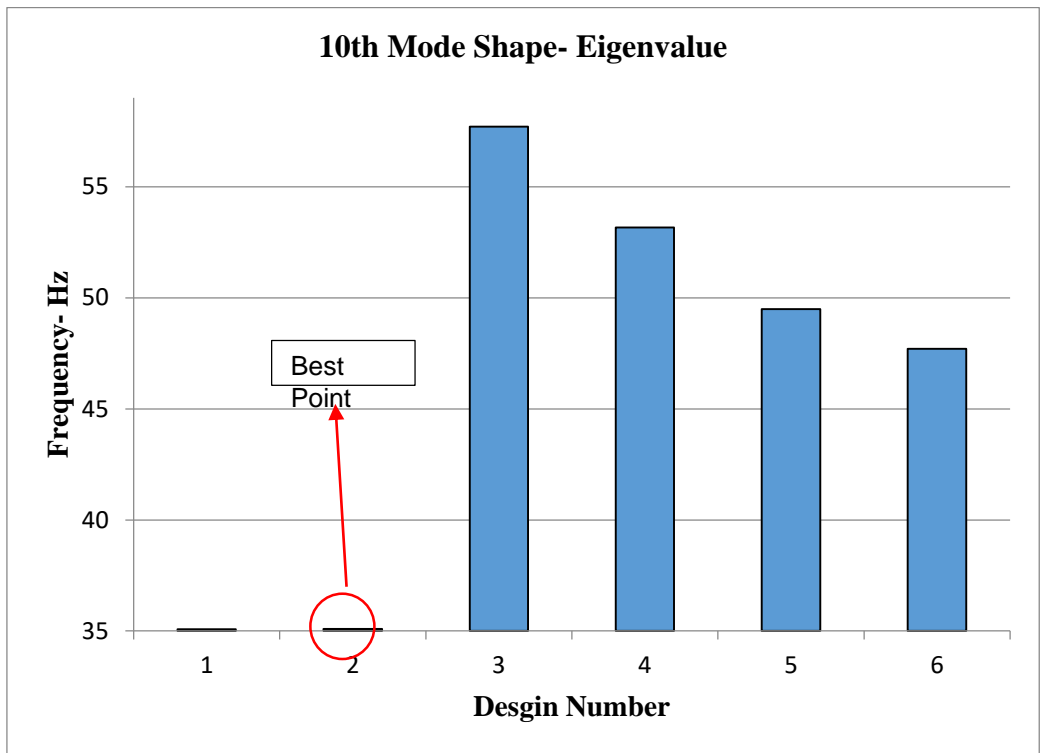


Figure 3-54. Mode Shape and Design Number in DOE Analysis

Investigated zone displacement and design number changes are given in Figure 3-55:



Figure 3-55. Displacement and Design Number in DOE Analysis

The correlation table of input and output variables are given in Figure 3-56. From this table, the effect of each input on each output can be seen exclusively.

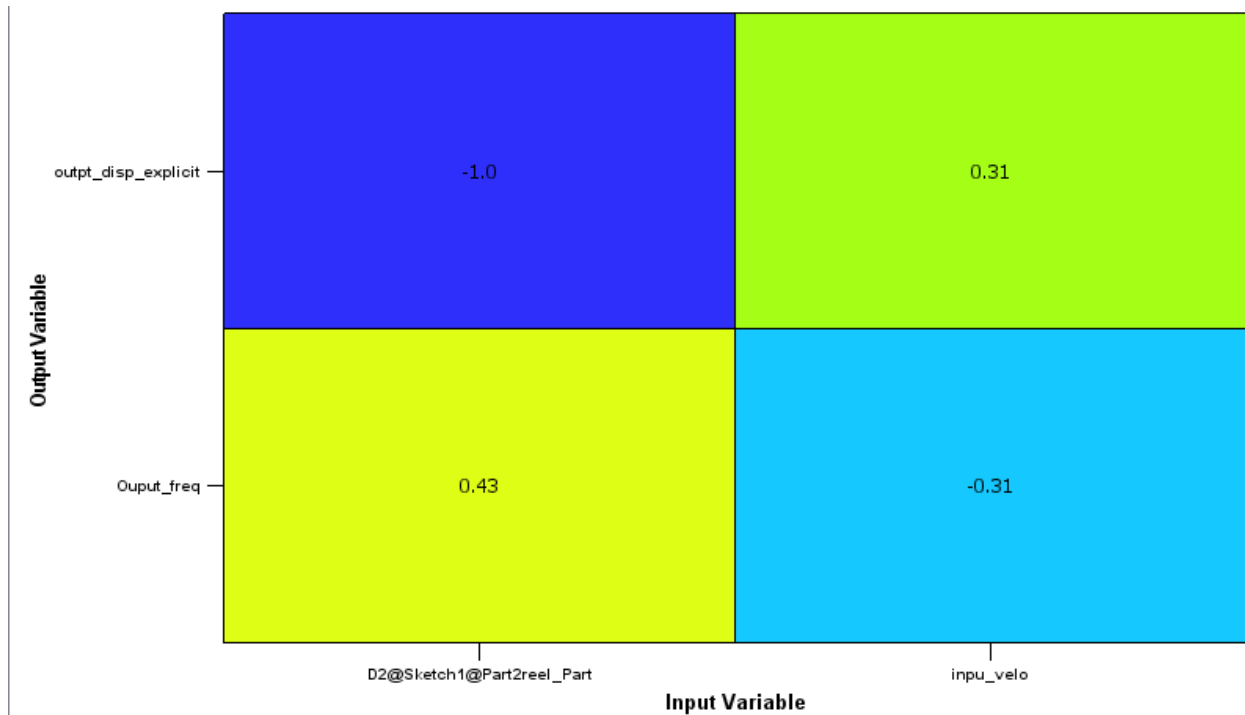


Figure 3-56. Correlation of Input and Output

From the figure given below every input and outputs relation can be investigated as continuous graph.

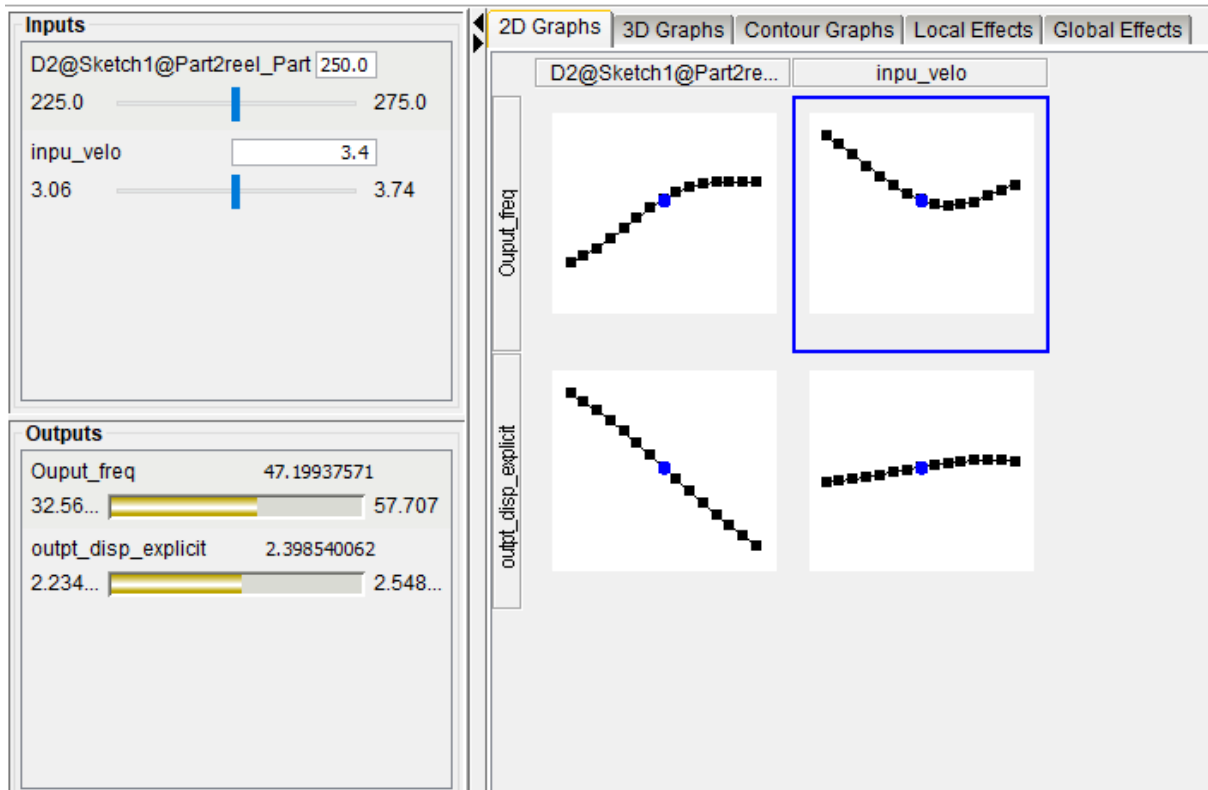


Figure 3-57. Every Input's effect on Outputs

## 4. SCALED SLIDER CRANK MECHANISM ANALYSIS

### 4.1 Introduction

In this part of the thesis, a scaled and more realistic slider-crank was investigated.

In this part of the thesis, stress analysis was separated from the explicit analysis. Performing these analyses together requires so much computational force and time. Also, when there is a change that needs to be made, the process becomes harder to accomplish. Since all the inputs are related to each other and taking results causes enormous time. In order to eliminate this issue, an explicit analysis was made with rigid bodies and obtaining acceleration values from them. After then, the static analysis was performed and accelerations were implemented on the system.

### 4.2 SolidWorks Model

In order to create consistent analysis, CAD data must be simple and easily understandable. The simple crank slider mechanism was modelled in SolidWorks and it was assembled based on some geometrical constraints.

The model was given below:

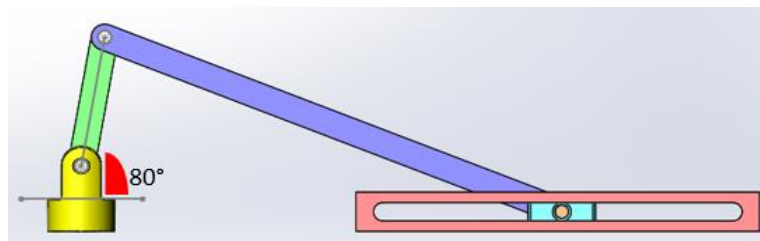


Figure 4-1. General View of Crank Slider

As it can be seen from Figure 4-1, it is established from five parts.

The first one is piston/slider:

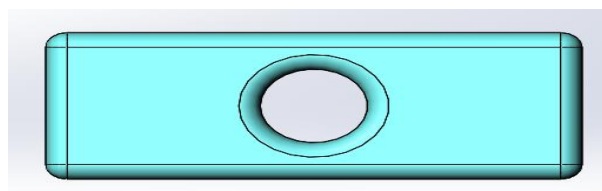


Figure 4-2. Slider/Piston

Table 4-1. Slider Geometrical Properties

Geometrical Feature	Dimension (mm)
Width	20
Length	50
Depth	20
Hole Diameter	10



The second one is slider fitting /slider road:



Figure 4-3. Slider Fitting -Slider Road

Table 5-2.

Table 4-2. Slider Fitting Geometrical Properties

Geometrical Feature	Dimension (mm)
Width	30
Length	300
Depth	30
Inner Cut Length	260

The third one is connecting rod:



Figure 4-4. Connecting Rod

Table 4-3. Connecting Rod Geometrical Properties

Geometrical Feature	Dimension (mm)
Width	10
Length	350
Depth	20
Hole Diameter	10

The fourth one is crank arm:



Figure 4-5. Crank Arm

Table 5-4.  
Table 4-4. Crank Arm Geometrical Properties

Geometrical Feature	Dimension (mm)
Width	10
Length	100
Depth	20
Hole Diameter	10

The fifth one is crank arm fitting:

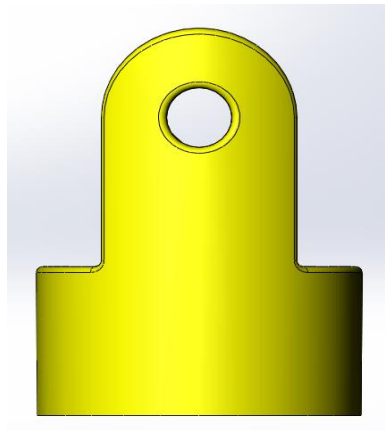


Figure 4-6. Crank Arm Fitting

Table 4-5. Crank Arm Fitting Geometrical Properties

Geometrical Feature	Dimension (mm)
Depth	50
Center Diameter	50
Hole Diameter	10

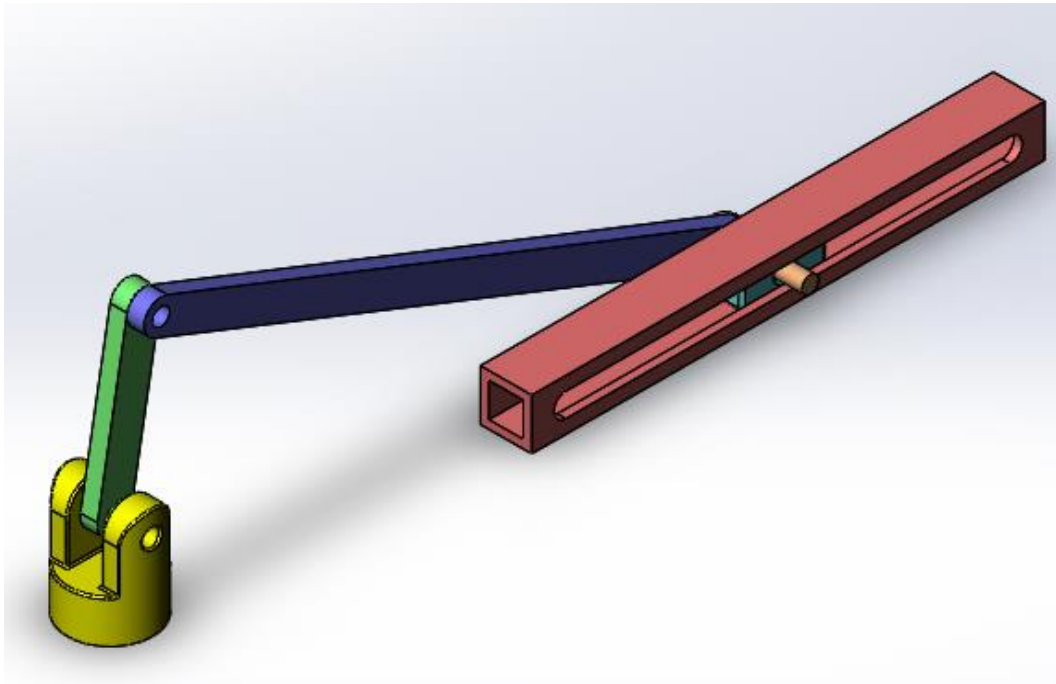


Figure 4-7. Simple Slider Crank Isometric View

Isometric view of assembly is displayed in. At start-off, the angle between crank and connecting rod is  $80^\circ$ .

### 4.3 Abaqus Model

Since this thesis interests in both modal analysis and dynamic response of the system, two different separated models should be constructed. However, for dynamic model, using only explicit analysis is not effective due to the analysis total time enormously large. In order to avoid large analysis time, firstly explicit analysis was modelled as a rigid body and obtained the acceleration values from the selected time step. After that, these acceleration values were imported from static model and implemented as force input. The analysis was run and obtained the stress values for the selected area.

#### 4.3.1 Modal Analysis Model

##### 4.3.1.1 Introduction

In the Abaqus model first, the SolidWorks model is imported a '.sat' file type. Importing the assembly as a '.sat' file rather than '.SLDASM' helps one create a python file that assists the automation process. The whole process must be automated in order to construct the design optimization correctly.

In this study, steel AISI 4340 was chosen. Required Material Properties of 4340:

Table 5-6. Mechanical Properties of Steel  
Mechanical Properties of Steel

E/Young Modulus	$2 \times 10^9$ Pa
$\nu$ /Poison Ratio	0.3
$\rho$ /Density	7800 kg/m <sup>3</sup>

### 4.3.1.2 Analysis Step

In Abaqus, in order to create modal analysis steps mechanism should be in a static position, additionally, mechanical movement should be made at the same time. To be more specific, the mechanism should move according to its regular motion and in some points, the modal analysis should be made. Modal Analysis Model analysis' results obtained the necessary data for the optimization process.

To create the necessary environment for the analysis, firstly in the SolidWorks modelling phase, a global variable was used as the angle between crank and crankshaft fitting. For further usage, this global variable is fed by a '.csv file, so the angle can be changed along with configuration in Isight.

In the step option Lanczos method selected as Abaqus Solver. Lanczos method works with the maximum frequency of desired or the number of eigenvalues desired. In Modal Analysis 10 eigenvalues were requested in Figure 4-8.

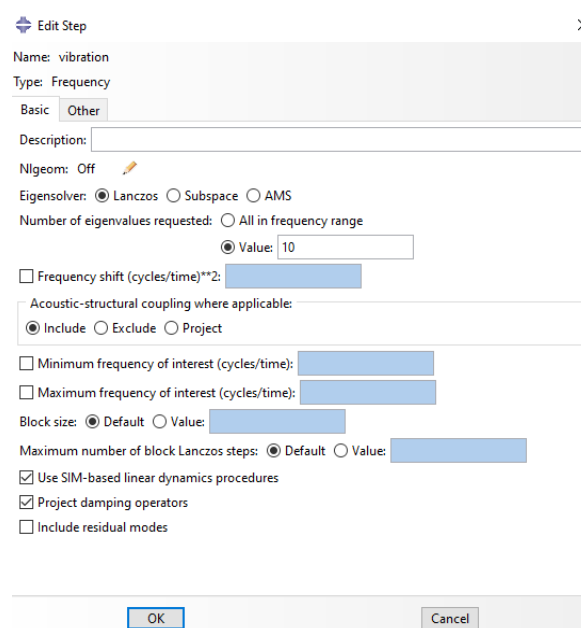


Figure 4-8. Step Definition

### 4.3.1.3 Interaction and Load Step

In this section, necessary joints and boundary conditions were assigned. As it can be seen from the Figure 4-9 and Figure 4-10, there were two types of connectors and two types of boundary conditions were defined. For rotational movement 'hinge' and for translational movement 'translator' joints were defined. The translator joint was assigned between the ground and piston. To assign correctly this hinge joint, the encastre boundary condition was used on the point where on the ground. Also, connector displacement was used on the hinge joint that was located on the crank part. Furthermore, the motion freedom in the joint locations should be restrained because if there is a motion during the process, the analysis will distort due to mechanism being unstable. In order to eliminate the uncontrollable motion, connector displacement was assigned to the hinge joint between crank and fitting, and translator between slider fitting and slider. Finally, connector displacement was assigned zero to prevent motion.

Moreover, in order to save more time some parts were modelled as rigid bodies in explicit and static analysis. This intervention was not accurate but prevent large analysis time and does not largely corrupt the modal analysis logic. And crank fitting was modelled as display body which

had no contribution to the analysis, this action eliminates the part from the equation of the system and makes it just an image in the general model. Body types are shown in Figure 4-11.

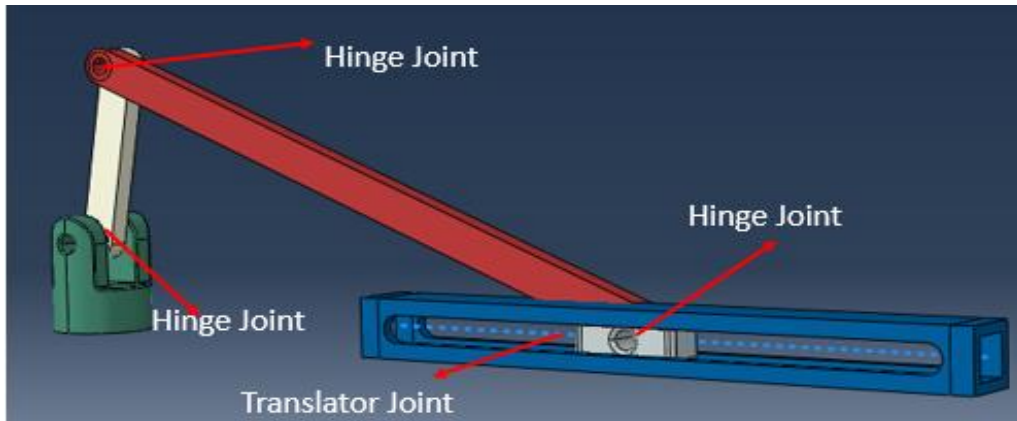


Figure 4-9. Joints on the Assembly

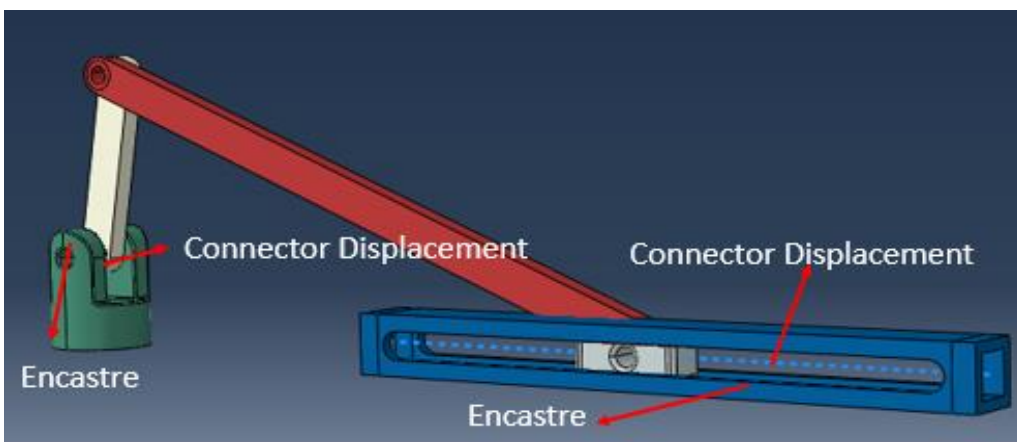


Figure 4-10. Boundary Conditions on the Assembly

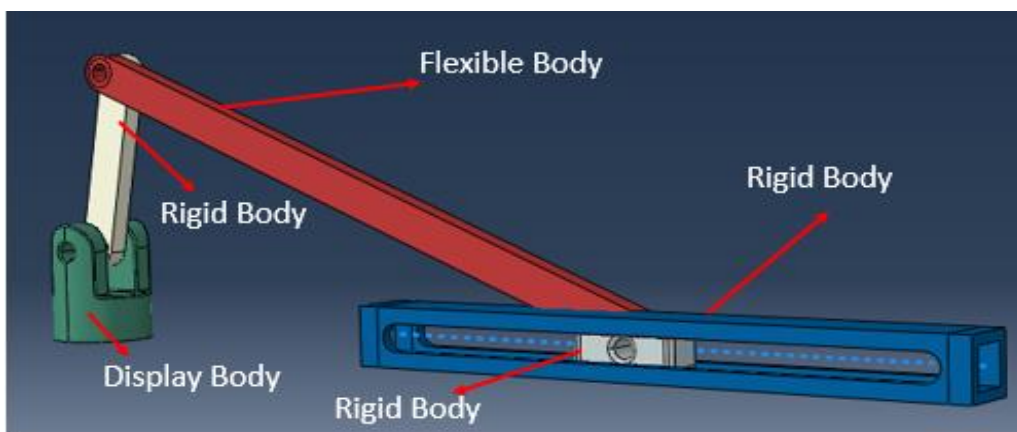


Figure 4-11. Body Type Demonstration on the Assembly

#### 4.3.1.4 Meshing

In the aspect of total computational time, meshing is a crucial issue. Because, if not enough seed is assigned to the parts, the analysis may give incoherent and meaningless results, if more than the required seed is assigned to the parts, this only increase the computational time. For

only one analysis, analysis time increment may not be a problem but since the real issue is optimization, unnecessary analysis total time increments have an enormous effect on the total process.

In this case, for each part assigned mesh are given below Figure 4-12 and Table 4-6:

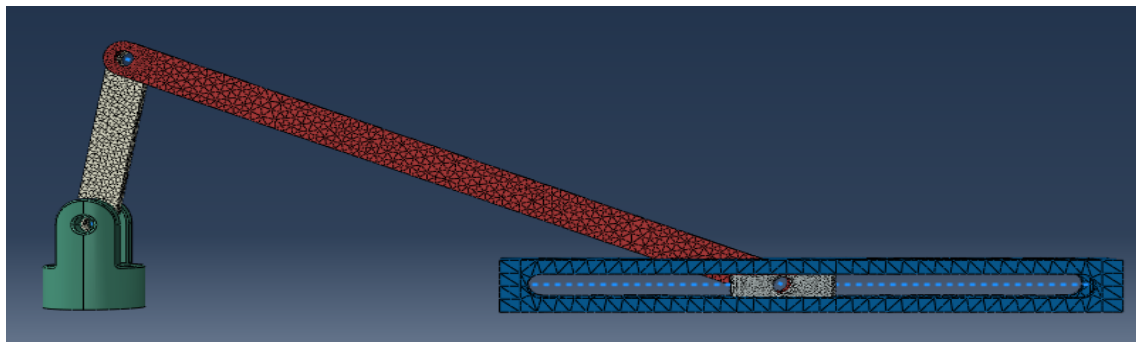


Figure 4-12. Meshed Parts

Table 4-6. Element Type and Node Number

Part	Element Type	Element	Node
Connecting Rod	C3D8R	6168	8183
Slider	C3D8R	24351	35914
Crank Arm	C3D8R	852	1324
Crank Fitting	C3D8R	2706	5806

In Table 4-7 mesh quality was investigated and there are no errors on the assigned mesh. Some errors which are no greater than %5.5 occurred, but this does not affect the analysis quality defectively. Hence, the mesh quality is acceptable.

Table 4-7. Mesh Quality Analysis

Part Name	Number of Elements	Quality
Connecting Rod	6168	Analysis errors:0 (0%), Analysis warnings: 0 (0%)
Slider	24351	Analysis errors:0 (0%), Analysis warnings: 1333 (5.47411%)
Crank	852	Analysis errors: 0 (0%), Analysis warnings: 6 (0.704225%)
Crank Fitting	2706	Analysis errors: 0 (0%), Analysis warnings: 46 (1.69993%)

#### 4.3.1.5 Results and Conclusion

In this section, an analysis job was constructed and run the analysis job. After given the run for the 80° between the crank and connecting rod, results are:

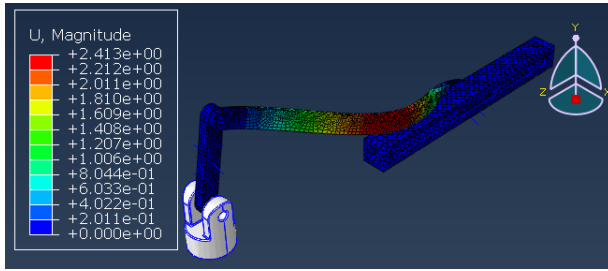


Figure 4-13. 1<sup>st</sup> Mode Shape

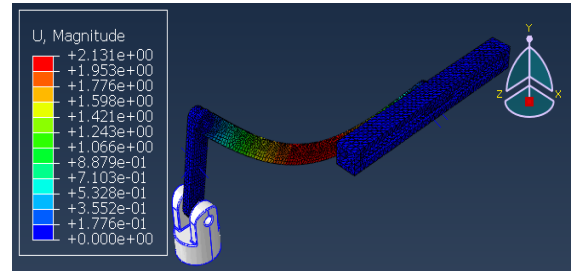


Figure 4-14. 2<sup>nd</sup> Mode Shape

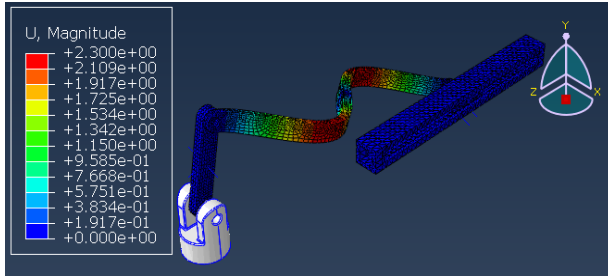


Figure 4-15. 3<sup>rd</sup> Mode Shape

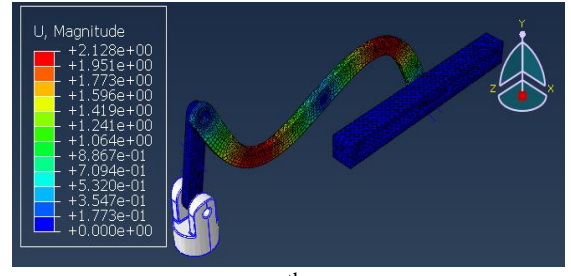


Figure 4-16. 4<sup>th</sup> Mode Shape

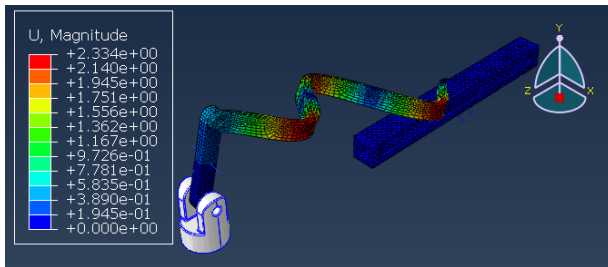


Figure 4-17. 5<sup>th</sup> Mode Shape

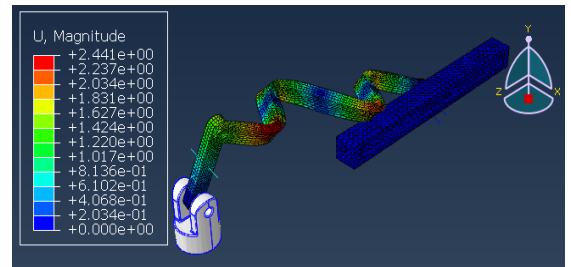


Figure 4-18. 6<sup>th</sup> Mode Shape

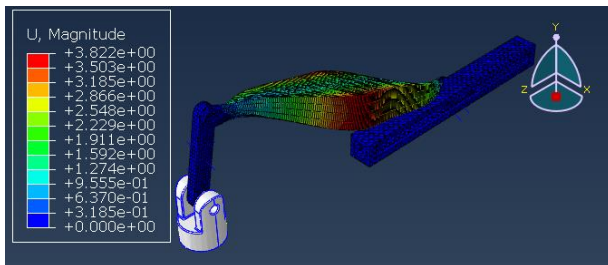


Figure 4-19. 7<sup>th</sup> Mode Shape

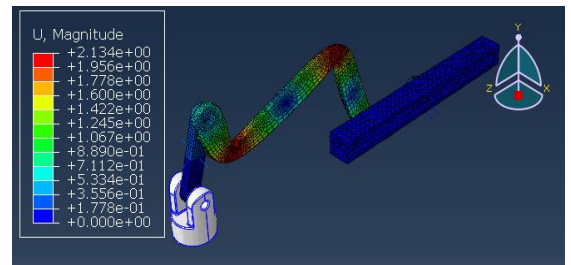


Figure 4-20. 8<sup>th</sup> Mode Shape

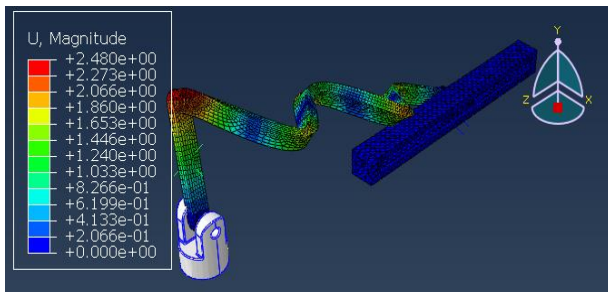


Figure 4-21. 9<sup>th</sup> Mode Shape

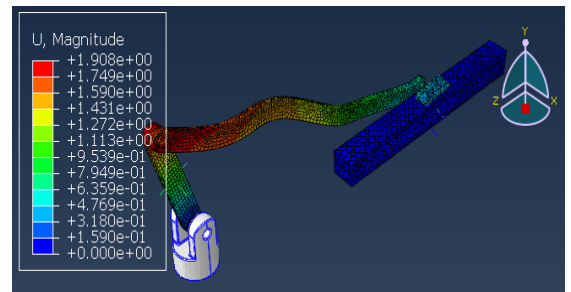


Figure 4-22. 10<sup>th</sup> Mode Shape

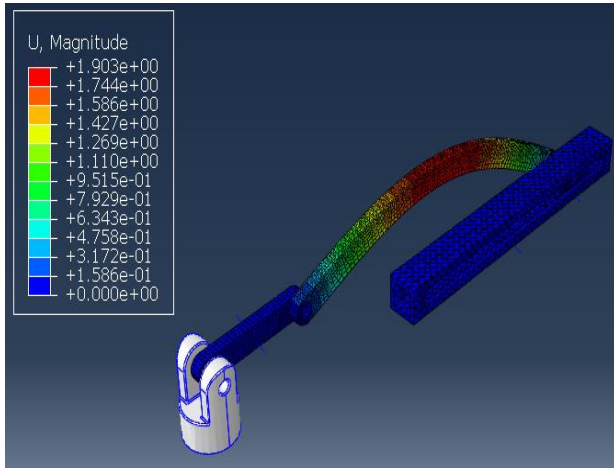


Figure 4-23. 0° Configuration- 1<sup>st</sup> Mode

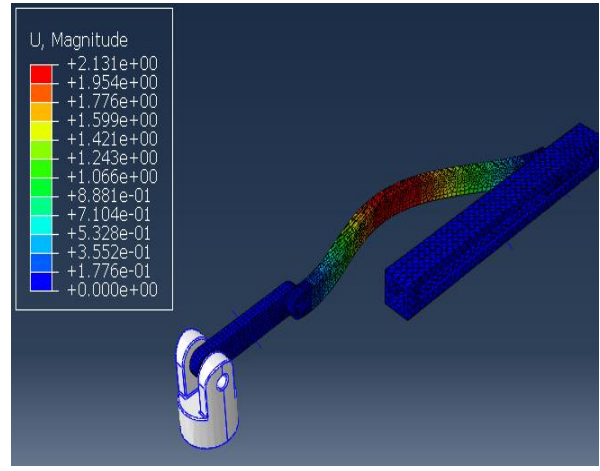


Figure 4-24. 0° Configuration- 2<sup>nd</sup> Mode

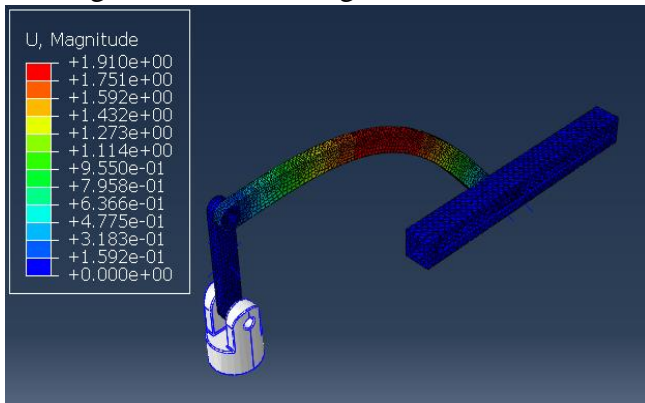


Figure 4-25. 90° Configuration- 1<sup>st</sup> Mode

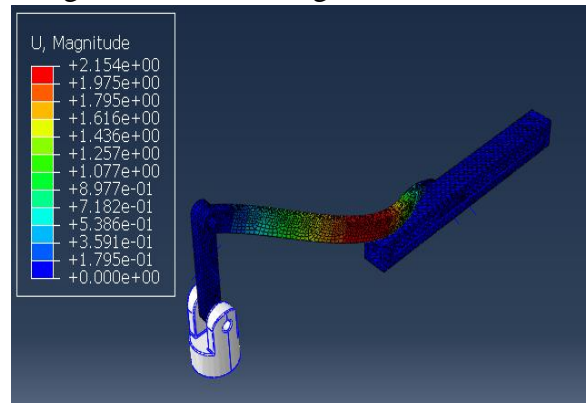


Figure 4-26. 90° Configuration- 2<sup>nd</sup> Mode

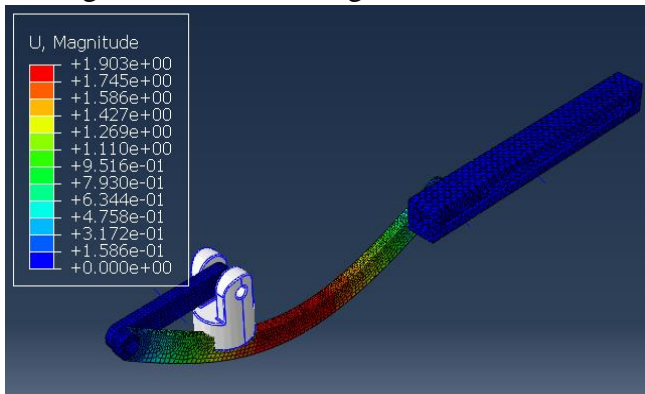


Figure 4-27. 180° Configuration- 1<sup>st</sup> Mode

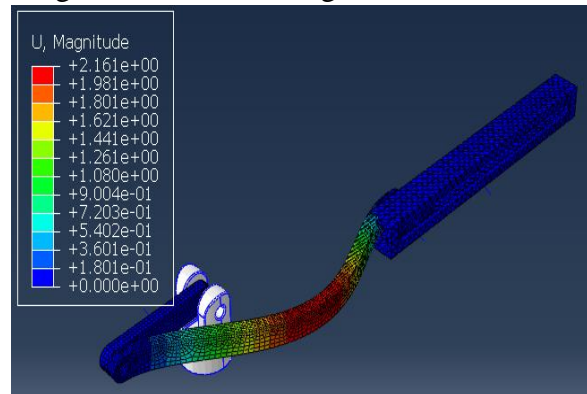


Figure 4-28. 180° Configuration- 2<sup>nd</sup> Mode

As it can be seen from the Table 4-8, after 2<sup>nd</sup> mode shape, natural frequency values increase widely. In real life consideration, after the 2<sup>nd</sup> mode shape results are not encountered for the resonance cases for slider-crank mechanisms.

Moreover, solely connecting rod is distorted in the figure. Because other parts were modelled as a rigid body and only connecting rod was modelled as a flexible body in order to reduce the analysis time. Modelling all parts as flexible requires huge computational time. Moreover, since dealing with the most critical part which is connecting rod, performing modal analysis with this part's flexible feature is sufficient.



Table 4-8. Natural Frequency Results for Simple Crank Slider

MODE NO	EIGENVALUE	FREQUENCY/(RAD/TIME)	FREQUENCY/(CYCLES/TIME-Hz)
1	5.68E+06	2383.3	379.31
2	7.25E+06	2693.2	428.64
3	5.17E+07	7190.7	1144.4
4	8.68E+07	9316.3	1482.7
5	1.67E+08	12917	2055.8
6	3.14E+08	17716	2819.5
7	3.97E+08	19915	3169.6
8	4.24E+08	20586	3276.3
9	4.44E+08	21077	3354.5
10	6.22E+08	24950	3970.9

#### 4.3.1.6 Different Configurations

Modal analysis was directly affected by the configuration of the mechanism. The angle between links changes the mode shapes.

To be able to see different angles-configurations effects on the mode shapes, for 0°, 90°, 180° configuration angles, modal analysis was run and figures for the first two-mode shapes were given below.

As it can be seen from the above figures, different configurations affected the maximum displacement values for each mode shape. Because the configuration of the system changes the stiffness matrix. Since the eigenvalue can be written as  $\omega_n = \sqrt{k/m}$  these changes on the eigenvalues are expected and showed us the modal analysis depends on the configuration of the system.

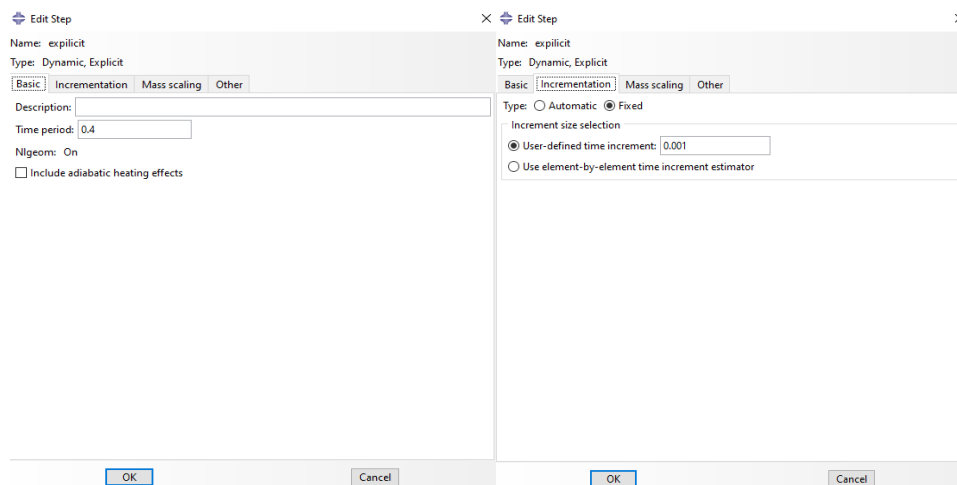


Figure 4-29. Step Definition

## 4.3.2 Dynamic Explicit Model

### 4.3.2.1 Introduction

Since the main idea is to extract the acceleration and later implement it on the static model, in this section whole model was built as a rigid body.

In this section, only dynamic analysis was performed according to the given momentum. After applying the momentum system started to move and reaction forces and displacements occurred. The goal is here to analyse the system according to those reaction forces, obtaining the acceleration, displacements and stress values.

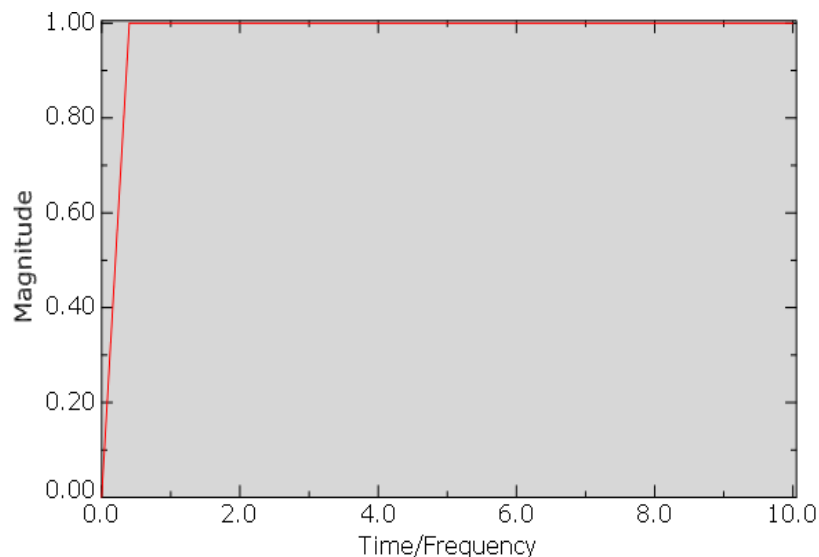


Figure 4-30. Amplitude for Input Moment

### 4.3.2.1 Analysis Step

In this section, the 'Dynamic-Explicit' option was selected as a step type. Furthermore, 0.4 seconds was given as a time period and since the system has been established from a rigid body, Abaqus cannot resolve the step increment size. In order to avoid this problem manually increment size was given and in this section, it is 0.001.

Moreover, in the step section, output time was divided into 50 steps by adjusting the field output section. So, at the end of the analysis, there were 50 frame-step that was used during the data collecting process.

### 4.3.2.2 Interaction and Load Step

Since the mechanism should be moved according to force, the same joints were used as in 'Modal Analysis': Hinge and Translator Joints. However, only one boundary condition was applied for this case which was the encastre type. It was assigned both crank and slider fitting. The displacement boundary condition is unnecessary for this case because the continuous movement of the assembly was required and this type of boundary condition was insufficient for this. The hinge joint on the crank allowed the motion.

This analysis required external force or moment. The moment was applied on the hinge which is connected between crank fitting and crank arm. Since the crank arm fitting is only displayed body, actually the hinge is between the ground and the crank arm. 10 Nm is implemented along the global 'x' direction. Furthermore, the load or moment is not applied as a ramp method, it

is applied as a time function in real life. In addition, when the ramp input is given system acts rapidly, in this way it causes stress concentration. In real life, the loading process starts at 0 seconds and goes to a specific time. The amplitude is given in Figure 4-30.

Joint, boundary types and body types are given in Figure 4-31, Figure 4-32 and Figure 4-33:

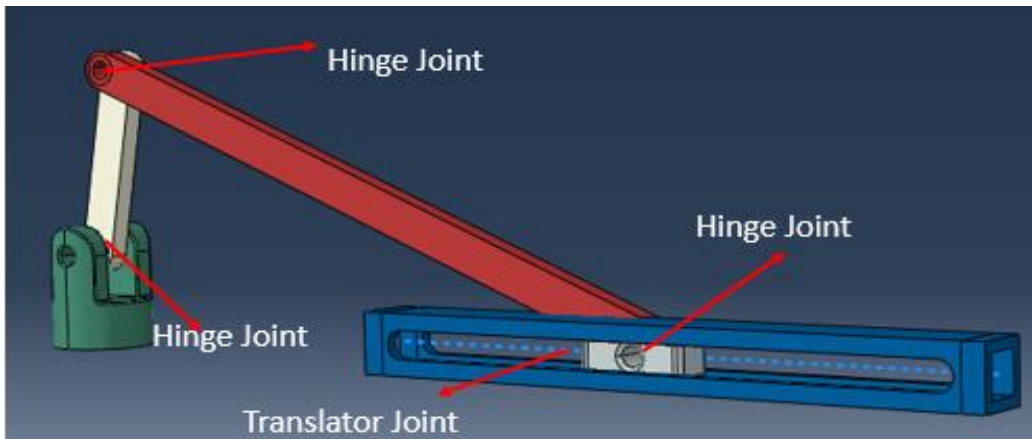


Figure 4-31. Joints on the Assembly

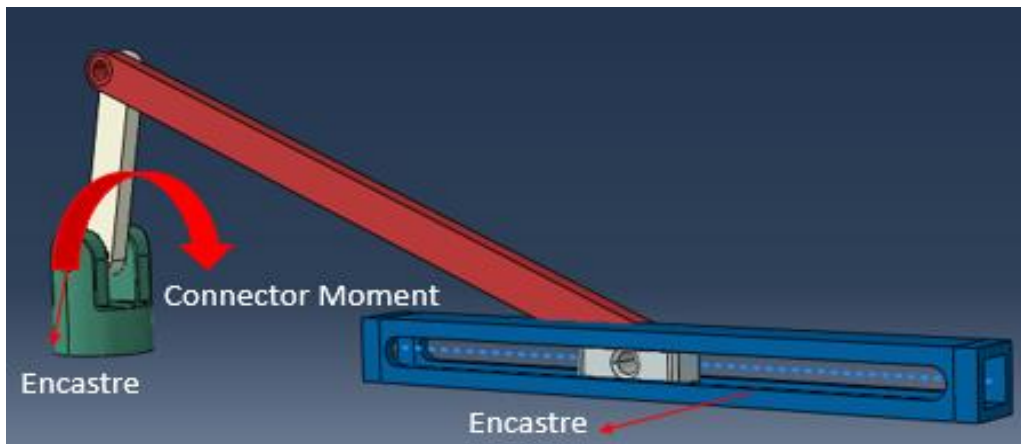


Figure 4-32. Moment and Boundary Conditions on Assembly

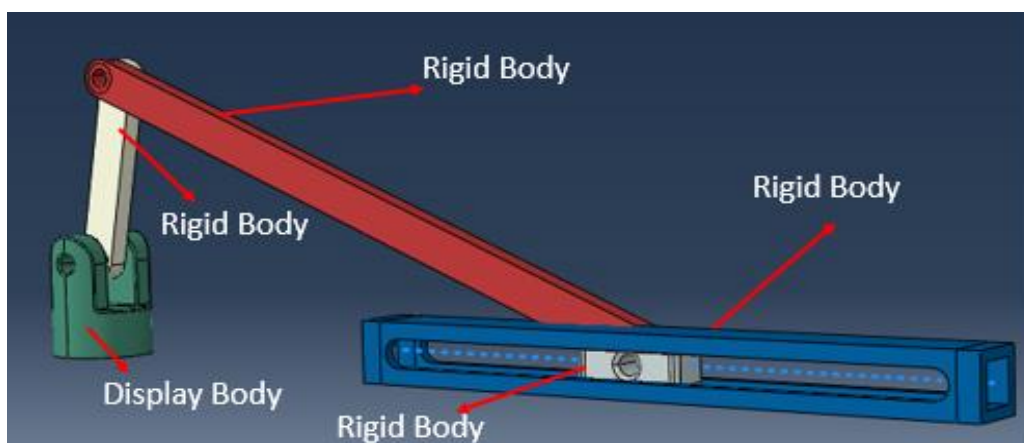


Figure 4-33. Body Type Demonstration on Assembly

#### 4.3.2.3 Meshing

The same seed number and type was implemented as it was in Modal Analysis.

In this case, for each part assigned mesh are given below Figure 4-34 and Table 4-9:

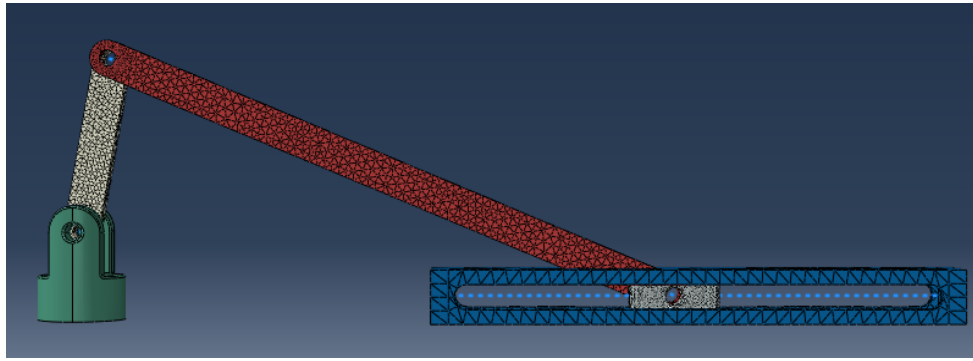


Figure 4-34. Meshed Parts

Table 4-9. Element Type and Node Number

Part	Element Type	Element	Node
Connecting Rod	C3D8R	6168	8183
Slider	C3D8R	24351	35914
Crank Arm	C3D8R	852	1324
Crank Fitting	C3D8R	2706	5806

#### 4.3.2.4 Results and Conclusion

In this section, an analysis job was for 0.4 s created and ran the job in Figure 4-35. No parallelization method was used. Because in some cases Abaqus may need to use extra licences in the parallelization method and may not extract the licence, which cause the analysis could fail. Displacement and Acceleration results with 0.04 s intervals are given below figures:

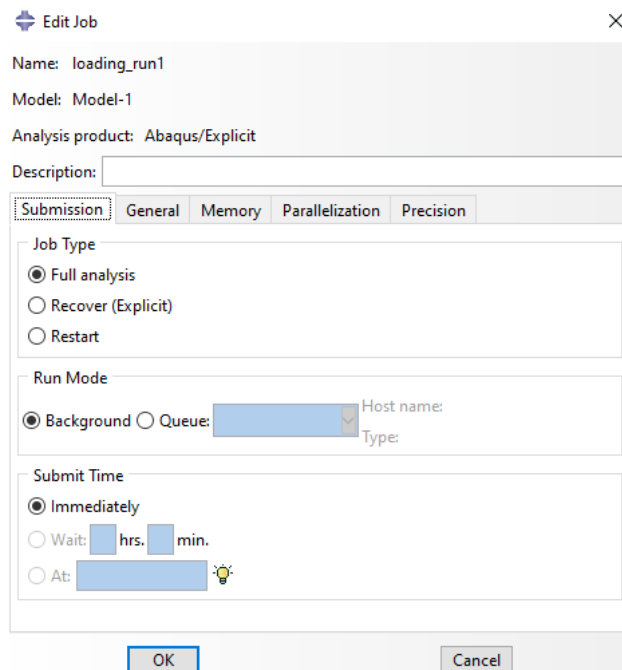


Figure 4-35. Dynamic Explicit Job

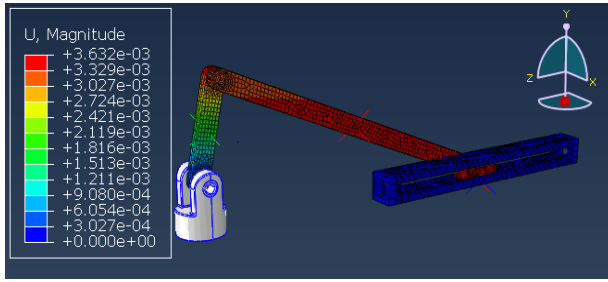


Figure 4-36. Displacement at 0.04 s

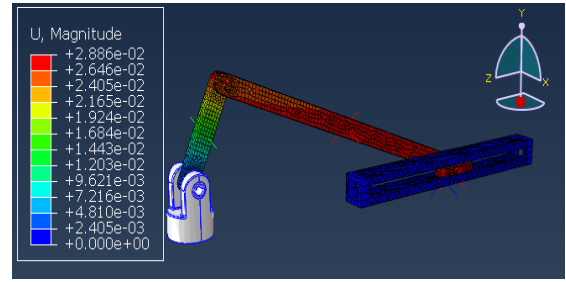


Figure 4-37. Displacement at 0.08 s

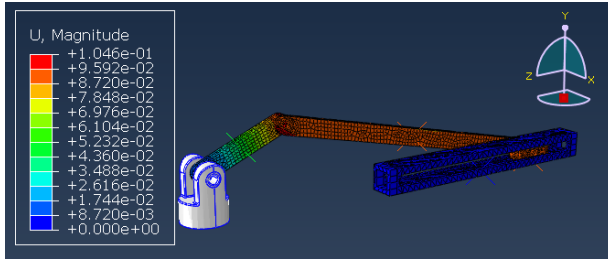


Figure 4-38. Displacement at 0.12 s

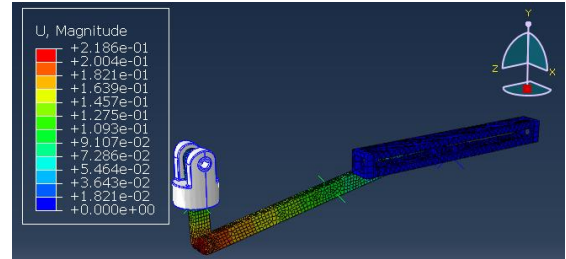


Figure 4-39. Displacement at 0.16 s

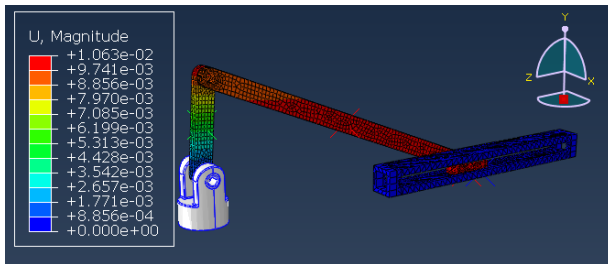


Figure 4-40. Displacement at 0.20 s

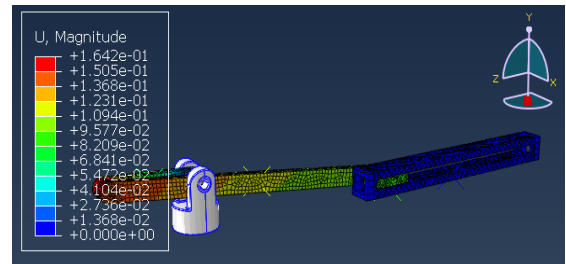


Figure 4-41. Displacement at 0.24 s

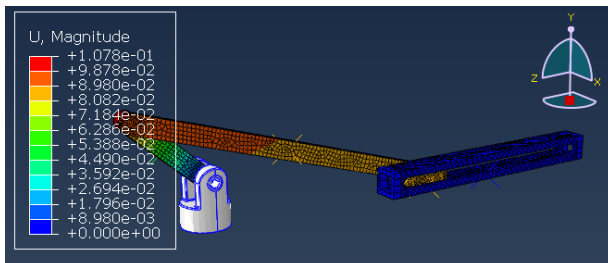


Figure 4-42. Displacement at 0.28 s

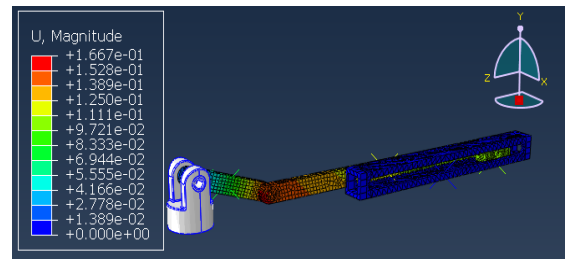


Figure 4-43. Displacement at 0.32 s

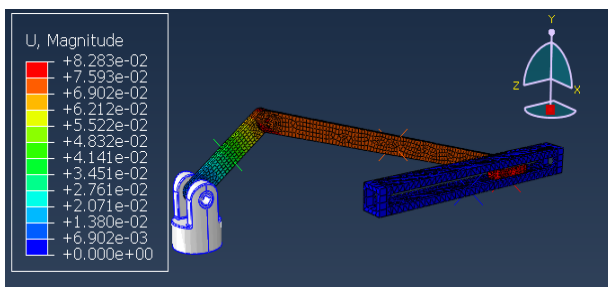


Figure 4-44. Displacement at 0.36 s

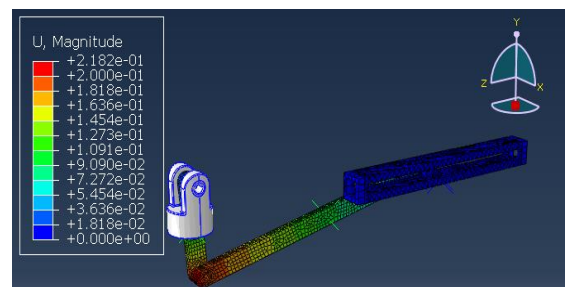


Figure 4-45. Displacement at 0.40 s

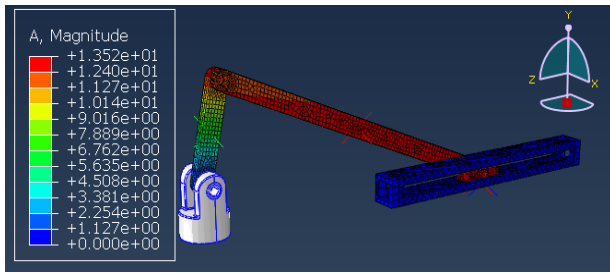


Figure 4-46. Acceleration at 0.04 s

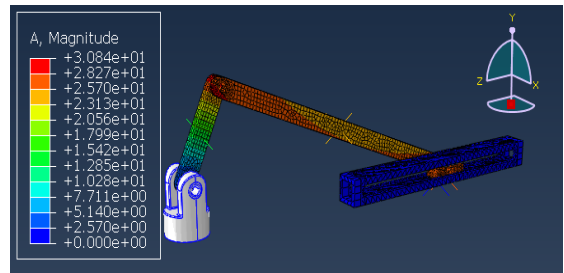


Figure 4-47. Acceleration at 0.08 s

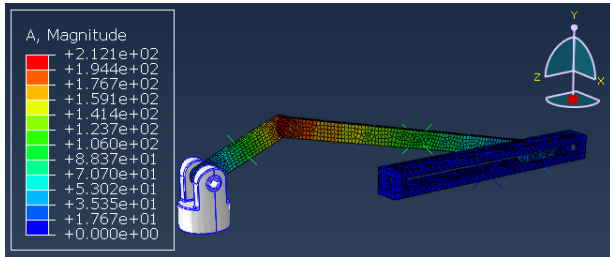


Figure 4-48. Acceleration at 0.12 s

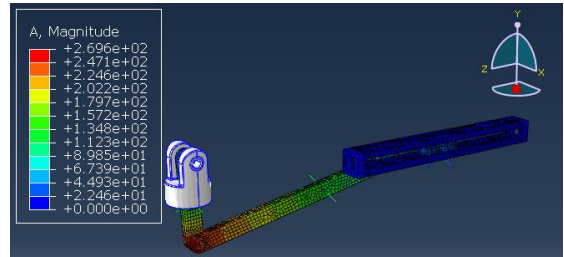


Figure 4-49. Acceleration at 0.16 s

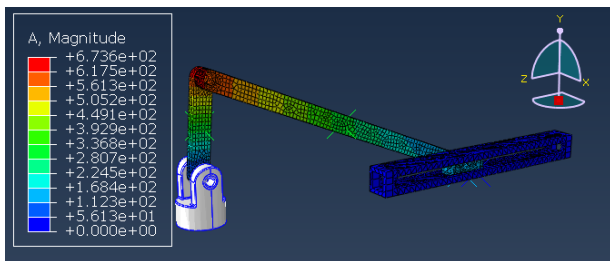


Figure 4-50. Acceleration at 0.20 s

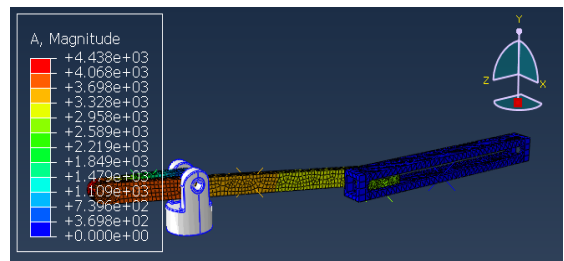


Figure 4-51. Acceleration at 0.24 s

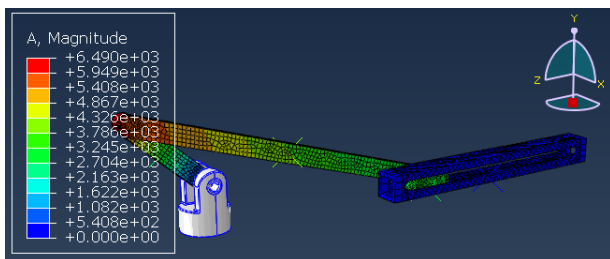


Figure 4-52. Acceleration at 0.28 s

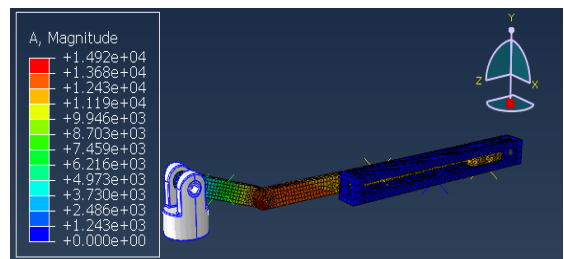


Figure 4-53. Acceleration at 0.32 s

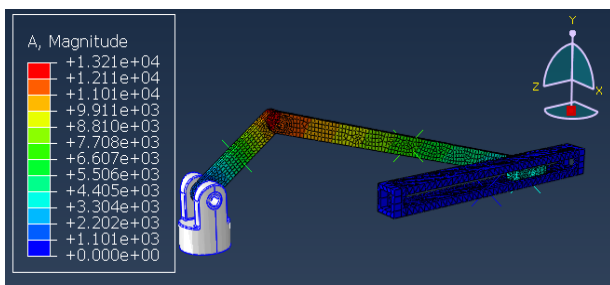


Figure 4-54. Acceleration at 0.36 s

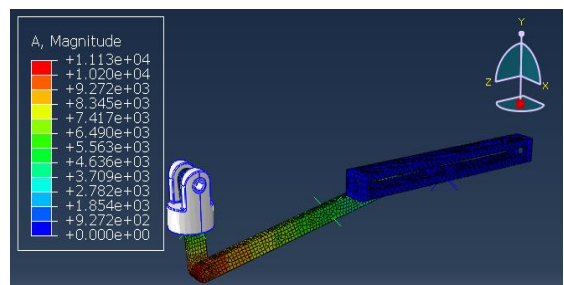


Figure 4-55. Acceleration at 0.40 s

From the above figures, connecting rod is deflected more than other parts and in addition acceleration values are higher on the connecting rod. Moment affects the connecting rod higher than other parts due to the length of the connecting rod. Moreover, the width of the rod is not sufficient enough to resist deflection. All these effects are the reason the connecting rod was selected for the optimization problem case part.

As it can be seen from acceleration figures, acceleration values stand extremely high. Because the given momentum is excessively huge for the system. But since optimization is the main concern, changes in results will be more noticeable, so this momentum will be applied.

Also at the end of the analysis, the angle between the crank arm and crank fitting was extracted as a '.txt' file to be information for Static Analysis.

#### 4.3.2.5 Matlab Step

At the end of dynamic analysis, a frame is selected and for the connecting rod acceleration and coordinates of every node is extracted as a '.txt' file. This file was later processed by Matlab Script. The Matlab Script creates acceleration functions for each X-Y-Z coordinate combining nodal coordinates with nodal acceleration values with the 'polyfit' tool. These 3 acceleration function was used as the input value for static analysis.

### 4.3.3 Static Model

#### 4.3.3.1 Introduction

In the Static Model, the SolidWorks model angle needs to be calibrated according to the preselected frame's angle which comes from extracted file. After the calibration angle was adjusted, the model can be built.

#### 4.3.3.2 Analysis Step

In this section, 'static-general' is selected as the step. Furthermore, 0.1 second was given as a time period and since the system has been established from a rigid body, Abaqus cannot resolve the step increment size. In order to avoid this problem manually increment number was given and in this section, it is 10000. Nonlinear geometry was set to on. The step definition is given in Figure 4-56.

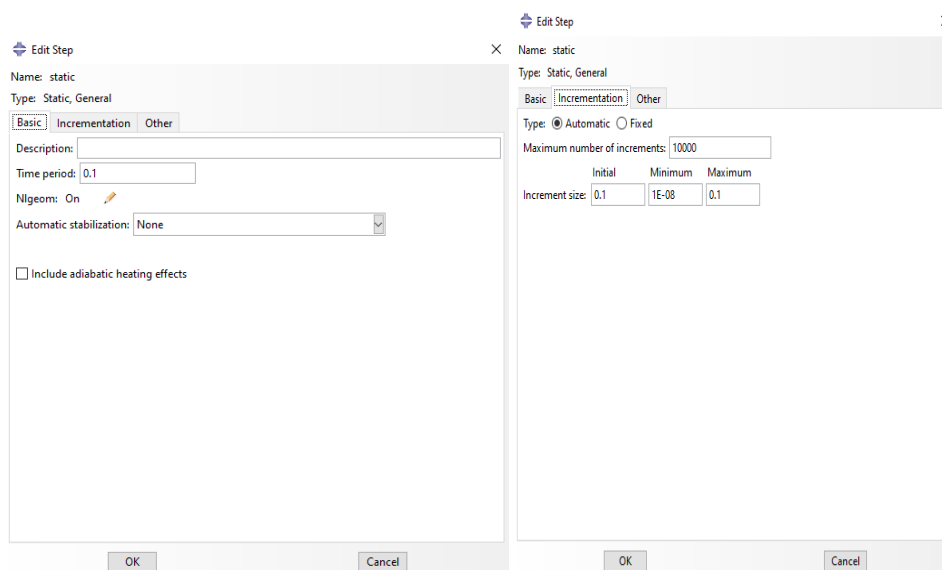


Figure 4-56. Step Definition of Static Analysis

### 4.3.3.3 Interaction and Load Step

The same joint types were applied as in ‘Modal Analysis’: Hinge and Translator Joints. In addition, boundary conditions were applied for this case same as ‘Modal Analysis’. Hinge joint between links, translator joints between the slider and slider fitting was used. Also to attach the assembly to the ground, an encastre joint on the crank arm fitting and slider fitting was used. Furthermore, to eliminate the motion from the mechanism, zero displacement boundary conditions at the hinge and translator joint were used. The reason behind giving 0 to boundary conditions is because if the system has the ability to move then the Abaqus solver diverge since the step type is selected ‘static’. So eliminating movement is crucial in this step.

In addition, to be able to shorten the analysis process time, the only connecting rod was modelled as flexible other parts were the rigid body. But, since the Abaqus ‘static solver’ cannot solve the being joint locations rigid, these locations were modelled as flex.

Joints, boundary conditions and body types are given in Figure 4-57, Figure 4-58 and Figure 4-59.

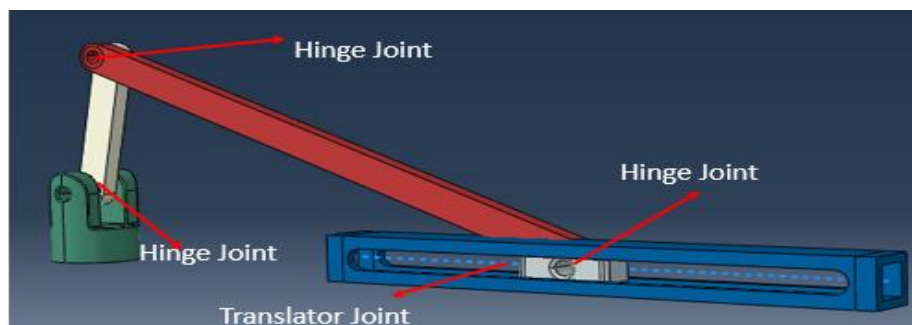


Figure 4-57. Joints on Assembly

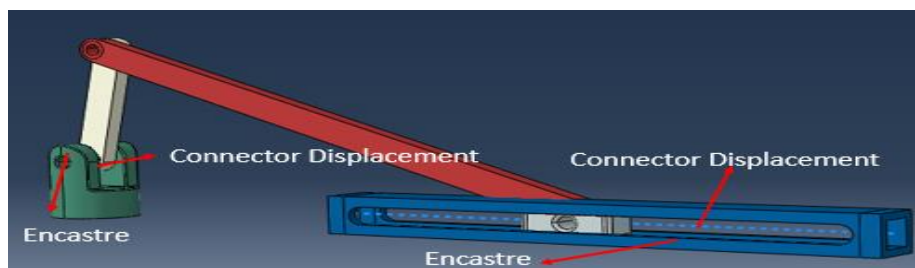


Figure 4-58. Boundary Conditions on Assembly

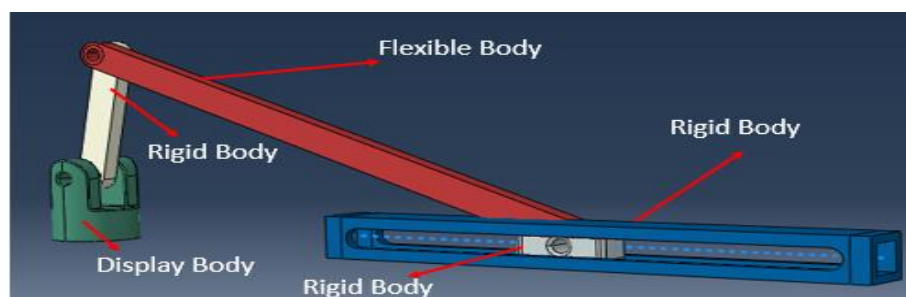


Figure 4-59. Body Type Demonstration on Assembly



The loading process was made by applying 'acceleration values', that extracted from 'Dynamic Analysis', into the 'gravity loading' section. Selecting this option actually is an obligation rather than a choice, since the Abaqus does not create 'Body Forces' in the 'explicit analysis'. During the loading step, the 'Analytical Field' tool was used. In this tool, the polynomial equation created in Matlab was imported and used nodal coordinates values as the unknown variables in the equation. So mesh quality and count must be equal between the 'explicit' and 'static' models. If the mesh is not identical 'acceleration equations' will be wasted due to inconsistent and gives incorrect results. Furthermore, since the output acceleration and coordinate data has 3 axes, the force must be applied in 3 axes.

The calculated polynomial equation was written in Analytical Field in Figure 4-60.

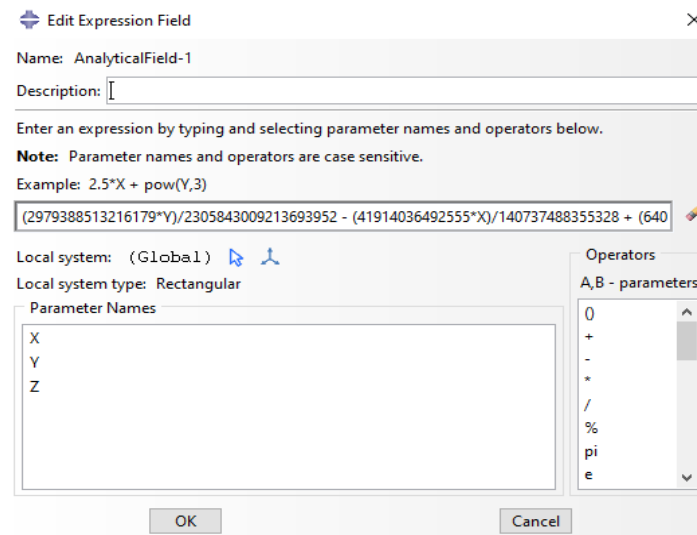


Figure 4-60. Analytical Field Creation of Static Analysis

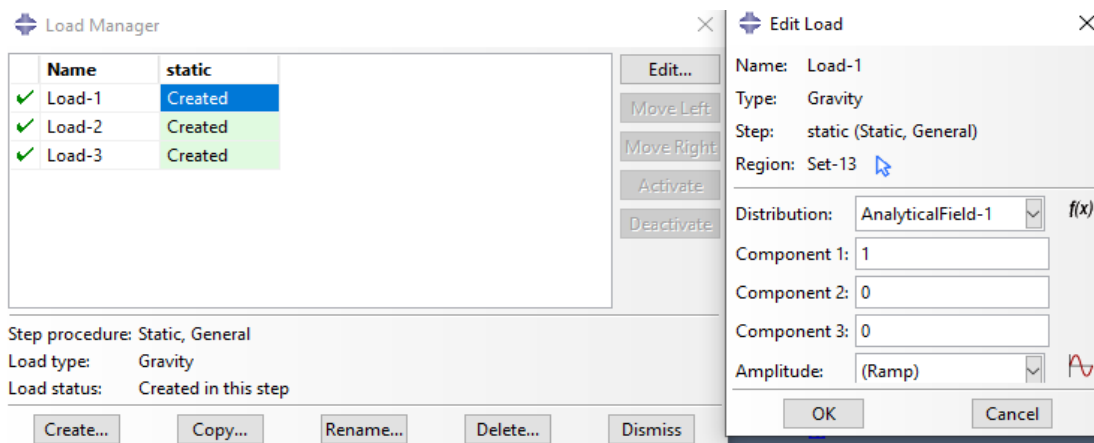


Figure 4-61. Loading Process of Static Analysis

Implemented load was given for 'x-y-z' axes in Figure 4-61 and Figure 4-62.

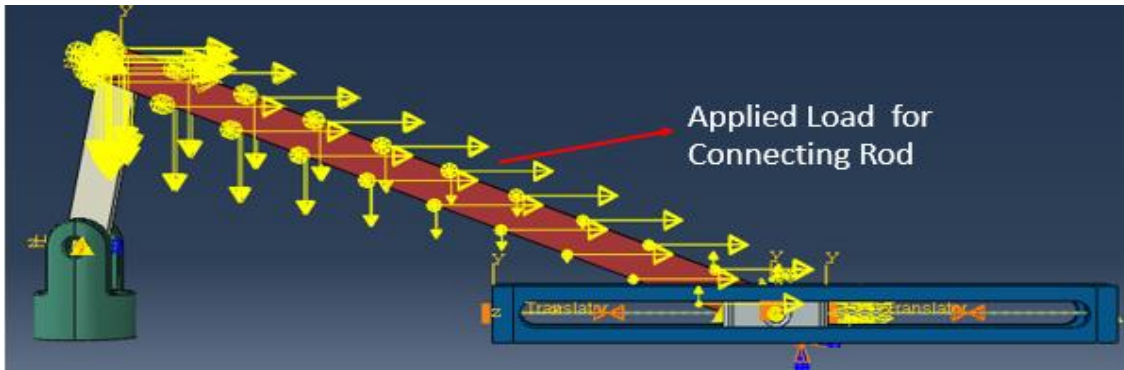


Figure 4-62. Applied Force on the System

#### 4.3.3.4 Meshing

The same seed number and type is implemented as it was in Modal Analysis.

In this case, for each part assigned mesh are given below Figure 4-63 and Table 4-10:

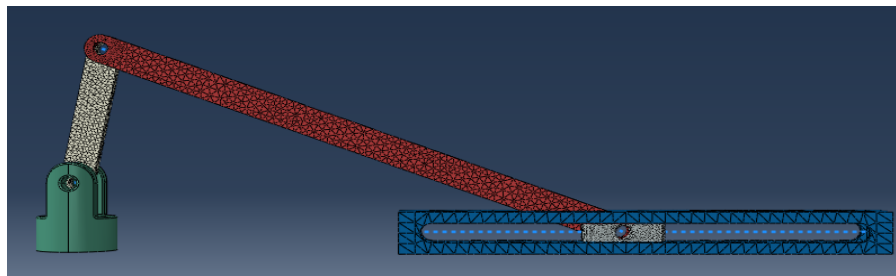


Figure 4-63. Meshed Parts

Table 4-10. Element Type and Node Number

Part	Element Type	Element	Node
Connecting Rod	C3D8R	6168	8183
Slider	C3D8R	24351	35914
Crank Arm	C3D8R	852	1324
Crank Fitting	C3D8R	2706	5806

#### 4.3.3.5 Results and Conclusion

At the end of the analysis which is 0.1 s, the stress distribution is consistent with acceleration distribution in explicit analysis. The middle area of the connecting rod is exposed to the highest stress and it can be predicted from the explicit graph (Figure 4-36 to Figure 4-45). The same pattern can be observable in acceleration graphs (Figure 4-46 to Figure 4-55). Because the middle area of the connecting rod is exposed to more rotational and linear acceleration than the start and end regions of the connecting rod. The stress is affected directly by force which depends on the acceleration. Furthermore, the thickness-width of the connecting rod is not enough to encounter a high-stress outcome. In addition, it can be observable from Figure 4-66, the acceleration grew in the edge of the connecting rod, which causes high stress (Figure 4-64 and Figure 4-65).

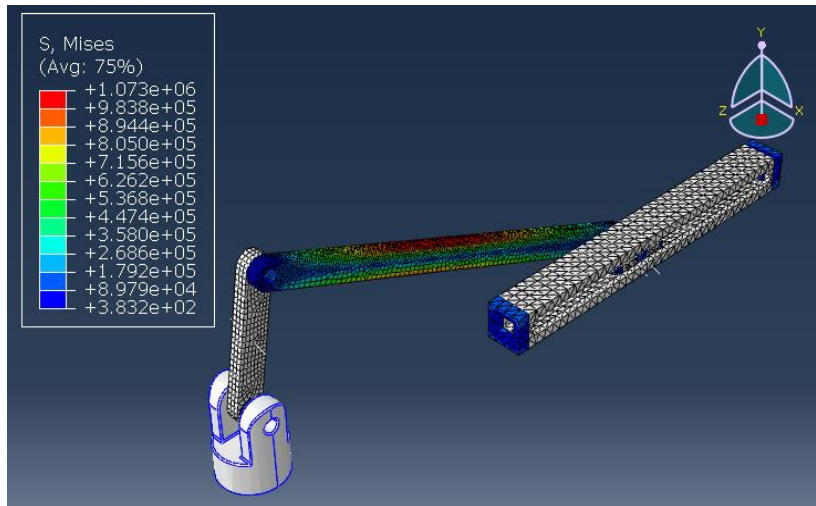


Figure 4-64. Von Mises Stress at the end of The Analysis

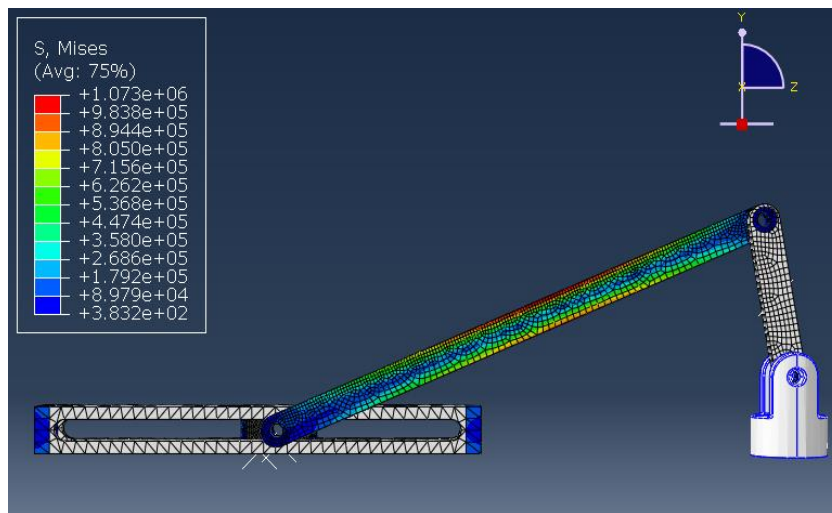


Figure 4-65. Von Mises Stress at the end of The Analysis

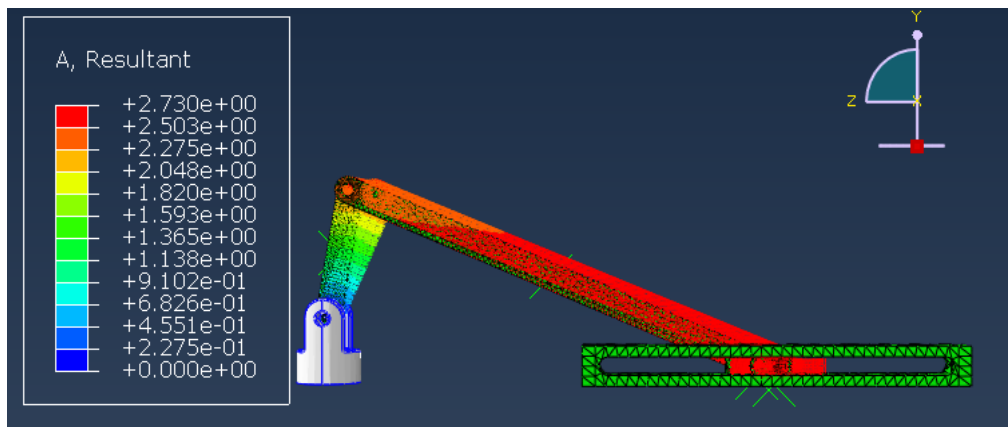


Figure 4-66. Acceleration on the Case Study Time-End of the Analysis

At the end of the static analysis (at 0.1 s), the connection location (hinge joint location) between the slider and connecting rod was selected as investigated area and via python coding average stress value and nodal stress were extracted to use in Isight.

The investigated zone is shown in Figure 4-67.

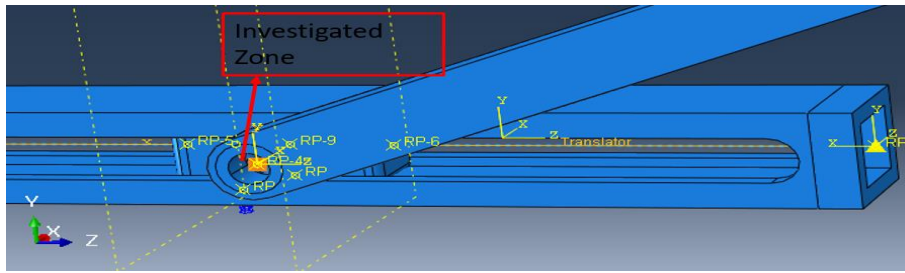


Figure 4-67. Von Mises Stress investigated Zone

#### 4.4 Isight Model

In the Isight model, the goal is to create a multi-model that enables ‘Modal Analysis’, ‘Dynamic Explicit’ and ‘Static Analysis’ models, run them and find the best solution according to constraints.

##### 4.4.1 General Overview of Model

General overview of Isight model given below figure:

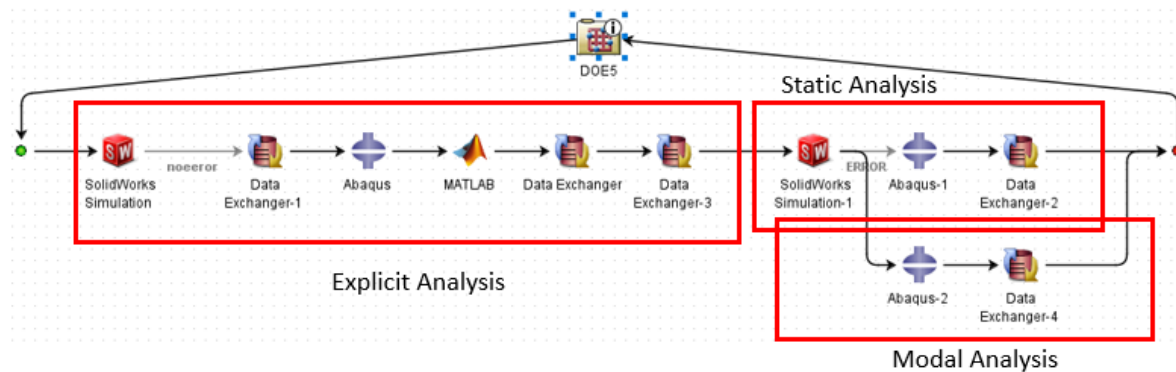


Figure 4-68. General Overview of Isight Model

As it can be seen there are 3 analysis workflows: Dynamic Explicit, Static and Modal.

Since these models use the same CAD data, both of the workflows is fed by the SolidWorks Model.

For Explicit Workflow, first Abaqus imports the SolidWorks via Python Code that is created during the initial Abaqus Model. After that, it process the ‘.SAT’ file and started the building and running model according to the python file. This file actually repeated the first initial Abaqus model in the previous. It creates the same parameters, same analysis, same job. After the job is finish in the Abaqus component, the ‘Data Exchanger’ component extracts the solution from the ‘Abaqus .odb’ file. The solution then is sent to the ‘Design of Experiment’ component. Also during the preparing python code extracting ‘node locations’, ‘angle changes’ and ‘acceleration’ values are written in separated text files. After this process ends, the Matlab script starts to work and create 3 polynomial functions for each axis based on nodal coordinate and acceleration raw data. These functions are acceleration vector polynomials. Later, these are implemented into the static analysis.

For Static Analysis Workflow, another SolidWorks Components is required. The first SolidWorks component that was used in the explicit analysis must be independent of angle calibration to avoid confusion. This SolidWorks Component obtain a different model from the explicit model’s usage. Actually, the dimensions are the same but this model has the ability to

change its angle. To be able to accomplish this model has the ability to import output value as the global variable (angle). This imported file was fed by an 'explicit analysis' output angle text file. In this situation, the only unknown is how to select the angle from the output angle text. This was achieved via the Isight optimization design variable part. Also to be sure of working with the same dimensions, in both SolidWorks Components, the same parameters were selected in Isight. After the required angle was uploaded from SolidWorks and calibrating the angle is finished, Abaqus started to work. After finishing the analysis, for the selected area a file is generated which includes the Von-Misses Stress for every node in the selected area. To access easily these values and make comment on the selected area, the average value was calculated with Stress Output. This Average Value was used in the design optimization process with help of a Data Exchanger.

For Modal Analysis Workflow, the same SolidWorks model was used with 'Static Analysis'. Obtaining the calibrated angle with SolidWorks simplified the process. After that, Abaqus analysis started and Modal Analysis was performed. At the end of the analysis, Data Exchanger

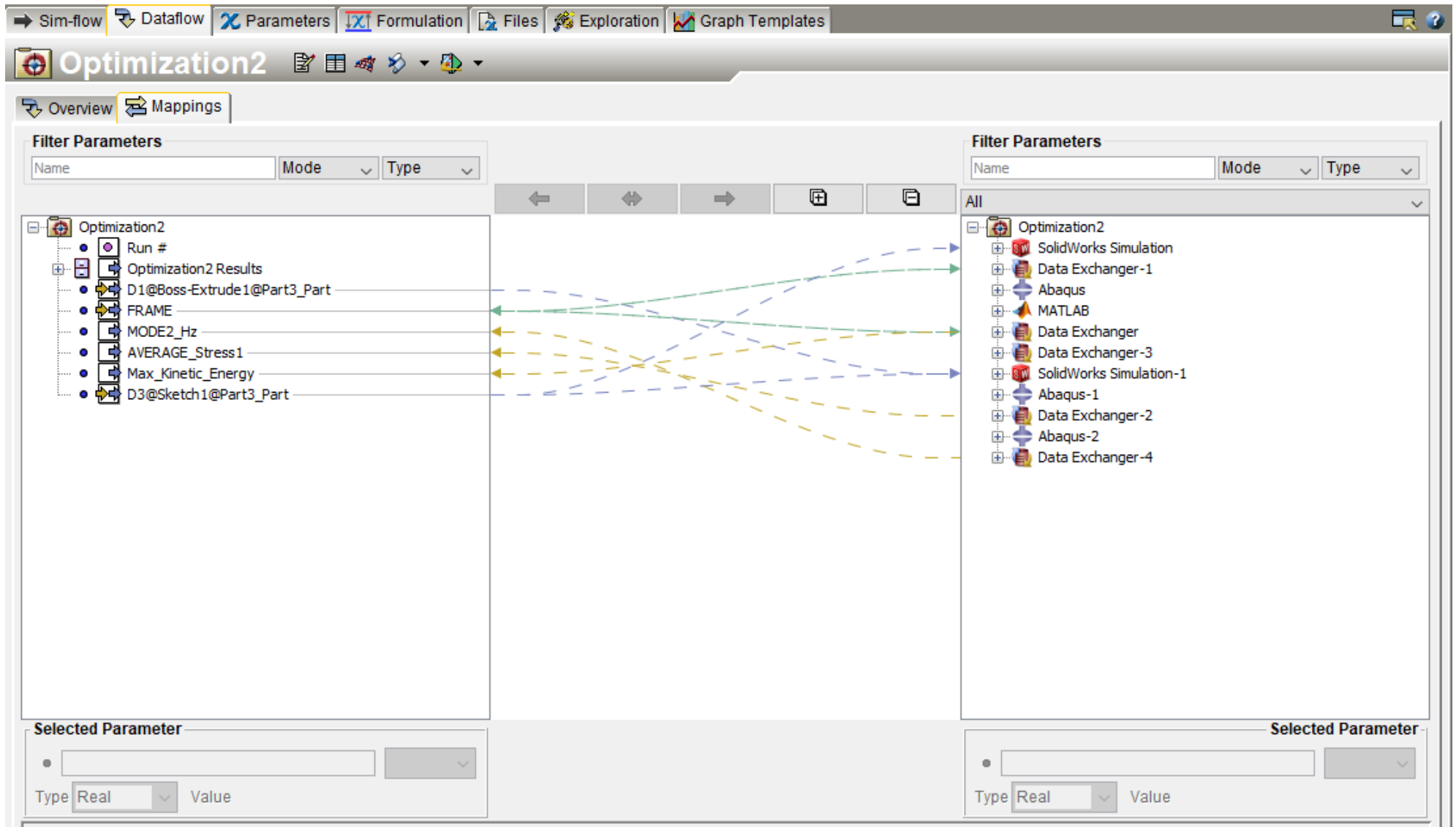


Figure 4-69. General View of Isight Design

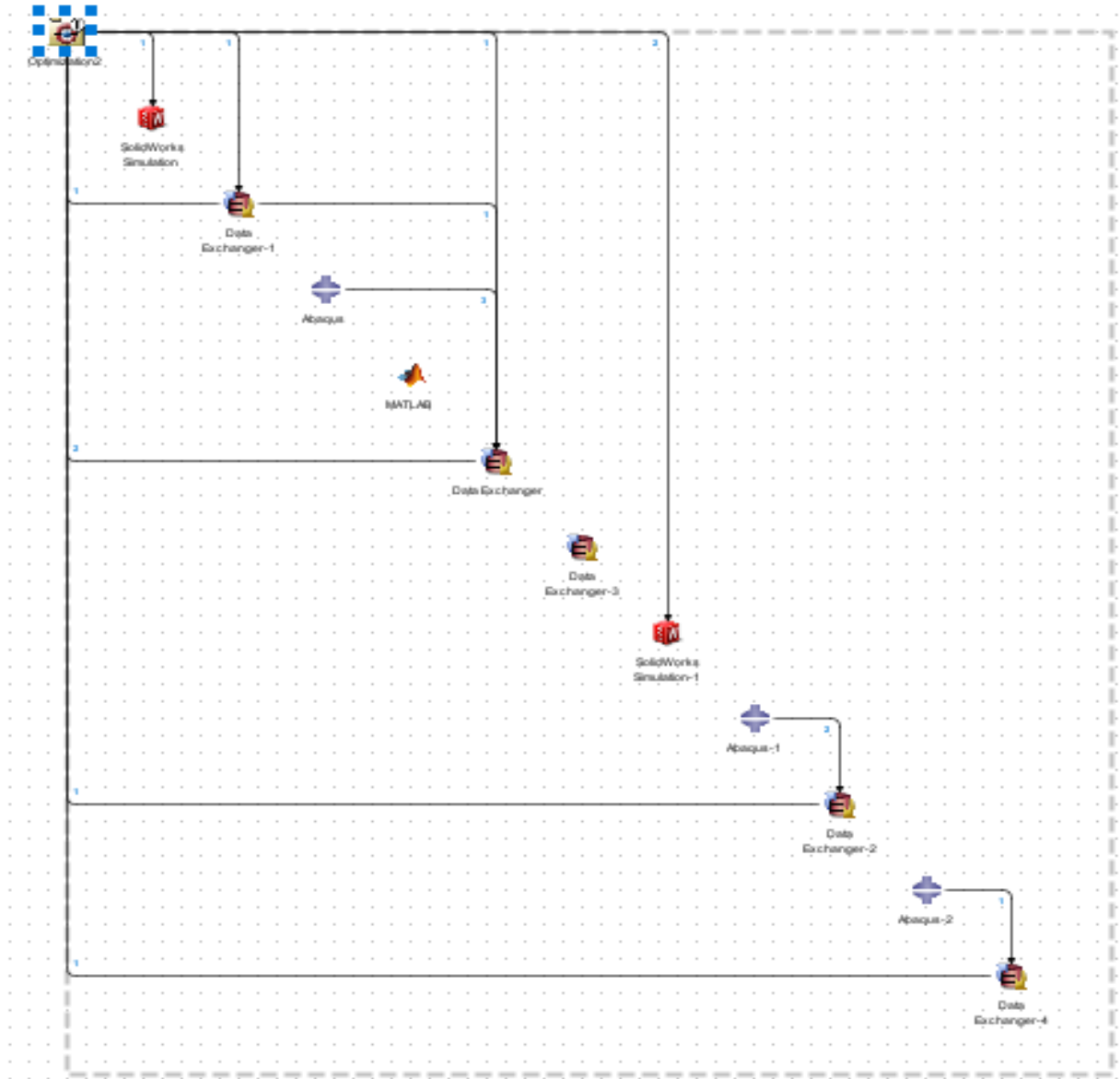


Figure 4-70. General View of Isight Design

worked and extracted the results from the ‘Abaqus.dat’ file. The solution then was sent to the ‘Design of Experiment’ component.

The Isight component input and output relationship configuration is given in Figure 4-69 and Figure 4-70:

#### 4.4.2 Design Inputs and Outputs Selection

SolidWorks provides the main input as CAD data. In the Isight SolidWorks component, every design parameter can be accessible.

In this part, the length and width of the connecting rod were selected as design parameters for Dynamic Explicit, Static and Modal Analysis models. The same CAD parameters must be chosen, because nodal coordinates of explicit analysis CAD data and static analysis CAD data must be the same in order to create correct force input for ‘static analysis’. However, the second CAD data is able to change its angle based on the information that comes from ‘explicit analysis’.

Figure 4-71 shows the all geometrical parameters and which geometrical parameters was selected. It can be seen based on Explicit, Modal and Static Analysis results the length and width of connecting rod are crucial, so these inputs were selected as geometrical inputs.

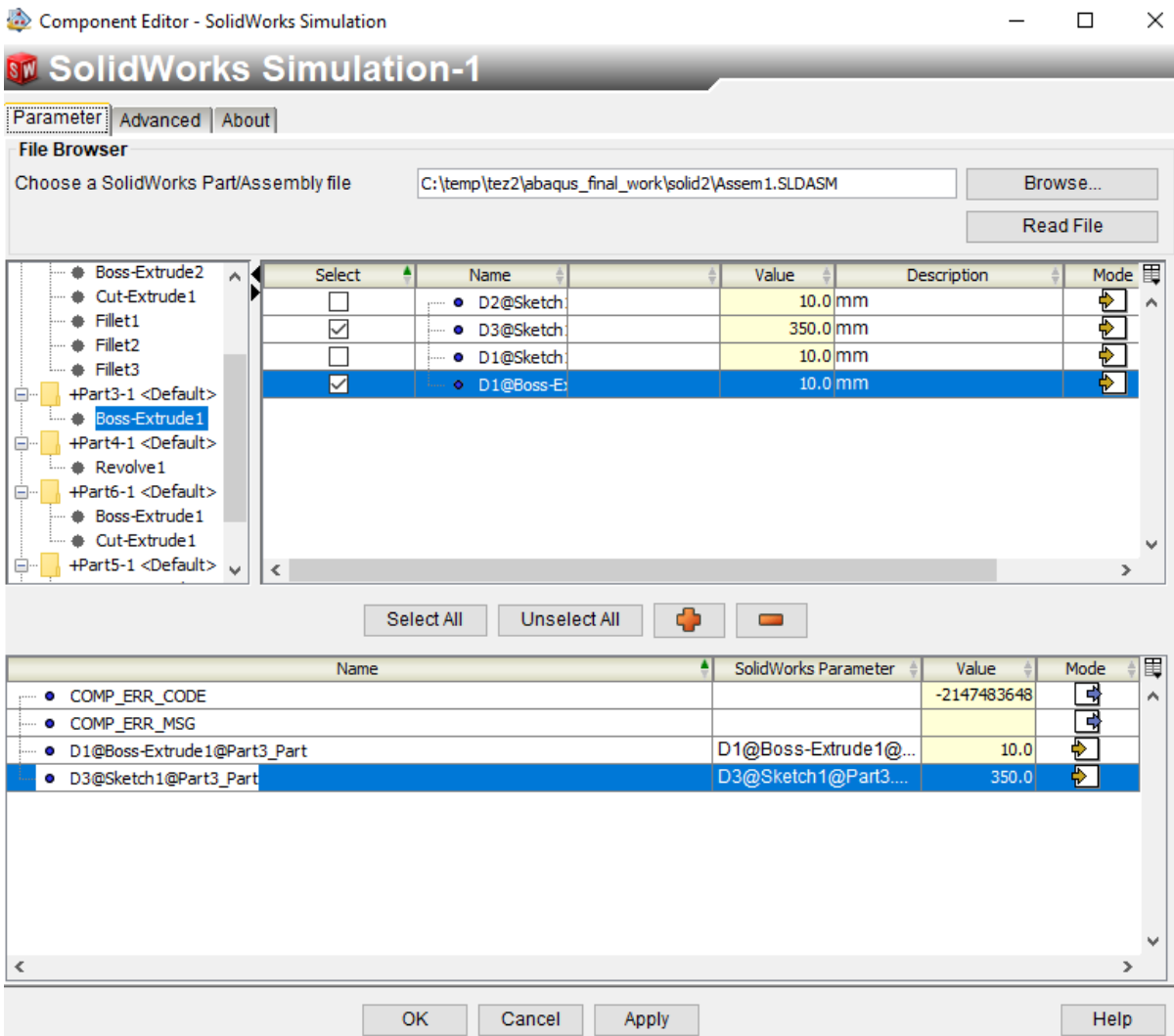


Figure 4-71. SolidWorks Input Selection



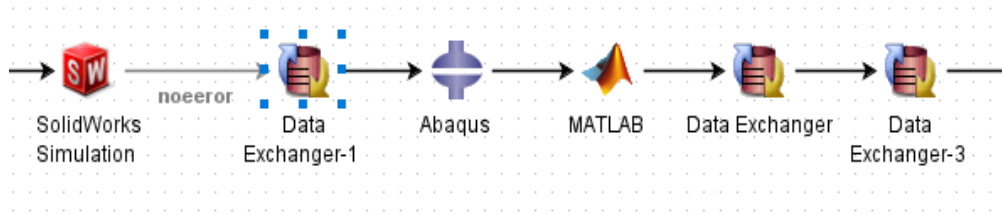


Figure 4-72. Dynamic Analysis Workflow

After SolidWorks inputs were given, Data Exchanger-1 starts and gives the investigated frame-angle extraction as the input for the Static Part to Explicit Analysis. After that, Abaqus Component started the analysis for the explicit part and it ran with its automated python code. The Python Script allows generating the required outputs for the analysis which are, angle change during the motion of analysis, total system kinetic energy and nodal coordinates and accelerations for the connecting rod. Following the Abaqus job analysis finished, nodal coordinates and accelerations were sent into Matlab as input responses, and they were processed with the 'polyfit tool' to create acceleration polynomial equations. After generating equations, they were printed on a specific folder in a text file format with help of Matlab.

The Dynamic Explicit Analysis process is expressed in Figure 4-72.

The screenshot shows a software interface with two main panels. The left panel displays a CSV file named 'data\_input.csv.tmp1' with the following content:

```

1 1.0
2

```

The right panel, titled 'Parameters', shows a table of input parameters for the analysis:

Op	Name	Value	Mode	Type
•	COMP_ERR_CODE	-2147483648	[Icon]	Integer
•	COMP_ERR_MSG		[Icon]	String
•	AVERAGE_Stress1	71508.73751	[Icon]	Real
•	d	0.0	[Icon]	Real
•	Diam	0.0	[Icon]	Real
⊕	DOE6 Results		[Icon]	
•	Max_Kinetic_Energy	479.221863	[Icon]	Real
•	MODE2_Hz	624.42	[Icon]	Real
•	n	0.0	[Icon]	Real
•	D1@Boss-Extrude1@Part3_Part	10.0	[Icon]	Real
•	D3@Sketch1@Part3_Part	350.0	[Icon]	Real
•	FRAME	10	[Icon]	Integer

Figure 4-73. Data Exchanger-1 Input Selection

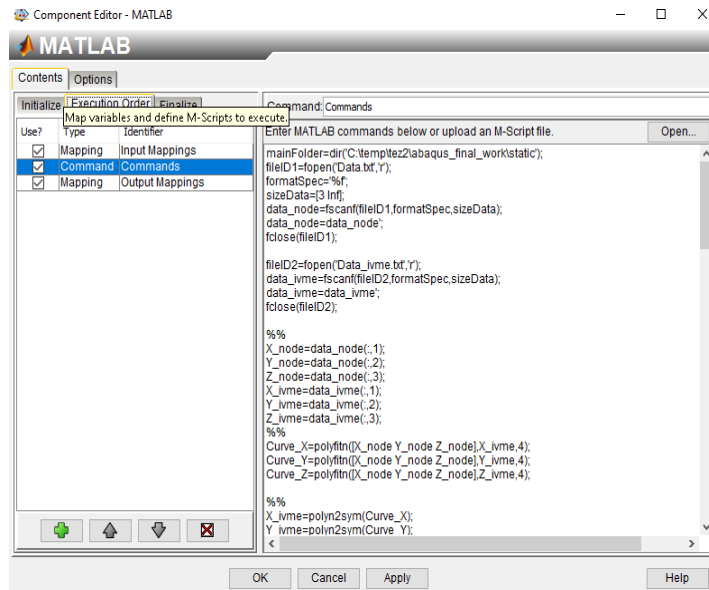


Figure 4-74. Matlab Function Calculator and Printer

The Matlab component which composes the polynomial function is shown in Figure 4-74. The system's maximum kinetic energy extractor Data Exchanger component is given Figure 4-75:

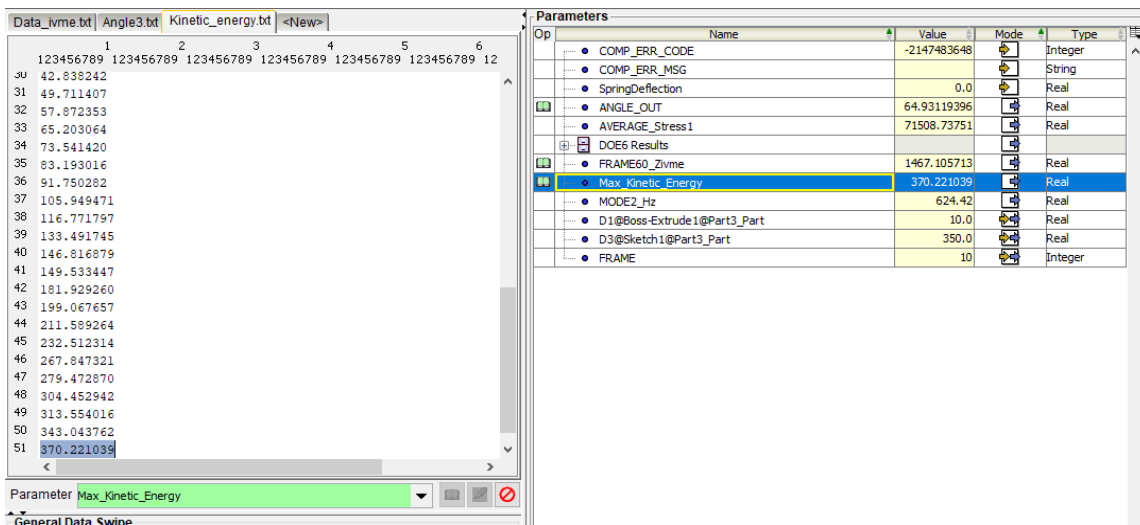


Figure 4-75. Data Exchanger Output Selection- Max Kinetic Energy of Dynamic System

After the Matlab component worked, the angle information that depends on the selected frame was written in a text file with 'Data Exchanger-3' to read by SolidWorks second component and modify the CAD data according to the new angle.

The Data Exchanger-3 information is given in Figure 4-76:

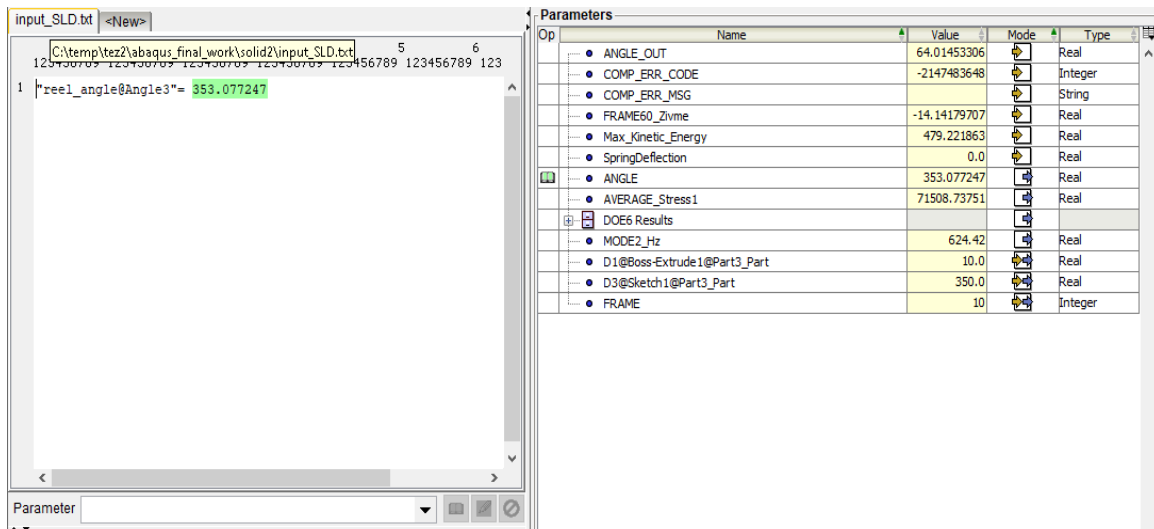


Figure 4-76. Data Exchanger-3 Input Selection- Static-Modal Model, Angle

After this step finishes, the second SolidWorks Component runs and create modified CAD data for static and modal analysis. As it was mentioned before, geometrical dimensions are the same as the previous component. The starts with the second CAD data is being process, The Static and Modal Analysis process begins, as it can be seen from Figure 4-77:

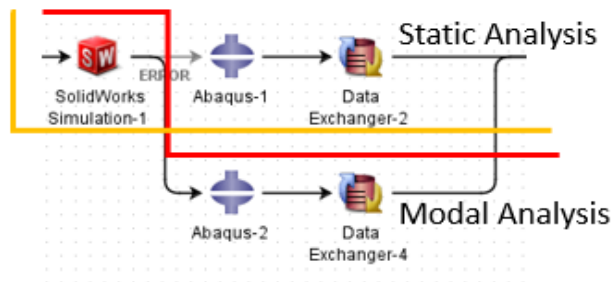


Figure 4-77. Static and Modal Analysis Workflow

After the second SolidWorks finished its job, information of CAD data was sent to both Modal and Static Analysis. For Static Analysis Abaqus-1 component ran with python. With help of python, desired area average Von-Misses Stress value was calculated and extracted by Data Exchanger-2 (Figure 4-78).

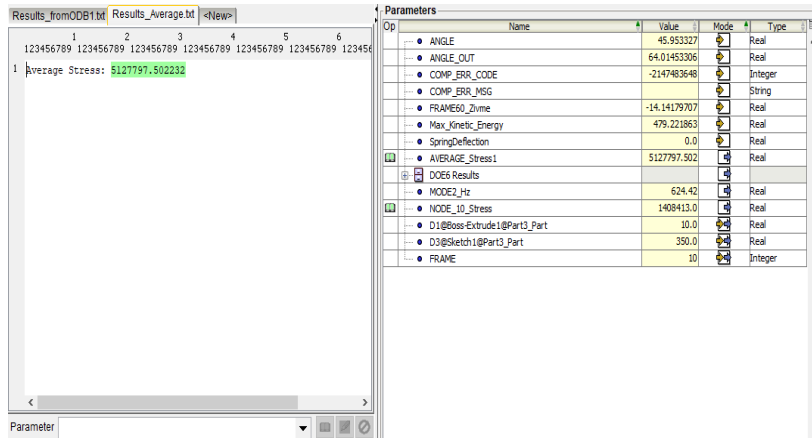


Figure 4-78. Data Exchanger-2 Output Selection- Static Model Average Stress

For Modal Analysis Abaqus-2 component runs with python. With help of python, from the '.dat' file Mode 2 is selected and delivered to Data Exchanger-4, and the 2<sup>nd</sup> mode shape was selected as design output response as it can be seen from Figure 4-79.

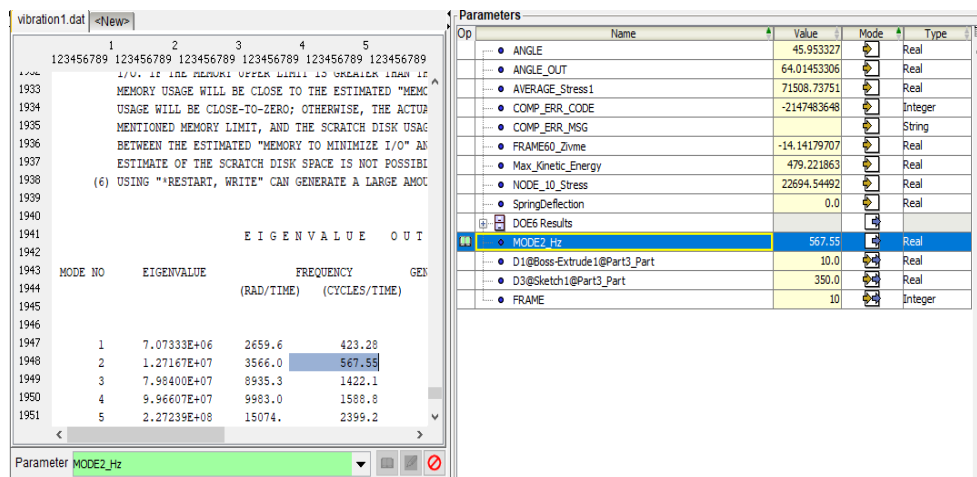


Figure 4-79. Data Exchanger-4 Output Selection- Modal Analysis-Mode 2

#### 4.4.3 Design of Experiment

In this case Design of the Experiment was selected as an optimization technique. In the Design of Experiment, there are several methods. Some of them are gradient-based algorithms. These are:

- Adaptive DOE
- Box-Behnken
- Central Composite
- Fractional Factorial
- Full Factorial
- Latin Hypercube
- Optimal Latin Hypercube
- Orthogonal Array
- Parameter Study

The main idea is to change the angle of configuration and not to affect the Explicit Analysis. However, the change in the configuration should affect both Modal and Static Analysis. In addition, the CAD data is needed to update geometrically, for all analysis types. These are the rules of obtaining input parameters.

The geometrical inputs' limits should be indicated in order to avoid defects in analysis. For the length of connecting rod upper limit should be 385 and the lower limit should be 315 mm. The CAD data mechanism permits these variables kinematically. Moreover, off-limits values cause the connecting rod to clash with slider fitting. On the other hand, the width of connecting rod's limit values can be selected arbitrarily.

In Explicit Analysis, Abaqus divides the results into a certain time step. The time step is given by the user and in this analysis, it is given as 50 steps. So, the angle of the mechanism under explicit analysis conditions is divided into 50 angles and these are represented as the term 'frame'. Therefore, for the angle of configuration, the upper and lower limits are 1 and 50 frames which are shown in Table 4-11:

Table 4-11. Frame- Angle Conversion

Frame	Angle (°)	Frame	Angle (°)	Frame	Angle (°)
0	80	17	305.3879	34	296.389
1	79.98065	18	282.3688	35	187.2749
2	79.84343	19	257.4196	36	61.95979
3	79.47076	20	226.169	37	288.6216
4	78.74595	21	179.5826	38	142.5433
5	77.55405	22	124.0838	39	10.81648
6	75.7823	23	81.87482	40	220.4469
7	73.31915	24	40.73325	41	52.55348
8	70.05076	25	333.5056	42	244.8961
9	65.85181	26	278.1163	43	58.96344
10	60.56651	27	219.2677	44	240.5305
11	53.97014	28	127.1465	45	46.58821
12	45.68665	29	61.13996	46	219.52
13	34.98688	30	330.9237	47	18.70474
14	20.205	31	253.9313	48	168.3309
15	357.5628	32	142.0905	49	319.457
16	329.6842	33	52.38023	50	115.0253

For this study Frame number 4, 27, 50 was selected (Angle: 70.05°, 219.26°, 115.02°).

Based on this information, other than Full Factorial and Fractional Factorial methods does not fully obey the rules preceding. Other methods, build a design matrix with focuses the satisfying the objective function in any circumstances, they ignore the scan of all angle configurations. They find the best possible proper angle and dimension yielding the objective and start to focus on their zone. Therefore, most of the angle configurations are ignored. In order to avoid this problem, angle input should be given earlier and optimization of geometry should be made on the imputed configurations. 'Full Factorial and Fractional Factorial' accept the input from the user for changing the angle and create a geometrical design matrix based on the imputed angle. Moreover, 'Full Factorial' allows investigating every factor were on the response variable. During this process, it permits the interaction between responses.

So, the Full Factorial Method was selected. The selected inputs for the Full Factorial DOE are given in Figure 4-80:

General Factors Design Matrix Postprocessing						
	Parameter	# Levels	Levels	Relation	Baseline	Values
<input type="checkbox"/>	• d					
<input checked="" type="checkbox"/>	• D1@Boss-Extrude1@Part3_Part	2	-25.0 25.0	%	10.0	7.5 12.5
<input checked="" type="checkbox"/>	• D3@Sketch1@Part3_Part	6	315.0 329 343 357 371 385.0	values	350.0	315.0 329 343 357 371 385.0
<input type="checkbox"/>	• Diam					
<input checked="" type="checkbox"/>	• FRAME	5	4 16 27 39 50	values	10	4 16 27 39 50
<input type="checkbox"/>	• n					

Figure 4-80. DOE Inputs

Responses				
	Parameter	Objective	Weight	Target
<input checked="" type="checkbox"/>	• MODE2_Hz	minimize	1.0	
<input checked="" type="checkbox"/>	• Max_Kinetic_Energy	minimize	1.0	
<input checked="" type="checkbox"/>	• AVERAGE_Stress1	minimize	0.001	
<input type="checkbox"/>	• NODE_10_Stress			
<input type="checkbox"/>	• SpringDeflection			
<input type="checkbox"/>	• ANGLE_OUT			
<input type="checkbox"/>	• FRAME60_Zivme			
<input type="checkbox"/>	• ANGLE			
<input type="checkbox"/>	• COMP_ERR_MSG			
<input type="checkbox"/>	• COMP_ERR_CODE			

Figure 4-81. DOE Outputs

For arranging DOE outputs, weight constant needs to be given according to design variables' number of digits. Stress values have the highest number value among the natural frequency and kinetic energy value, therefore its weight constant should be considerably low. In contrast, if all these three variables weight functions are similar to each other, the design solution optimization

Table 4-12. Design Matrix for DOE-Full Factorial

Run#	Width of Connecting Rod (mm)	Length of Connecting Rod (mm)	Angle (degree)
1	7.5	315	70.05°
2	7.5	315	219.26°
3	7.5	315	115.02°
4	7.5	338.333	70.05°
5	7.5	338.333	219.26°
6	7.5	338.333	115.02°
7	7.5	361.667	70.05°
8	7.5	361.667	219.26°
9	7.5	361.667	115.02°
10	7.5	385	70.05°
11	7.5	385	219.26°
12	7.5	385	115.02°
13	12.5	315	70.05°
14	12.5	315	219.26°
15	12.5	315	115.02°
16	12.5	338.333	70.05°
17	12.5	338.333	219.26°
18	12.5	338.333	115.02°
19	12.5	361.667	70.05°
20	12.5	361.667	219.26°
21	12.5	361.667	115.02°
22	12.5	385	70.05°
23	12.5	385	219.26°
24	12.5	385	115.02°

only considers the Stress Values. Because its weight constant 'x value' is much higher than others and it will dominate the others.

The weight coefficients and output responses are given in Figure 4-81.

- Cost Function:

$$Y = \beta_1 x X_1 + \beta_2 x X_2 + \beta_3 x X_3 + \epsilon$$

Where;

$$X_1 = \text{Average Stress}$$

$$X_2 = \text{Kinetic Energy}$$

$$X_3 = \text{2nd Mode Shape}$$

$$\beta_1 = 0.01$$

$$\beta_2 = 1$$

$$\beta_3 = 1$$

$$\epsilon = \text{Total Error}$$

- Objective Function:

$\min\{f(\zeta): \zeta \in \mathbb{R}^n\}$  is the objective generalized function.

Table 4-13. Result Table of DOE

Design Number	Width of Connecting Rod (mm)	Length of Connecting Rod (mm)	Investigated Zone-Average Stress (Pa)	Max Kinetic Energy of System (J)	2 <sup>nd</sup> Mode Shape (Hz)
1	7.5	315	21849.06475	341.923309	466.56
2	7.5	315	1099458.818	341.923309	465.28
3	7.5	315	5856411.344	341.923309	465.78
4	7.5	338.333	22344.6096	401.807343	405.3
5	7.5	338.333	801035.0098	401.807343	405.02
6	7.5	338.333	801035.0098	401.807343	405.02
7	7.5	361.667	22537.30525	429.207703	354.94
8	7.5	361.667	654166.3131	429.207703	355.52
9	7.5	361.667	7067822.019	429.207703	355.36
10	7.5	385	23663.69305	381.97995	313.76
11	7.5	385	624971.1164	381.97995	313.84
12	7.5	385	10633646.64	381.97995	312.17
13	12.5	315	14952.73124	353.942078	642.39
14	12.5	315	461004.9863	353.942078	624.22
15	12.5	315	6440357.092	353.942078	663.62
16	12.5	338.333	15435.49093	315.283173	559.36
17	12.5	338.333	314379.3701	315.283173	551.63
18	12.5	338.333	7443040.783	315.283173	542.75
19	12.5	361.667	14832.4923	326.39035	491.12
20	12.5	361.667	246472.874	326.39035	489.68
21	12.5	361.667	3193723.808	326.39035	494.04
22	12.5	385	15602.94083	321.202911	434.75
23	12.5	385	254933.8096	321.202911	436.34
24	12.5	385	5940465.328	321.202911	443.83



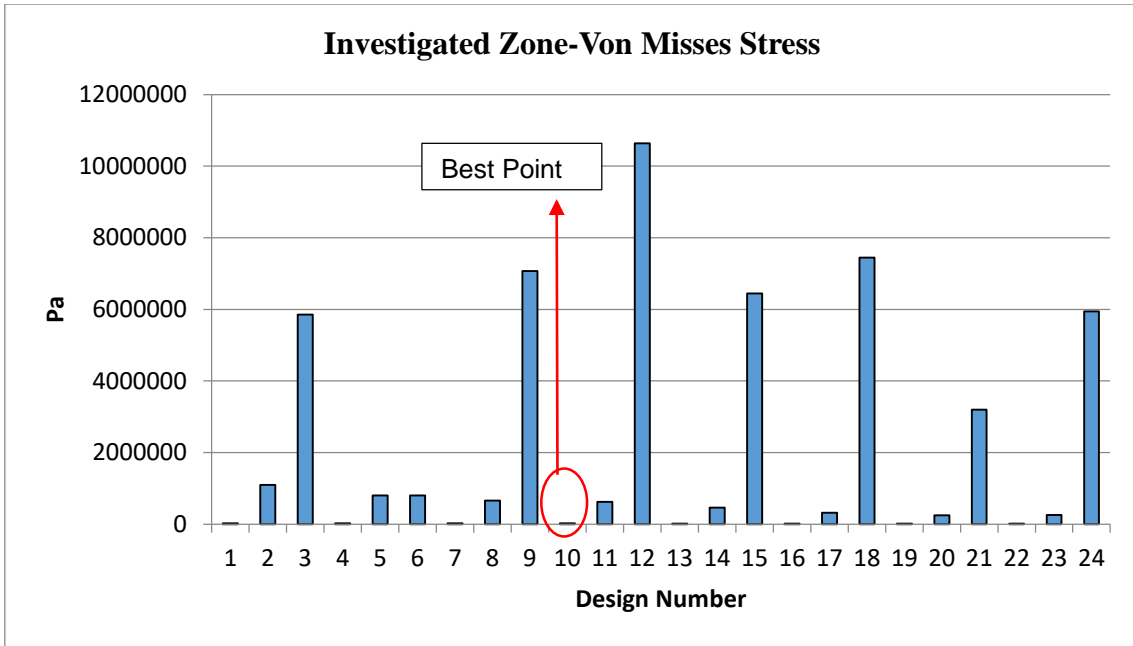


Figure 4-82. Investigated Zone Von-Misses Stress vs Design Number

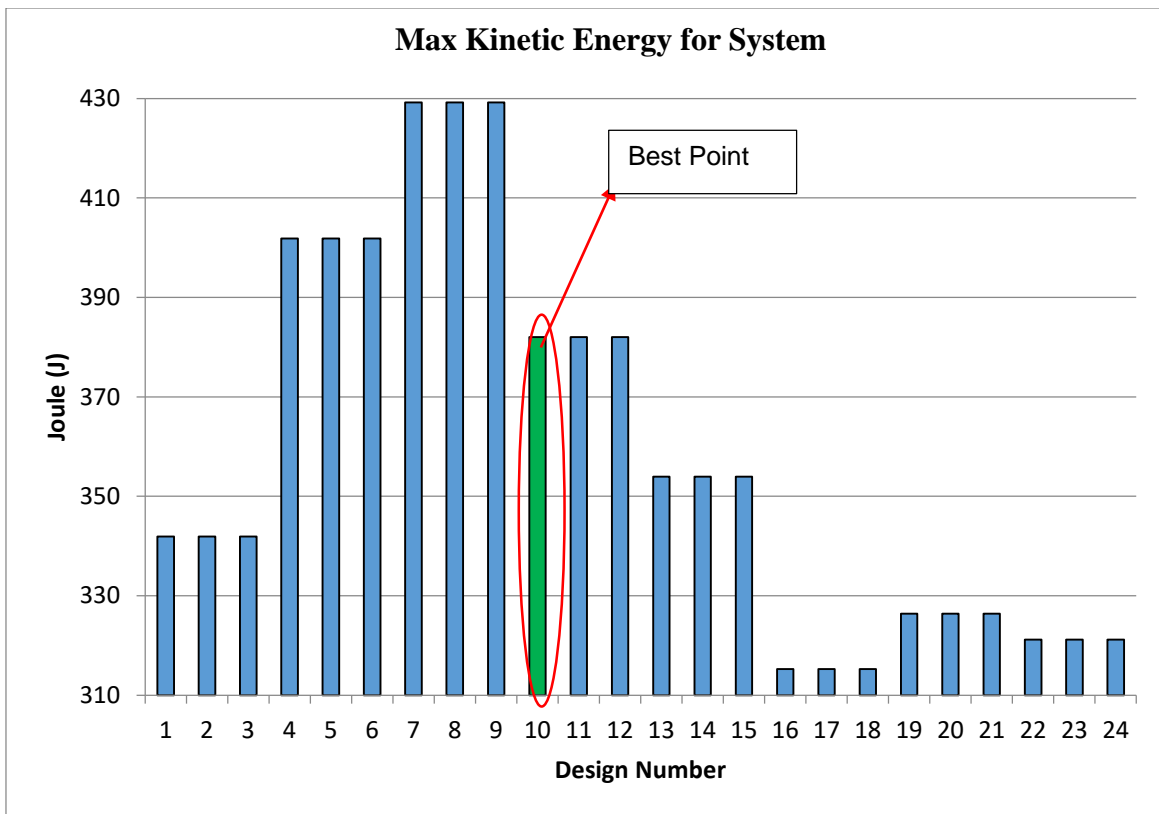


Figure 4-83. Kinetic Energy vs Design Number

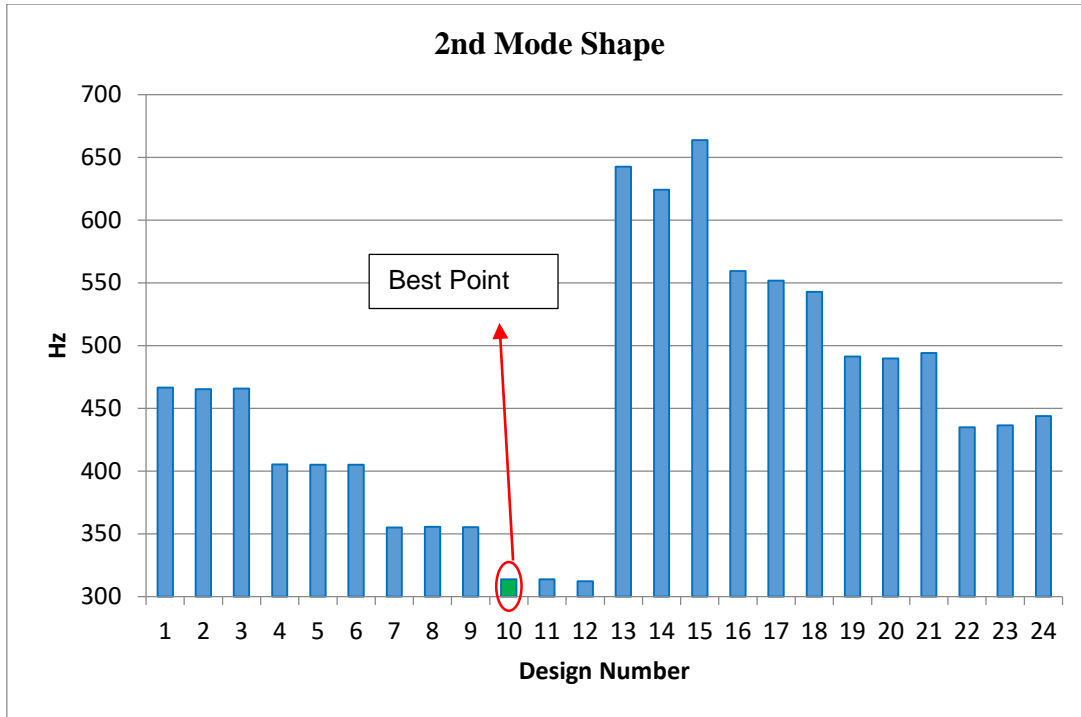
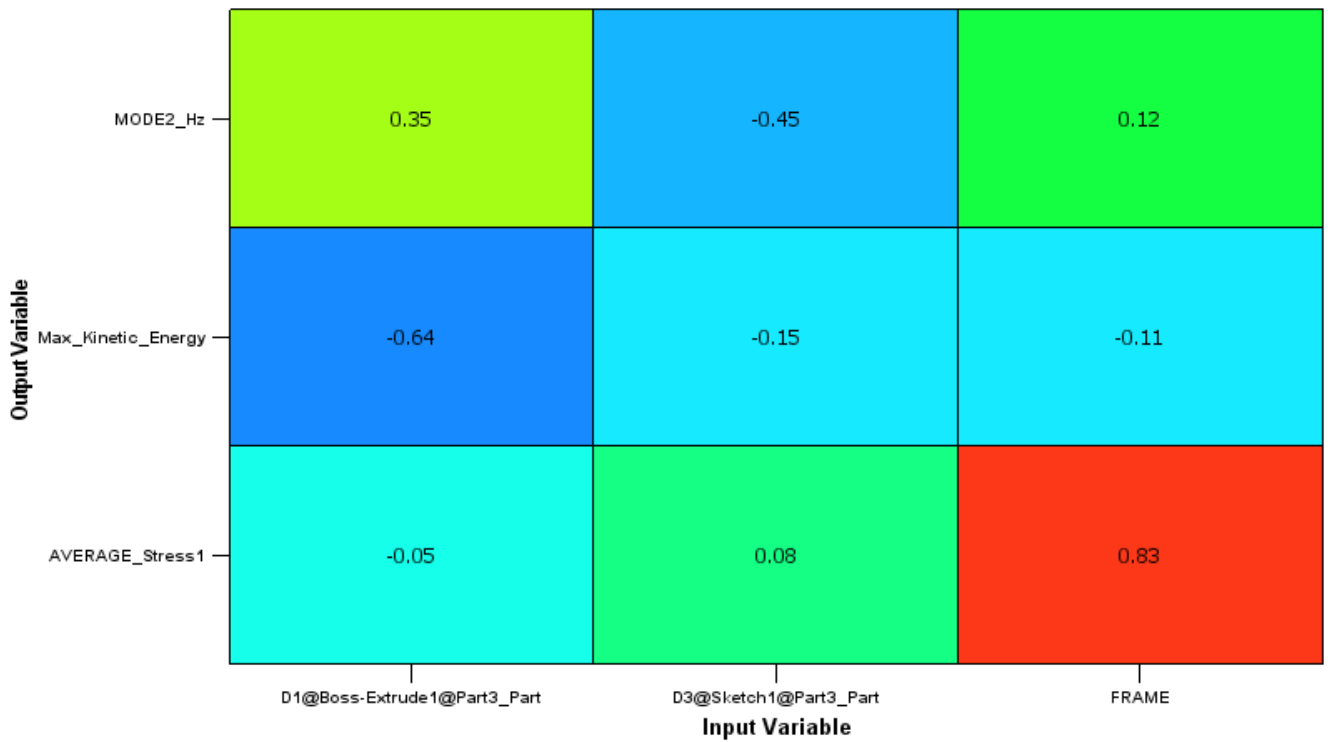


Figure 4-84. Mode Shape vs Design Number



Job(s): LOCAL\_12808024  
 Start Date: 20/09/21 19:38  
 Component: DOE6

Figure 4-85. Pareto Table between Input and Outputs

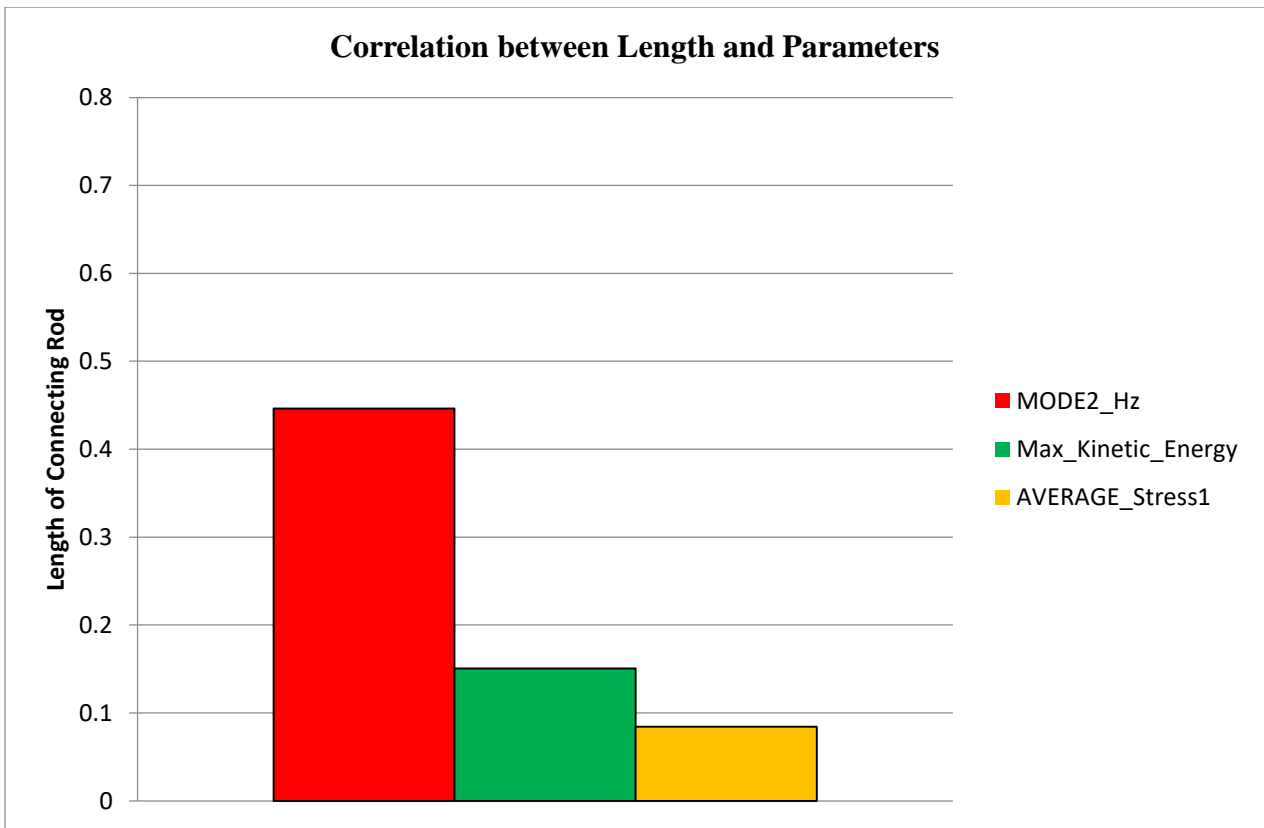


Figure 4-86. Correlation Graph of Rod Length and Other Parameters

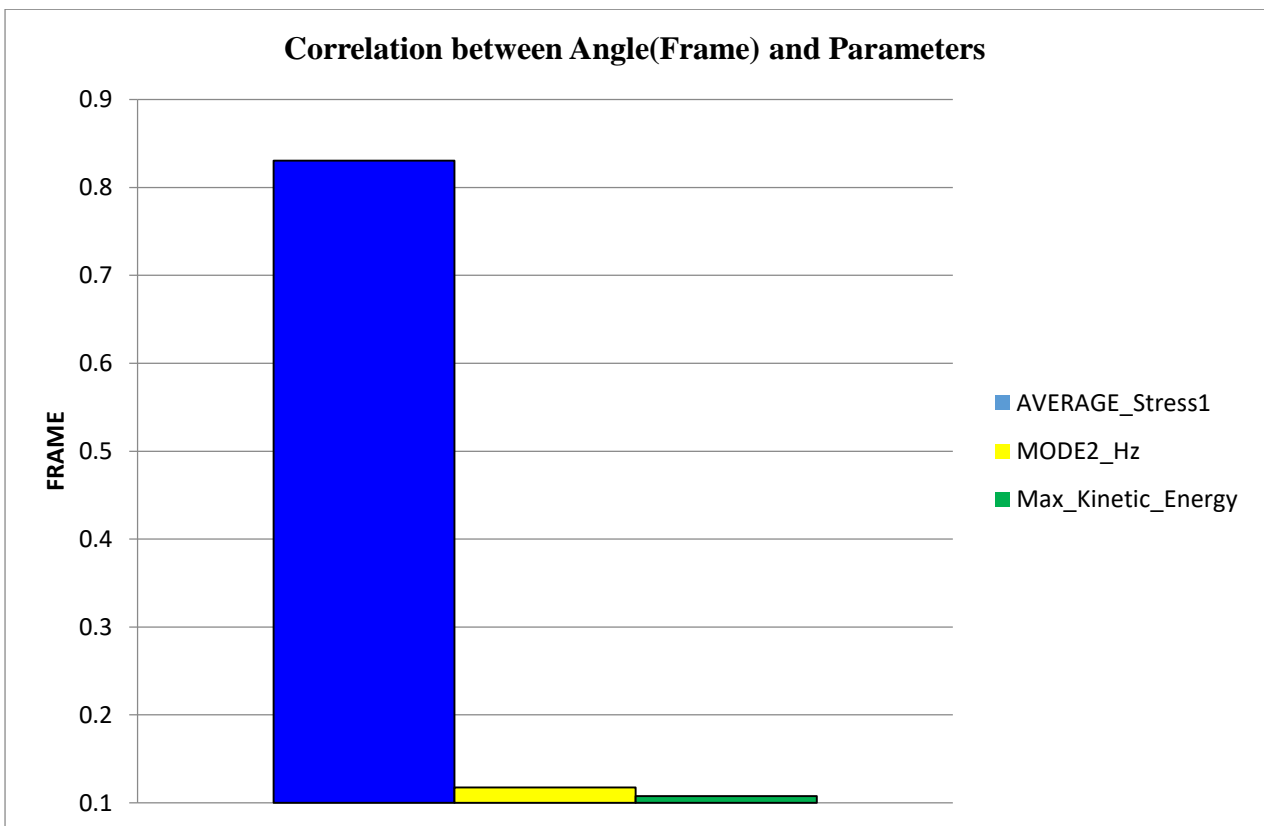


Figure 4-87. Correlation Graph of Angle (Frame) and Other Parameters

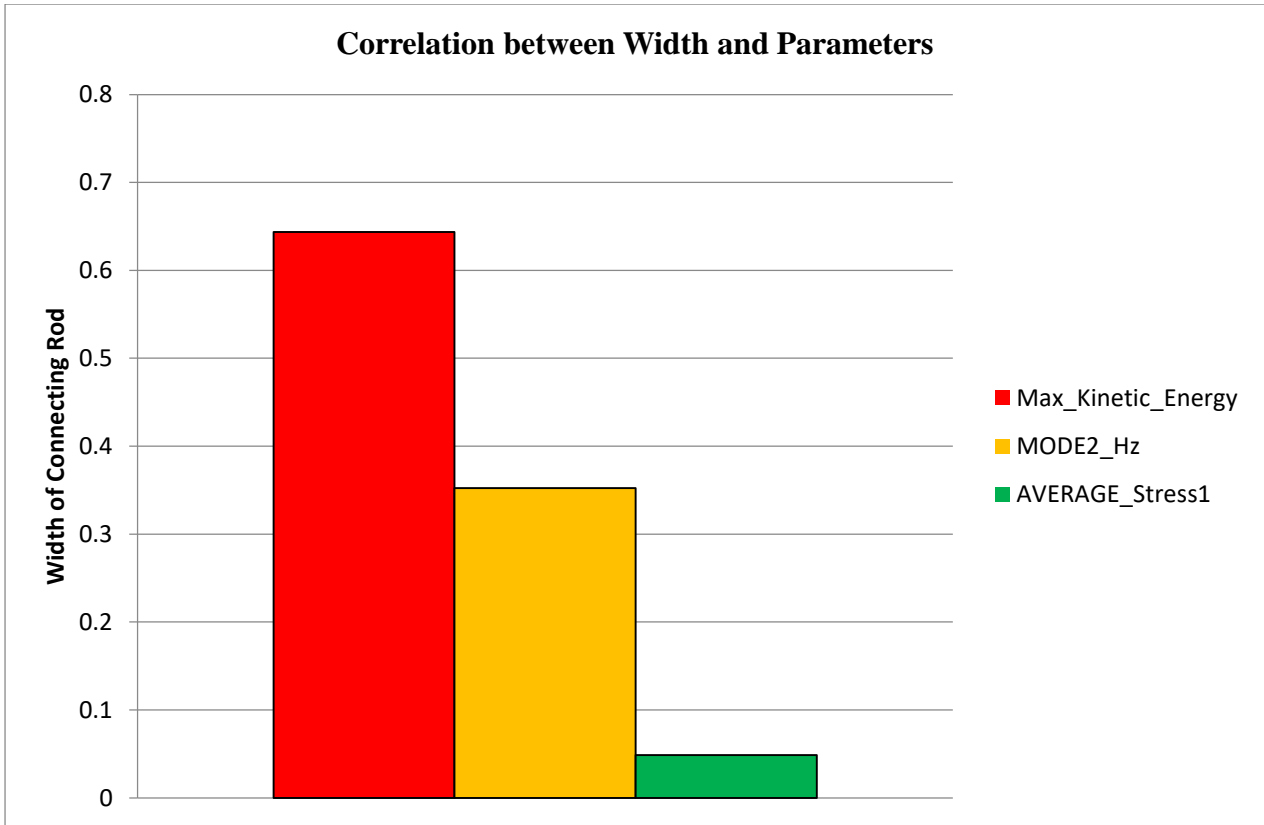


Figure 4-88. Correlation Graph of Width of Rod and Other Parameters

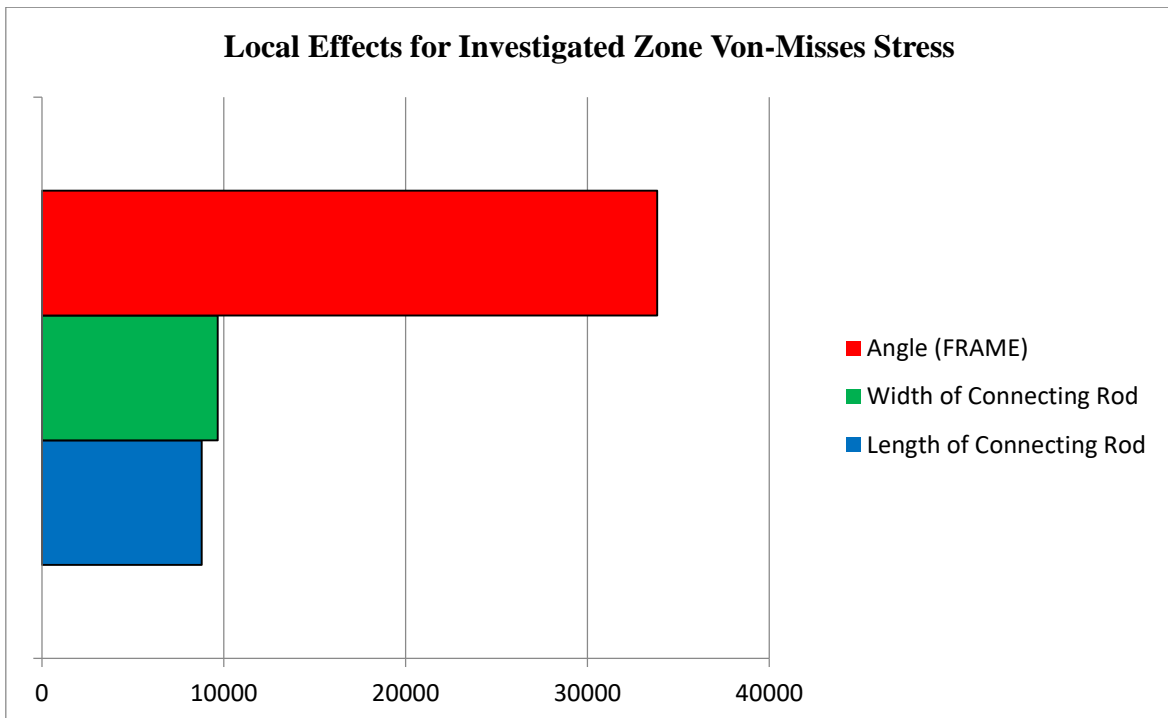


Figure 4-89. Local Effects for Stress

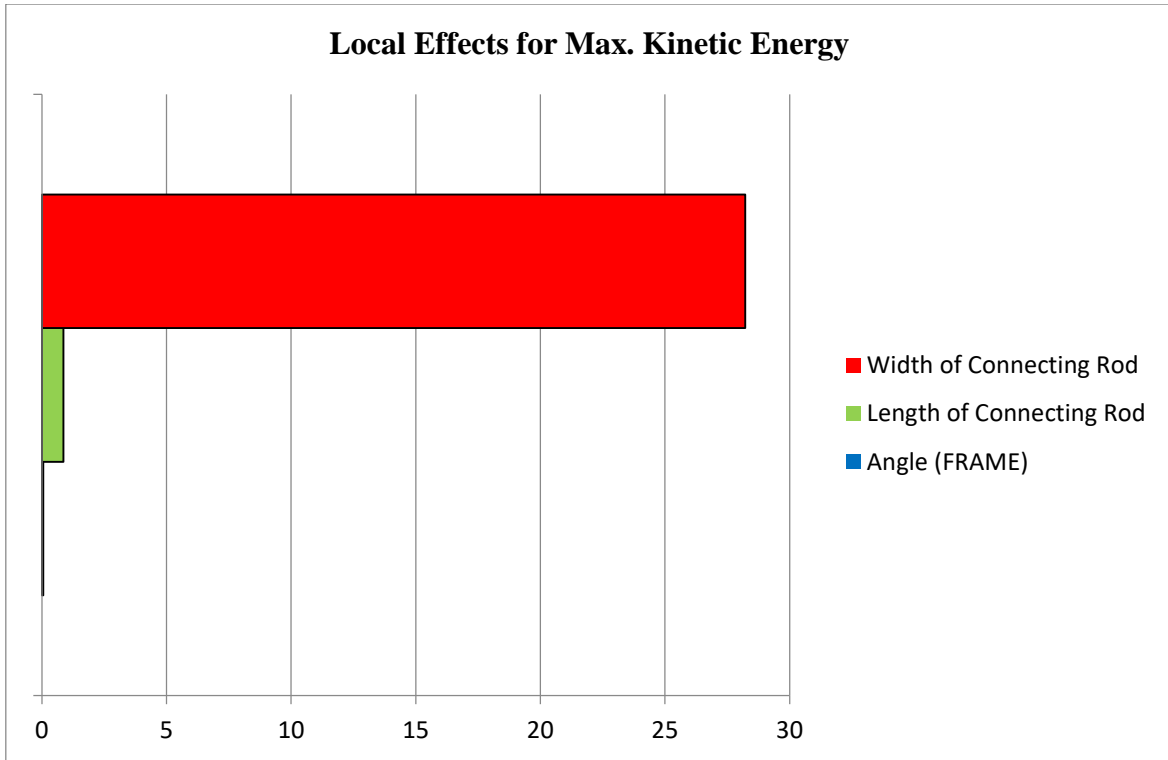


Figure 4-90. Local Effects for Kinetic Energy

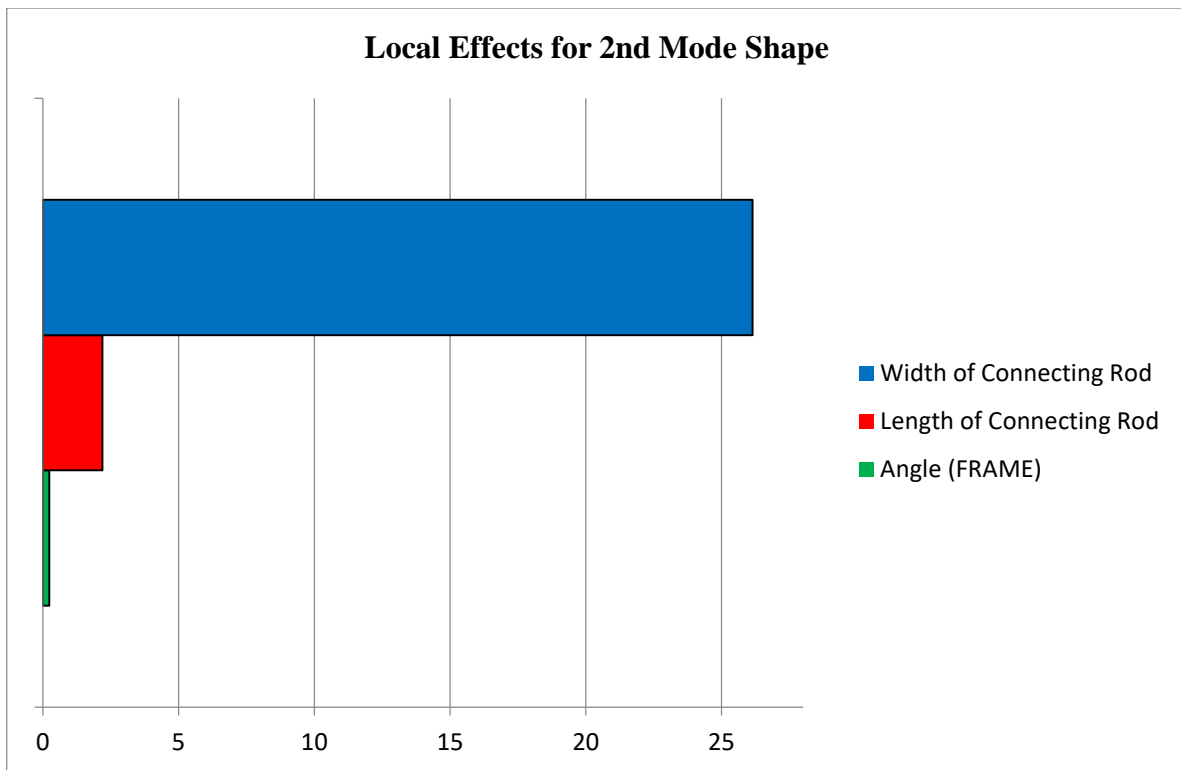


Figure 4-91. Local Effects for Mode Shape

$\zeta = [\zeta_1 \zeta_2 \zeta_3 \dots \dots \dots \zeta_n]^T$  is the vector variables of the cost function.

For each factor of design variables' level is defined and possible combinations of each design variable at each level are investigated in Table 4-12. For every geometrical design and angle change are categorized as a level. When the Table 4-12 is examined, it can be seen, same geometry given inputs are implemented for four design iteration with change in angle for each iteration, later the next four design the new geometry is implemented with the angle change for each iteration. Applying changes with this method, scans the all possible design inputs in given conditions.

- **Advantages:**

For any levels, all number of level minus 1 order effects can be investigated. Every possible interaction can be evaluated.

- **Disadvantages:**

Takes too much time since it works multiple factors for various factor at separated levels. As an example, 4 factors studied at 4 levels requires 256 design points.

#### 4.4.4 Results and Conclusion

The results that were produced by DOE-Full Factorial, are given in Table 4-13, the 10<sup>th</sup> design (green row) was selected the best optimum point by Isight:

According to the Isight DOE mechanism Design, 10<sup>th</sup> design stands the best solution among the 24 designs. When the results are investigated in Table 4-13, it can be seen from every design variable Full Factorial Method creates every possible variation. And the judgement process is done according to all these variables. However, when the table is investigated, there are better solutions for each investigated parameter. So in order to examine better the design variables, each design variable should be compared in their family tree.

According to Analysis results, stress output mostly depends on frame input which represents the angle of assembly as it can be seen from Figure 4-87 and Figure 4-89. This is truly understandable since the configuration of assembly affects directly the selected stress area which was the connecting point of the slider-connecting rod. Despite applying a short range for the width of the rod, being thicker or thinner has of course more effect on changing the length of the rod. Because, at the end of the rod, rotational accelerations almost get to zero and little accelerations produce small force and stress. After that kinetic energy and mode shape outputs depend on mostly the width of the connecting rod which is can be seen in Figure 4-86, Figure 4-88, Figure 4-90 and Figure 4-91. Again, the end of the rod has little acceleration and this cause less force and energy. Finally, the thicker width creates a more rigid structure which cause the change in the mass and stiffness matrix. From Figure 4-91 making thicker the rod has a positive effect on the mode shape.

Furthermore, historically the best solution comes in different positions for every output. For the kinetic energy obtained result is not best solution as it can be seen from Figure 4-83. However, it still obtained better solution than its initial value. DOE obtained the approximately best solution for other output responses (mode shape and stress), as it can be seen from Figure 4-82 and Figure 4-84. That indicates it is not possible to obtain the best design that meets every expectation. This

situation may be overcome by applying different weight constants but still, it will be in the range of some limitations.

Furthermore, the angle of configuration changes the response family and their best option. To investigate correctly, for selected angles and their response family, optimum solutions should be examined in their own family. Following, these optimum solutions should be compared to each other and the best design will be revealed.

In conclusion among all three inputs (2 geometrical, 1 angle), angle input has the most influence on the stress, kinetic energy and mode shape. The configuration of the system has the ability to affect the force distribution and it is the main cause of being the impact of the configuration on the output responses.

#### 4.4.5 Alternative Methods

As an alternative to Full Factorial Design of Experiment, NLPQLP method was implemented.

NLPQLP method is special application of SQP method. It applies a quadratic approach of the Lagrangian method with linearized the constraints, build a quadratic formulation and solved.

General   Variables   Constraints   Objectives							
	Parameter	Lower Bound	Value	Upper Bound	Allowed Values	Scale Factor	
<input checked="" type="checkbox"/>	● FRAME	13.0	1	50.0		1.0	
<input checked="" type="checkbox"/>	● D3@Sketch1@Part3_Part	315.0	350.0	385.0		1.0	
<input checked="" type="checkbox"/>	● D1@Boss-Extrude1@Part3_Part	7.5	10.0	12.5		1.0	
<input type="checkbox"/>	● n		0.0				
<input type="checkbox"/>	● d		0.0				
<input type="checkbox"/>	● Diam		0.0				

Figure 4-92. NLPQLP Inputs

General   Variables   Constraints   Objectives						
	Parameter	Direction	Target	Scale Factor	Weight Fac...	
<input checked="" type="checkbox"/>	● AVERAGE_Stress1	minimize		1.0	0.001	
<input checked="" type="checkbox"/>	● Max_Kinetic_Energy	minimize		1.0	1.0	
<input checked="" type="checkbox"/>	● MODE2_Hz	minimize		1.0	1.0	
<input type="checkbox"/>	● ANGLE					
<input type="checkbox"/>	● ANGLE_OUT					
<input type="checkbox"/>	● COMP_ERR_CODE					
<input type="checkbox"/>	● D1@Boss-Extrude1@Part3_Part					
<input type="checkbox"/>	● D3@Sketch1@Part3_Part					
<input type="checkbox"/>	● FRAME					
<input type="checkbox"/>	● FRAME60_Zivme					
<input type="checkbox"/>	● NODE_10_Stress					
<input type="checkbox"/>	● SpringDeflection					

Figure 4-93. NLPQLP Outputs

In Figure 4-92 and Figure 4-93, design input and outputs were selected and implemented in the NLPQLP method. The same weight factor and same objective which is minimizing the output responses were applied.

Inputs and upper-lower limitations were the same as in the Full Factorial method. The main difference is inputs are built during the analysis process based on the distance from the objective function.

In Table 4-14, the investigated angle and design number were given. The configuration angles were created during the analysis and final list of the angle inputs are constructed at the end of the analysis.

Table 4-15 is shown the geometrical input and outputs responses of the NLPQLP method. The output responses are the same as DOE, which is Investigated Zone Stress, Total Kinetic Energy and 2<sup>nd</sup> Mode Shape. In addition, it can be seen from the Table 4-15, 33<sup>rd</sup> design (green row) is the best optimum design selected by NLPQLP analysis.

Table 4-14. Investigated Angle-Frame

Design Number	Angle (degree)	Design Number	Angle (degree)	Design Number	Angle (degree)
1	60.56651	18	79.84343	35	79.98065
2	60.56651	19	79.84343	36	79.84343
3	60.56651	20	79.47076	37	79.98065
4	53.97014	21	79.98065	38	79.98065
5	75.7823	22	79.98065	39	79.98065
6	75.7823	23	79.98065	40	79.98065
7	75.7823	24	79.98065	41	79.98065
8	73.31915	25	79.84343	42	79.98065
9	70.05076	26	79.98065	43	79.98065
10	70.05076	27	79.98065	44	79.98065
11	70.05076	28	79.98065	45	79.98065
12	65.85181	29	79.84343	46	79.98065
13	45.68665	30	79.98065	47	79.98065
14	45.68665	31	79.98065		
15	45.68665	32	79.98065		
16	34.98688	33	79.98065		
17	79.84343	34	79.98065		



Table 4-15. NLQP Design Inputs and Outputs Results

Design Number	Width of Connecting Rod (mm)	Length of Connecting Rod (mm)	Investigated Zone-Average Stress (Pa)	Max Kinetic Energy of System (J)	2 <sup>nd</sup> Mode Shape (Hz)
1	10	350	46909.97093	374.174225	426.42
2	10.01	350	47037.68992	371.984131	426.78
3	10	350.35	46730.65745	371.463684	425.56
4	10	350	51432.41781	374.174225	425.79
5	12.5	360.7138699	23772.37373	329.075195	493.11
6	12.4875	360.7138699	23280.66926	335.962799	492.78
7	12.5	361.0745838	23268.14278	324.184357	492.21
8	12.5	360.7138699	26927.84626	329.075195	492.68
9	12.5	367.1073795	31095.11553	327.083038	475.47
10	12.4875	367.1073795	30431.99928	326.659149	475.19
11	12.5	367.4744869	31196.34407	326.656586	474.58
12	12.5	367.1073795	35528.13174	327.083038	474.87
13	12.04084278	385	50555.7838	313.134064	417.07
14	12.05288362	385	50293.72081	314.595184	417.42
15	12.04084278	384.615	52444.29944	311.479767	417.8
16	12.04084278	385	59605.26508	313.134064	415.99
17	11.93153585	385	7944.658292	324.419403	417.65
18	11.94346738	385	7834.294628	325.733063	418.09
19	11.93153585	384.615	7935.356456	322.137268	418.48

Design Number	Width of Connecting Rod (mm)	Length of Connecting Rod (mm)	Investigated Zone-Average Stress (Pa)	Max Kinetic Energy of System (J)	2 <sup>nd</sup> Mode Shape (Hz)
20	11.93153585	385	11707.45983	324.419403	417.71
21	11.88639816	384.5457915	3972.45325	329.770844	417.29
22	11.91054499	384.7887746	3912.593583	319.548737	417.6
23	11.92245554	384.7887746	3912.708161	321.177643	417.91
24	11.91054499	384.4039859	3973.773107	321.537903	418.3
25	11.91054499	384.7887746	7944.643803	319.548737	417.46
26	7.5	374.9182576	5843.33092	363.908447	330.86
27	7.5075	374.9182576	5765.508786	366.74884	330.51
28	7.5	375.2931758	5764.618515	368.605164	330.08
29	7.5	374.9182576	11413.16838	363.908447	330.94
30	7.5	374.7753778	5811.463684	401.194946	331.11
31	7.5	374.9039696	5843.76265	367.897644	330.75
32	7.5	374.9168288	5826.559927	364.270081	330.66
33	7.5	374.9181147	5853.341861	363.782471	330.71
34	7.5075	374.9181147	5853.707382	366.845795	330.63
35	7.5	375.2930328	5861.367313	368.734985	330.09
36	7.5	374.9181147	11412.08579	363.782471	331.05
37	7.5	374.1101744	5835.65524	731.613586	332.67
38	7.5	374.8373207	5742.989822	387.390717	331.01
39	7.5	374.9100353	5733.995255	366.033539	331

<b>Design Number</b>	<b>Width of Connecting Rod (mm)</b>	<b>Length of Connecting Rod (mm)</b>	<b>Investigated Zone-Average Stress (Pa)</b>	<b>Max Kinetic Energy of System (J)</b>	<b>2<sup>nd</sup> Mode Shape (Hz)</b>
40	7.5	374.9173068	5738.467239	364.162079	330.72
41	7.5	374.9180339	5867.142862	363.962677	330.56
42	7.5	374.9181066	5839.224899	363.725281	330.9
43	7.5	374.9181139	5847.828189	363.963654	330.82
44	7.5	374.9181146	5833.215704	364.156311	330.86
45	7.5	374.9181147	5841.701385	363.861389	331
46	7.5	374.9181147	5846.520657	363.922119	330.77
47	7.5	374.9181147	5853.341861	363.782471	330.71

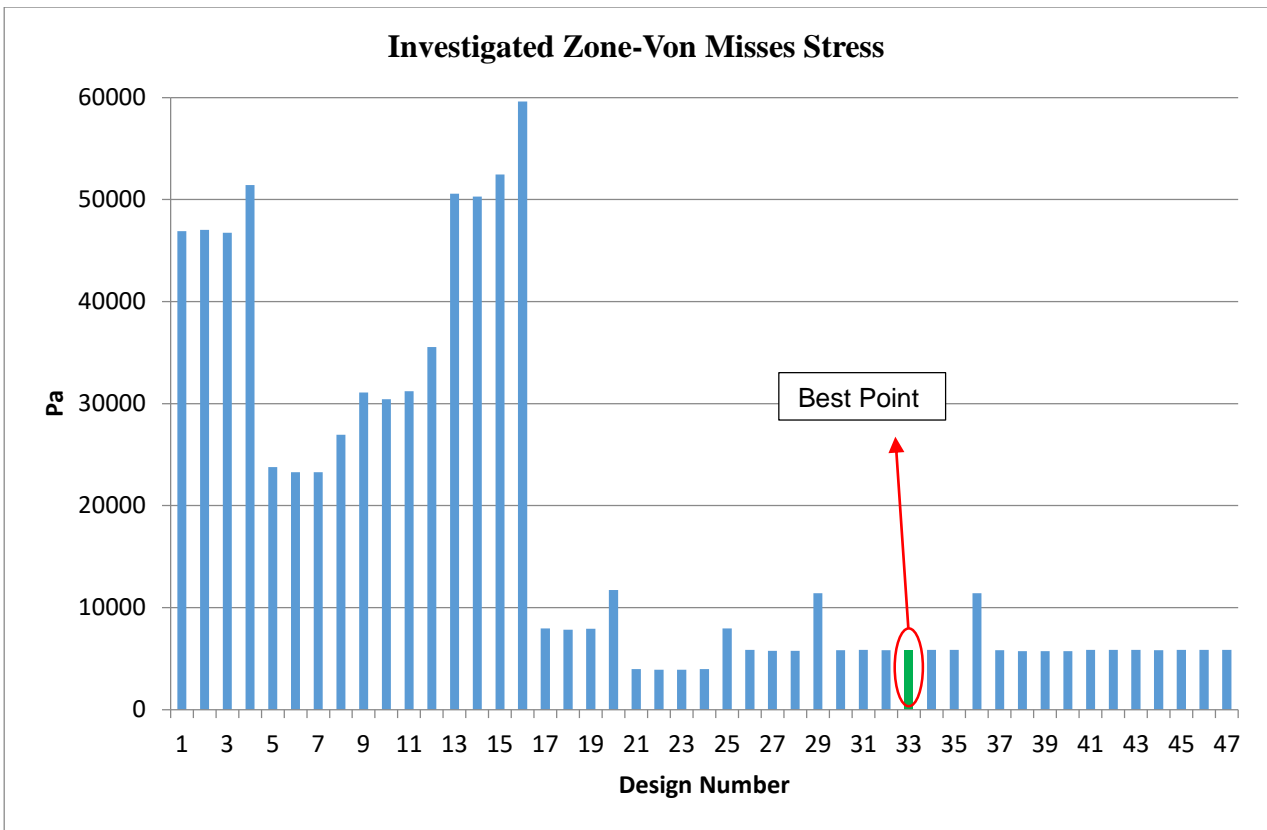


Figure 4-94. Stress vs Number of Design

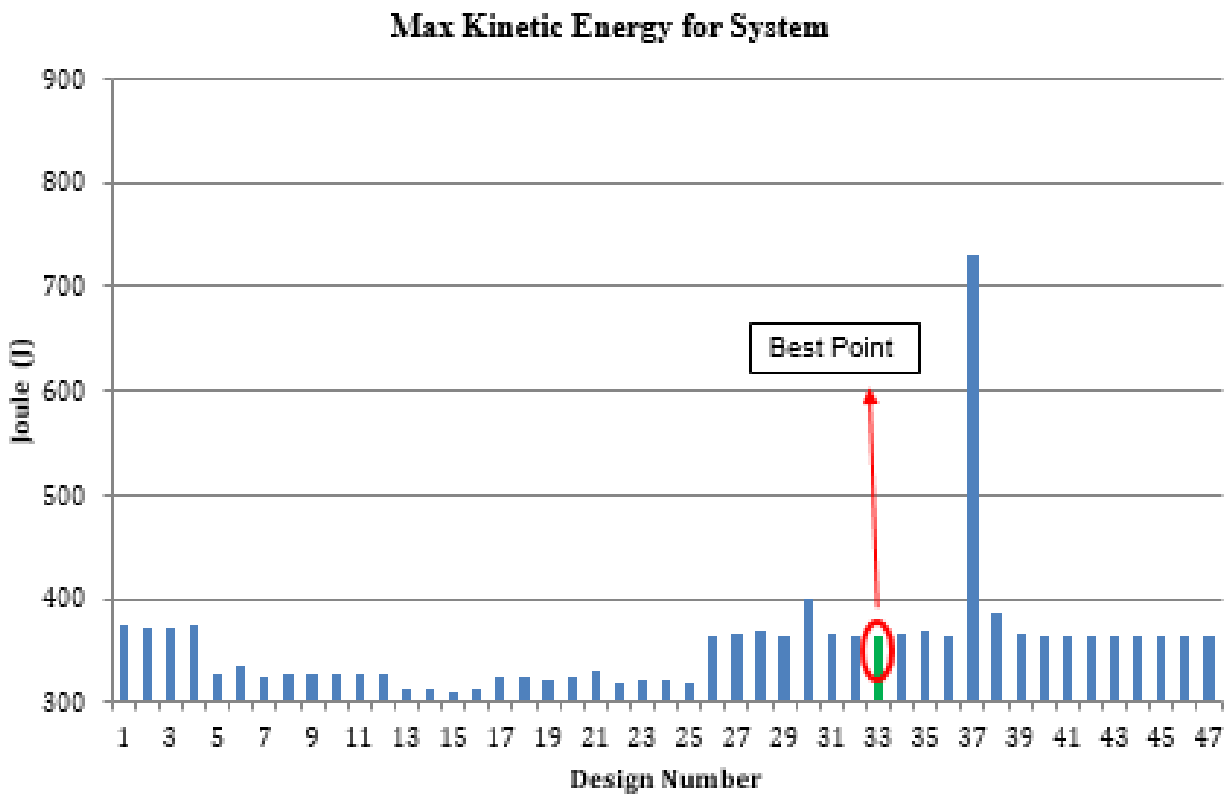


Figure 4-95. Kinetic Energy vs Number of Design

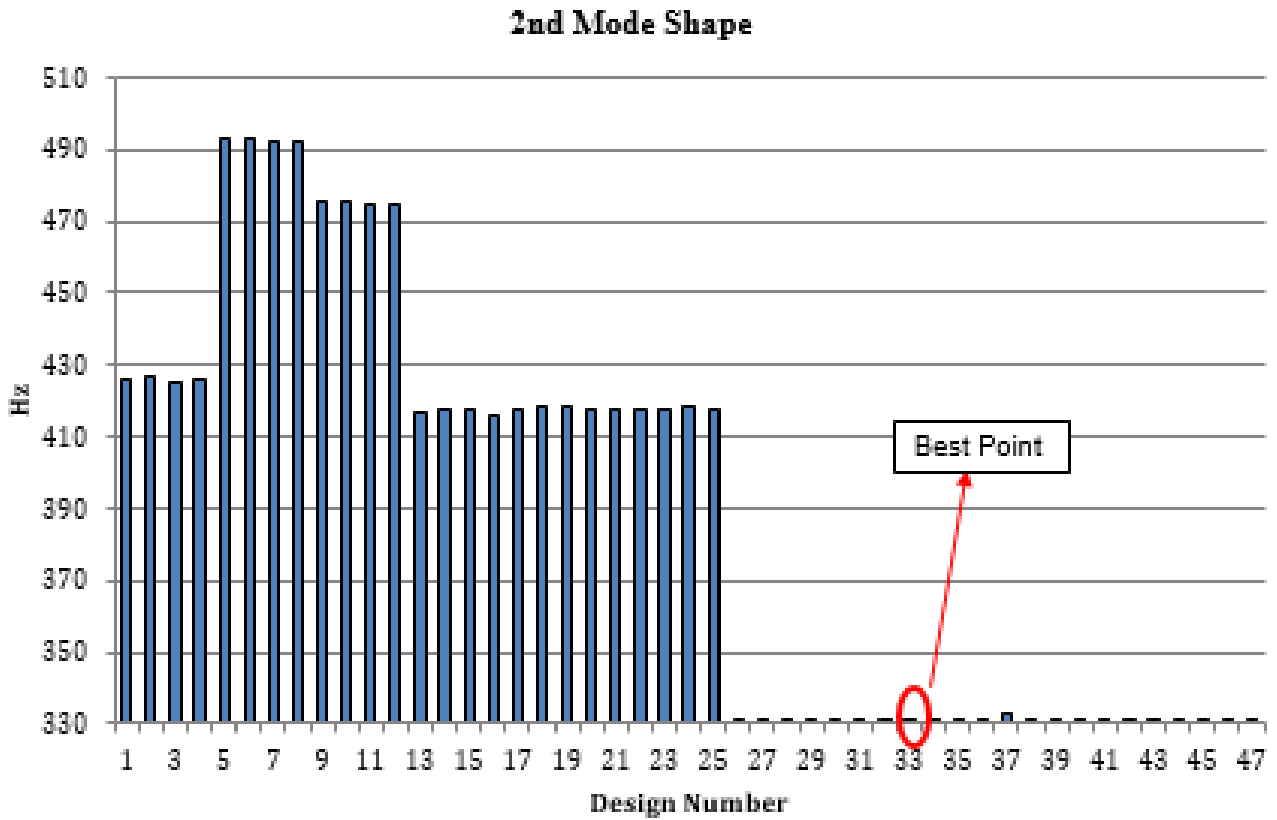


Figure 4-96. 2<sup>nd</sup> Mode Shape vs Number of Design

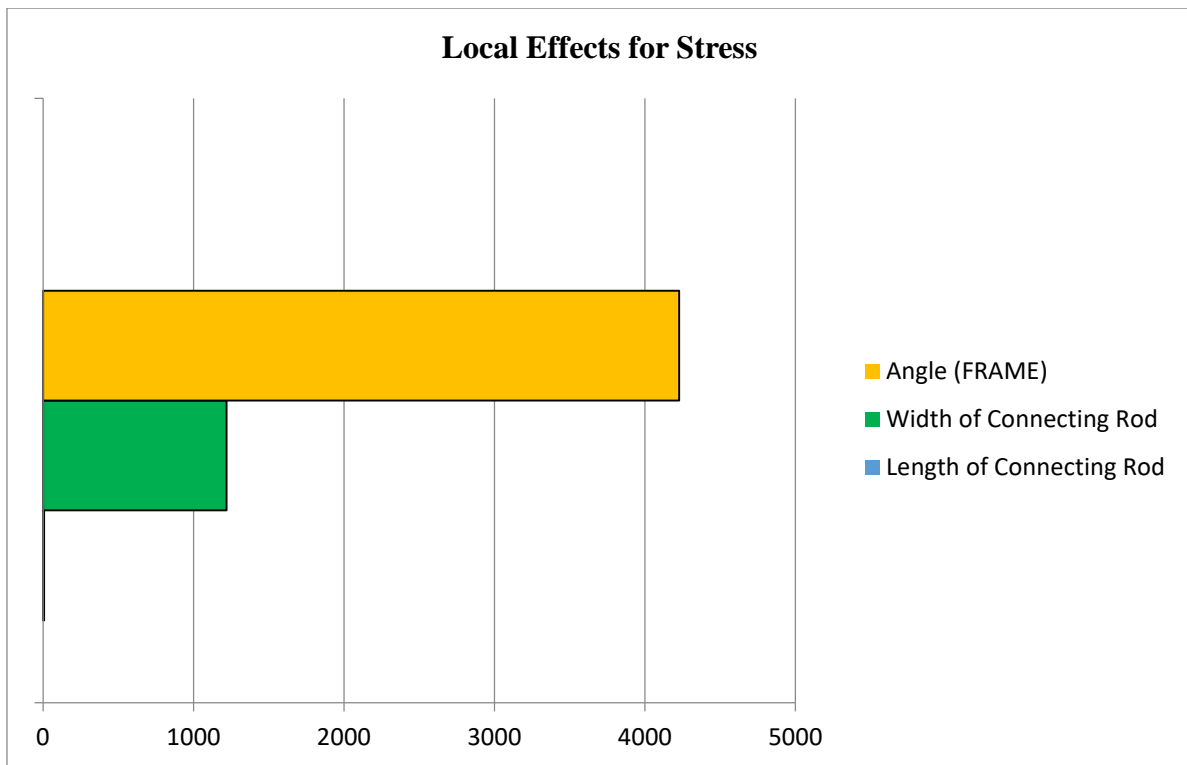


Figure 4-97. Local Effects for Investigated Zone Von-Misses Stress

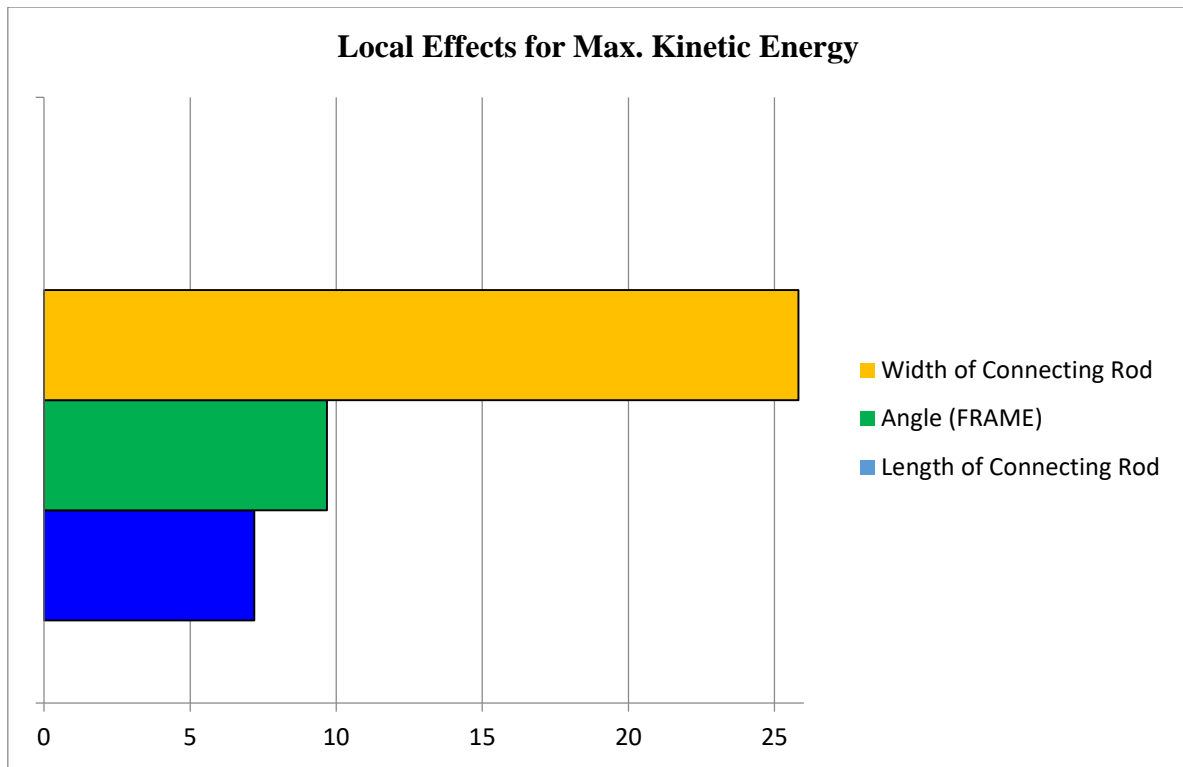


Figure 4-98: Local Effects for Kinetic Energy

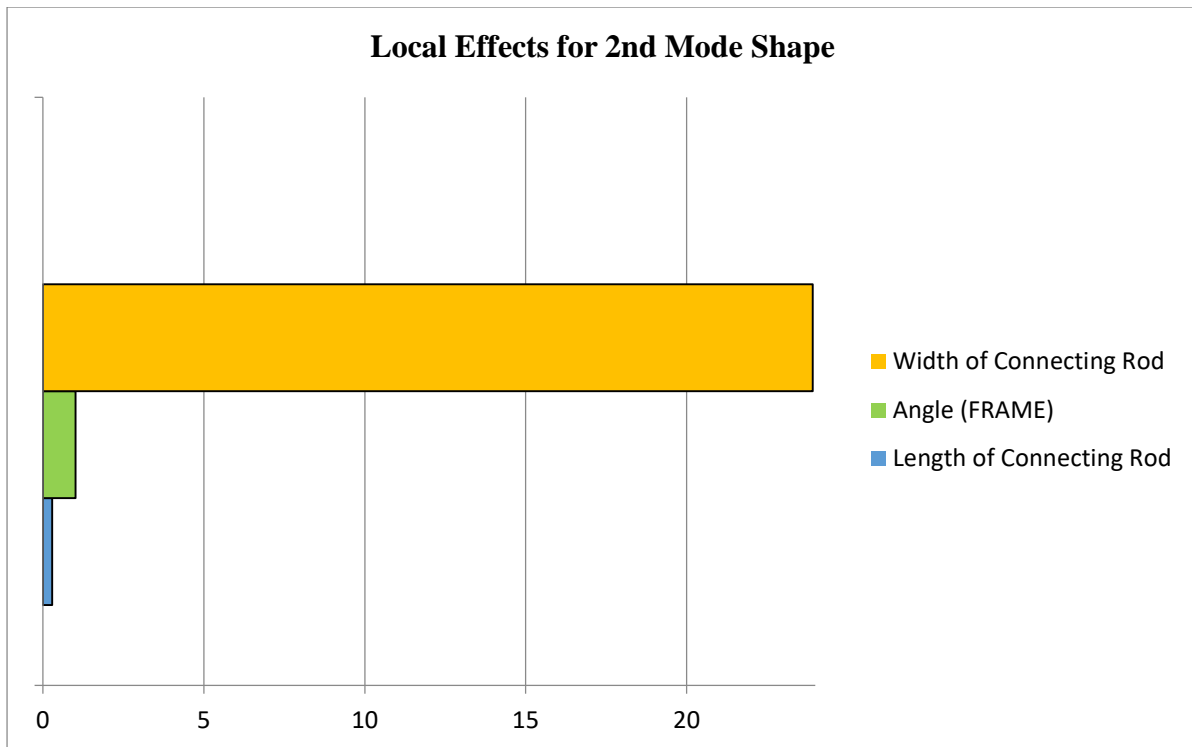


Figure 4-99. Local Effects for Mode Shape

In Table 4-15, it is shown the input and outputs of every parameter created during the NLPQLP method. As it can be seen, inputs are not discrete and they tend to behave in continuous variables. For example, from design number 5 to 12 length of connecting rod change is extremely low and continuous, there are no big changes in the length. This behaviour is the result of being the closest value of one of the objectives of output responses in these design numbers. In a simple explanation, the local extremum point near these design numbers.

The results of each output response were given in Figure 4-94, Figure 4-95 and Figure 4-96. From these figures, the best solution was discovered for the Mode Shape. However, the Maximum Kinetic Energy and Stress values were found one of the optimum solutions but not the best design.

The same effect encountered in the Full Factorial method was also observed in Local Effect graphics in this analysis type. The effects of length, width and frame (angle) almost same. This behaviour can be observable from Figure 4-97, Figure 4-98 and Figure 4-99.

In addition, as it can be seen from Table 4-14, NLPQLP method is mostly stuck on the same angle configuration. This method searches and find the best optimum minimum values for each design response and focus on these minimum areas. However, it lacks the ability to scan the whole angle configuration. It focuses on what it finds as minimum areas.

## 5. CONCLUSION

In this thesis, modal analysis, dynamic analysis and static analysis were made with parametric optimization via Isight. During the optimization process, 2 methods have been used, one of them Full Factorial which is a method of Design of Experiment and the other one is NLPQLP (Non-Linear Sequential Quadratic Programming). From the above results, it has been shown, the best optimal geometry was created for static and modal analysis, and for the dynamic analysis, the best geometrical solution has been extracted independently from the angle. When the local effects were investigated for each output, it can be observed this outcome clearly: That, stress analysis is based on mostly the width of the part and setup angle; for modal analysis, the width is the most crucial element and for the kinetic energy the length of the modelled part is essential. As you can see the comparative table the first and the best design solutions for each analysis;

Table 5-1. General Overview Comparison

<b>Run Number</b>	<b>Design Type</b>	<b>Width of Connecting Rod (mm)</b>	<b>Length of Connecting Rod (mm)</b>	<b>Angle</b>	<b>Investigated Zone- Average Stress (Pa)</b>	<b>Max Kinetic Energy of System (J)</b>	<b>2<sup>nd</sup> Mode Shape (Hz)</b>
NaN	Original Desin	10	350	80	31979415.68	345.742828	428.64
24	Full Factorial-1	7.5	385	78.74595	23663.69305	381.97995	313.76
47	NLQPLP	7.5	374.9181147	79.98065	5853.341861	363.782471	330.71

Among these, analysis Full Factorial method is more logical than NLQPLP method, since Full Factorial can scan every possible design solution with engineering sense, however, NLQPL stuck on a certain ‘frame angle for obtaining more close results to minimized results for kinetic energy and natural frequency. However, during this process, it overlooked the stress values. In this problem and this setup using only the NLQPL method does not give the best result.

NLQPLP method showed us, with multiple variables and multiple objectives, only local best points were achieved. Furthermore, the Full Factorial method achieved to close the global best point but it takes more time, more design parameters and computational force to get there. To be able to use more of Isight and optimization process, the problem can be simplifier or acquiring more computational force.



## 6. REFERENCES

- [1] Cohn, A.; Scheinberg, K.; Vicente, L. Introduction to Derivative-Free Optimization; MOS/SIAM Series on Optimization, SIAM: Philadelphia, PA, USA, 2009.
- [2] Lewis, R.M.; Torczon, V.; Trosset, M.W. Direct Search Methods: Then and Now. *J. Comput. Appl. Math.* 2000, 124, 191–207.
- [3] Pinter, J.D. Global Optimization: Software, Test Problems, and Applications. In *Handbook of Global Optimization*; Pardalos, P.M., Romeijn, H.E., Eds.; Kluwer Academic Publishers: Dordrecht, The Netherlands, 2002; Volume 2.
- [4] Kolda, T.G.; Lewis, R.M.; Torczon, V. Optimization by Direct Search: New Perspectives on Some Classical and Modern Methods. *SIAM Rev.* 2003, 45, 385–482.
- [5] R. Venkata Rao • Vimal J. Savsani *Mechanical Design Optimization Using Advanced Optimization Techniques*, Springer, 2012
- [6] G. Mastinu M. Gobbi C. Miano, *Optimal Design of Complex Mechanical Systems with Applications to Vehicle Engineering*, Springer, 2006
- [7] Slawomir Koziel and Xin-She Yang (Eds.), *Computational Optimization, Methods and Algorithms* Springer, 2011
- [8] Goldberg, D.E.: *Genetic Algorithms in Search*. In: *Optimization and Machine Learning*. Addison-Wesley, Reading, 1989
- [9] Tung Y, Erwie Z (2008) A hybrid genetic algorithm and particle swarm optimization for multimodal functions. *Appl Soft Comput* 8:849–857
- [10] Anonym, single variable optimization1.pdf , <http://cs.uok.edu.in/Files/79755f07-9550-4aeb-bd6f-5d802d56b46d/Custom/single%20variable%20optimization1.pdf> (Access Date: 08.04.2021)
- [11] P. R. AdbyM. A. H. Dempster, *Introduction to Optimization Methods*, Springer, 1974
- [12] Anonym, lec13.pdf, <https://services.math.duke.edu/~leili/teaching/duke/math212f15/lectures/lec13.pdf> (Access Date: 06.02.2021)
- [13] Anonym, businessmath\_1\_multivariable\_optimization.pdf, [https://web.northeastern.edu/dummit/docs/businessmath\\_1\\_multivariable\\_optimization.pdf](https://web.northeastern.edu/dummit/docs/businessmath_1_multivariable_optimization.pdf) (Access Date: 06.02.2021)
- [14] Abhijit Nagchaudhuri, *Dynamic Modeling and Analysis of a Crank Slider Mechanism*, University of Maryland Eastern Shore Princess Anne, MD 21853
- [15] Imed Khemili, Mohamed Amine Ben Abdallah & Nizar Aifaoui, *Multi-objective optimization of a flexible slider-crank mechanism synthesis, based on dynamic responses*, 2019
- [16] Shouguo Cheng and Shulin Liu, *Dynamic Analysis of Slider-Crank Mechanism with a Cracked Rod*, 2018
- [17] Dassault Systemes, ISIGHT & THE SIMULIA EXECUTION ENGINE, <https://www.3ds.com/products-services/simulia/products/isight-simulia-execution-engine/> (Access Date: 10.05.2021)

[18] Dassault Systemes, ABAQUS UNIFIED FEA, <https://www.3ds.com/products-services/simulia/products/abaqus/> (Access Date: 10.05.2021)

[19] CADTEK, <https://www.cadtek.com/5-reasons-use-solidworks/> (Access Date:18.05.2021)

[20] Shungen Xiao, Mengmeng Song, Zexiong Zhang, Dynamic analysis of slider-crank mechanism with clearance fault, *Vibroengineering Procedia*. November 2019